GA-C25413
07/07/2006

# High Energy Density Cryogenic Capacitors
# Final Technical Report (Phase 1)

**CDRL A002**

**Sponsored by the**
**Office of Naval Research**
**Contract # N00014-04-C-0297**

**Contractor:** General Atomics
**Address:** P.O. Box 85608
San Diego, CA 92186-9784

**DISTRIBUTION STATEMENT A**

**Approved for public release; distribution unlimited**

**GA PROJECT 30228**

GENERAL ATOMICS

# Table of Contents

# Tables

# Figures

# Acronyms

| | | | | |
|---|---|---|---|---|
| ABB | Asea Brown Boveri | | PE | Polyethylene |
| ANT | Albany Nano Technology | | PEN | Polyehtylene Napthalate |
| COTS | Commercial-Off-The-Shelf | | PET | Polyethylene terephthalate (polyester) |
| CPFF | Cost Plus Fixed Fee | | PF | Packing Factor |
| CPP | Chlorinated polypropylene | | PLC | Programmable Logic Controller |
| CTD-403 | Cryogenic epoxy | | PMMA | PolyMethyl MethAcrylate |
| CTE | Coefficient of Thermal Contraction | | PPL/PP | Polyproylene |
| DARPA | Defense Advanced Research Projects Agency | | | |
| DAS | Data Acquisition System | | PVdF | Polyvinylidene fluoride |
| DUT | | | PVA | Poly Vinyl Alcohol |
| ESR | Equivalent Series Resistance | | PVC | Poly Vinyl Chloride |
| FIB | Focused Ion beam | | RMS | Root Mean Square |
| FTIR | Fourier transform infrared spectroscopy | | RSO | Rapeseed oil |
| HEDCC | High Energy Density Cryogenic Capacitor | | SCR | Silicon controlled rectifiers |
| HVPS | High voltage power supply | | SF6 | Sulphur hexafluoride |
| GA | General Atomics | | SEM | Scanning Electron Microscope |
| GA-ESI | General Atomics – Electronic Systems, Inc. | | TPK | |
| GA-AMT | General Atomics Advanced Materials Technology | | VPI | Vacuum pressure impregnation |
| ICTC | Integrated Coefficient Of Thermal Contraction | | | |
| LCR | | | | |
| $LN_2$ | Liquid Nitrogen | | | |
| MHPPL | Metallized hazy polypropylene | | | |
| MPPL | Metallized Polypropylene | | | |
| MP | Metallized ( Kraft) paper | | | |
| NSWC | Naval System Warfare Center | | | |
| ORNL | Oak Ridge National Laboratory | | | |
| ONR | Office of Naval Research | | | |

# 1.0 Introduction

This is the final report for the High Energy Density Cryogenic Capacitor (HEDCC) program awarded to General Atomics (GA) as prime contractor with GA Electronic Systems Division (GA-ESI) and MTECH Laboratories, as major subcontractors, under the Offices of Naval Research (DARPA) CPFF contract: N00014-04-C-0297. Oak Ridge National Laboratory (ORNL) is also a team member but funded separately by ONR.

The HEDCC program is a two Phase project with just Phase 1 being funded to develop a 1 kJ cryogenic capacitor. Phase 2 when funded will support the development of a 100 kJ cryogenic capacitor.

## *1.1 Background*

General Atomics' pursuit of innovative technologies led to the development of improved stored energy density in capacitors. Recognizing the need for compact power conversion equipment and energy storage components in military applications, GA developed a new type of capacitor that could be operated at cryogenic temperatures such as 80K. Recent investigational studies by GA had indicated significant reductions in weight and size, and substantial improvements in efficiency for selected systems when electronic components, capacitors and bus work were operated at liquid nitrogen temperatures. Published data has also shown significant improvement in dielectric stress capacity and metal conductivity at cryogenic temperatures. Estimates indicate that substantial improvements in energy density can be achieved by operation at 80K and also by using new materials in capacitors specifically designed for operation in liquid nitrogen.

High Density Energy Cryogenic Capacitors can be used in a variety of commercial and military applications. An application for such a capacitor would be the Navy shipboard Railgun that requires ~200 MJ of energy storage. Electromagnetic Railguns are an example for Kinetic Energy Weapons. Power Conversion Modules can use these capacitors in Integrated Power Systems as do ship electric propulsion motor drives, Power Quality controls and pulse forming networks. High Power Microwave and Pulsed Laser are examples of Directed Energy Weapons that use High Density Energy Cryogenic Capacitors.

Commercial-off-the-shelf (COTS) capacitors have energy densities of 0.3–3.0 J/cc depending on the size, voltage, pulse width and lifetime. The HEDCC program was initiated to demonstrate density greater than 8 J/cc in 100 kJ cryocapacitors using metallized film capacitor technology with new materials. This can be achieved by developing a ten fold increase in energy density compared to conventional high energy capacitors at room temperature and also demonstrate a life time of $10^4$ cycles. The

target was to reduce the rate of dielectric aging, reduce dielectric and conductor losses with improved heat removal, thus extending the lifetime at high energy density.

The technical approach was to procure and evaluate COTS capacitors and associated materials for their performance under cryogenic temperatures. The failure modes and performace of these materials would lead to a down selection.

Using the selected material, custom capacitors designed to operate in cryogenic temperatures were developed. This development of the capacitors was an iterative process involving assessing the performance, determining failure modes, testing, and re-designing.

Capacitor testing was performed by GA, GA-ESI, and MTECH after developing test methods and also establishing a facility to conduct the testing.

GA-ESI performed the small scale materials screening tests.

GA and MTECH performed tests up to 15 kV and up to 1 kJ capacitors.

GA performed COTS life testing (DC and cyclic) at room temperatures and 77 K.

GA performed thermal and electrical cyclic tests.

Upon final down selection of the materials and design, the goal was to develop a 1 kJ capacitor.

The development of the 1 kJ Cryogenic capacitor involved the review of the Capacitor Materials, Requirements and Applications, the design and procurement of the capacitors, testing of capacitors and a final review of data. This involved the analysis of the high energy storage shipboard railgun applications and evaluation of candidate materials. Data collected on dielectric materials were reviewed and goals and parameters established for the cryocapacitors along with their testing ranges.

## *1.2 Data Summary and Review*

GA and the entire team reviewed all the data collected and downselect two (2) materials to pursue in the development of the 100 kJ capacitors for Phase 2.

# 2 Executive Summary

The successful deployment of advanced electromagnetic weapon systems will require significant improvements in the energy densities of the pulsed power supplies that drive those weapons. In fact the majority of an EM weapon system's weight and volume is dedicated to the power source, both prime power and the pulse-forming network. Weapons such as electromagnetic railguns, pulsed lasers, and high power pulsed microwave sources can be incorporated onto ships, aircraft, ground vehicles, and even space-based platforms if the energy density of their power sources becomes high enough. High energy density capacitors are a key technology that enables the deployment of weapons requiring pulsed power and capacitors designed to operate at cryogenic (77 K) temperatures represent a promising path toward the goal of high energy density.

The Naval Surface Fires Support (NSFS) mission being developed by the US Navy, for electromagnetic railguns requires a pulsed power supply that delivers approximately 200 MJ to the railgun breech per shot. A capacitor based pulsed forming network for such a weapon would occupy roughly 150 $m^3$ of deck space if the capacitors had an energy density of 3 J/cc. Army studies have indicated that a pulsed power supply of any architecture must deliver 10 J/cc for railguns to be practical on platforms roughly the size of a main battle tank. Given that COTS capacitors presently deliver approximately 1 J/cc with 10,000 shot lifetimes, it is clear that dramatic increases in energy density are required.

Early in the program, the likely requirements for capacitors for a shipboard railgun application were reviewed. The parameters as shown in Table 2-1, were selected as reasonable goals for the operating parameters for railgun cryocapacitors. The charge time and pulse interval of <5 s corresponds to a firing repetition rate of ~12 rounds per minute. The cryocapacitor discharge time of <5 ms assumes that several capacitor banks will be discharged in an overlapping pulse sequence into the same railgun circuit to achieve the required current delivery time to the railgun barrel of ~12 ms.

**Table 2-1**
**Target Requirements for Railgun Cryo-capacitors**

| | |
|---|---|
| Capacitor Energy Storage | >1 kJ then scale up to 100 kJ |
| Operating Temperature | ~80°K |
| Operating Environment | Liquid and/or gaseous nitrogen |
| Test Operating Voltage | 15 kV max |
| Charge time | < 5 s |
| Discharge time | < 5 ms |
| Pulse interval | < 5 s |
| Number of pulses per pulse train | > 100 |
| Time between pulse trains | < 300 s |
| Life expectancy | >10,000 shots at full energy |
| Capacitance loss at end-of-life | < 5% |
| Energy Density per Capacitor | >8 J/cc |

Figure 2-1 illustrates a 3 MJ capacitor bank using room temperature capacitors at 1 J/cc and includes the required inductor and switching. It also shows the projected reduction in size if the capacitors could be operated at 8 J/cc. The size reduction is dramatic.

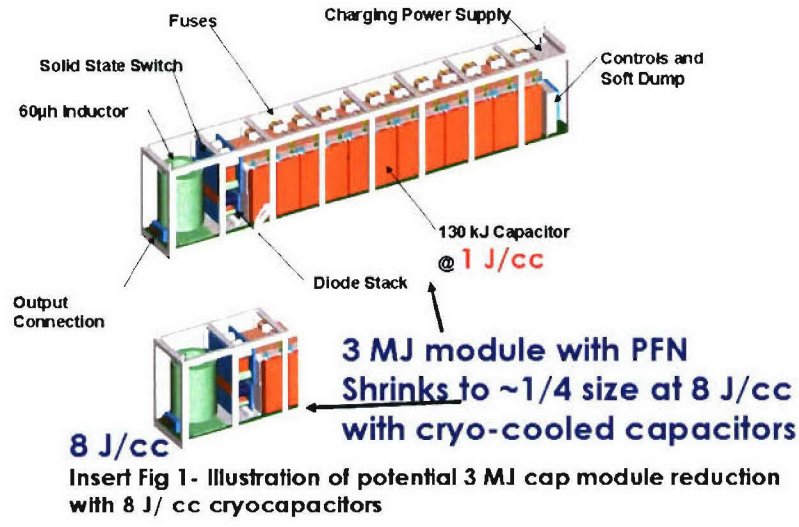


***Fig. 2-1. Potential advantages of a 8 J/cc for a 3 MJPFN module***

The impact is also shown in Fig. 2-2 which shows two of the 1 J/cc, room temperature modules, mounted in a standard 25 foot long sea-land container. Each container houses 6 MJ, hence, a shipboard railgun requiring 204 MJ would need 34 containers of this type. However, at 8 J/cc, this space requirement can be reduced to only 8.5 sea-land containers. Furthermore, our preliminary estimates indicate that there is sufficient room in the containers to accommodate the cryocoolers and insulation and cryostats for the cryocapacitors.

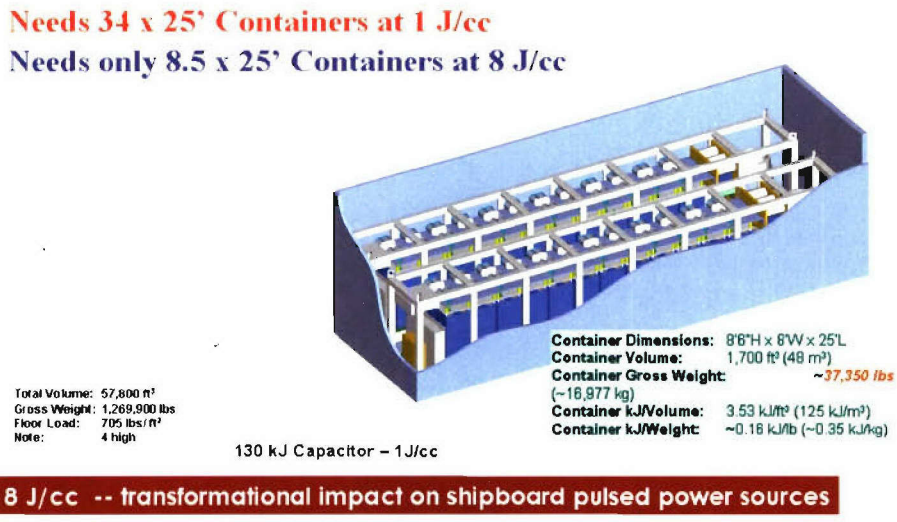


***Fig. 2-2. Configuration for 204 MJ Railgun Pulsed Power Facility Shows Potential Advantage of 8 J/cc***

The following report summarizes our Phase 1 cryocapacitor program. We found that we were unable to achieve the required voltage breakdown strength with COTS materials. However, a lab sample of specialized material and a first production run of the material that shows sections that have properties with ample margin to achieve 8 J/cc were produced. A reasonable follow on phase would be to tune the material production process, fabricate enough material to demonstrate several 5 KJ cryocapcitors at 8 J/cc, then operate the 5 KJ capacitors in series parallel at the 20 KJ level as a demonstration of the design approach and path toward a 100 KJ crycapacitor.

Phase 1 testing of COTS capacitors, indicated that the usual materials for capacitor impregnation were unsuitable for operation in LN2. However, using LN2 as the impregnation material improved both DC and AC lifetime of the capacitors significantly. Therefore GA does plan to continue this approach in any future effort.

Fundamentally, a capacitor stores energy in the electric field between two conductors. The challenge of increasing energy density then is to reduce the volume of the insulating dielectric material that separates those conductors since the thickness of the dielectric is orders of magnitude larger than the conductors in a typical energy storage capacitor. Figure 2-1 shows the requirements for an energy storage capacitor operating at 8 J/cc. High energy density can be achieved either with a high relative permittivity (sometimes called dielectric constant) or a high value of electric stress, the ability of a given thickness of dielectric to withstand an electric field across it. As shown by the governing equation in Fig. 2-3, the energy density is proportional to the relative permittivity and is proportional to the square of the dielectric breakdown strength. Recent room temperature capacitor development has focused on employing dielectric materials with high dielectric constants, either through the use of polar polymer materials and/or using dielectrics that are composites of polymers and nano-ceramics with high dielectric constants.

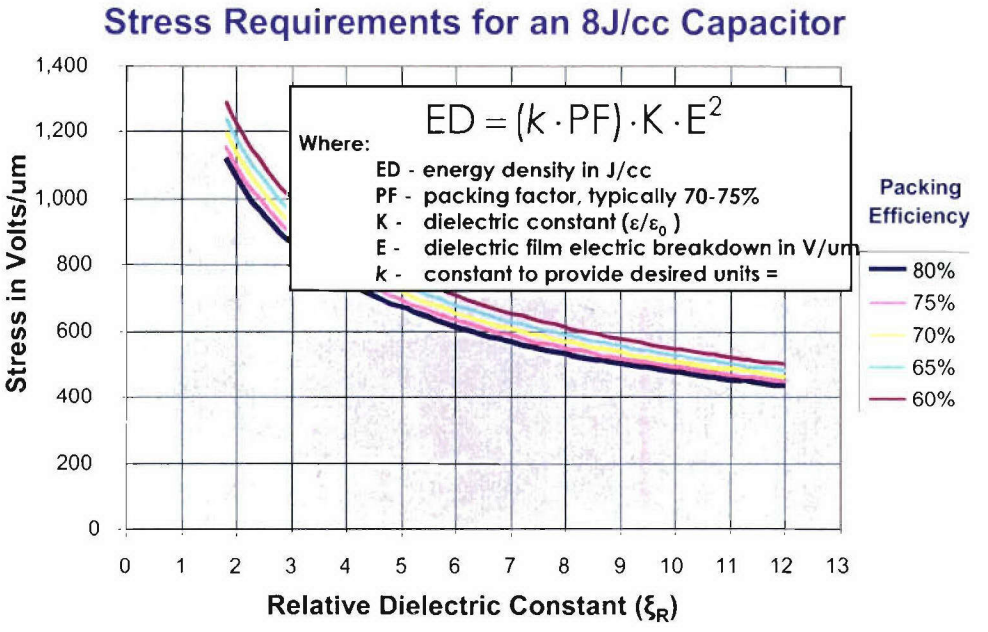


*Fig. 2-3. Basic operating requirements for an 8 J /cc energy storage capacitor*

One way to dramatically increase the dielectric breakdown stress in a polymer film is by reducing its temperature to 77K, the boiling point of liquid nitrogen at 1 bar. Evidence of this phenomenon was shown by Ball in 1951. Figure 2-4 is a reproduction of the data taken in that study that shows the increase in dielectric strength of a number of polymer films as a function of temperature from room temperature to 77 K.

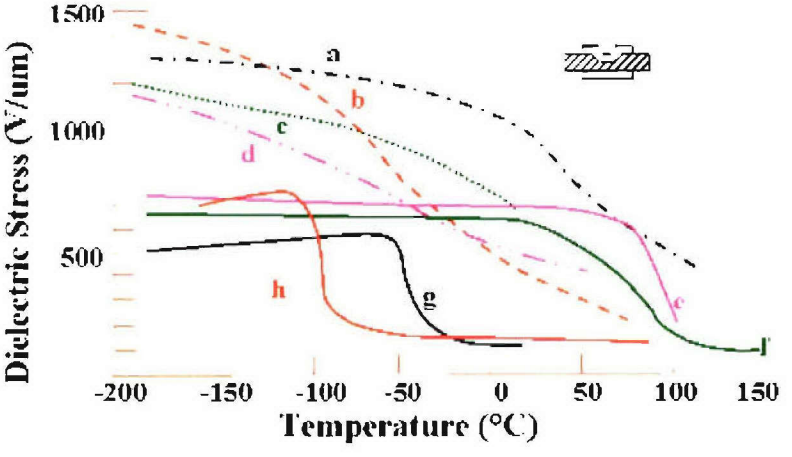


*Fig. 2-4. Results from 1951 study showing the temperature dependence of the dielectric breakdown strength for a number of polymers (from I.D.L Ball, Porc I.E.E.E 98. Pt 1, 84, 1951)*

The figure shows that four polar polymer materials exhibit breakdown strengths at 77 K adequate to yield a capacitor that operates at 8 J/cc, provided that the dielectric constant remains at approximately 2 or higher. These materials are polymethyl methacrylate (PMMA), Polyvinyl Alcohol (PVA), Polyvinylchloride Acetate (PVCA), and Chlorinated Polyethylene (PCE).

The initial goals of this program were to identify and test dielectric materials appropriate for use in a high energy density cryogenic capacitor (HEDCC); investigate the design, fabrication, and operational challenges involved; design and procure materials for a 1 kJ class capacitor; fabricate and test 1 kJ class capacitors; and finally design a 100 kJ class HEDCC based on the knowledge gleaned from the prior activities.

During the program began, however, testing indicated that commercially-available polymer films of the materials of interest, including but not limited to some of the materials shown in Fig. 2-4, did NOT exhibit high dielectric breakdown strengths at 77 K in either ball and plane or stamp capacitor tests. We determined that polymer films made by the common melt-extrusion process were too impure to repeat the performance shown in Fig. 2-4. In this case the impurities are in the form of additives used to facilitate the melt-extrusion process or provide the extruded film with desirable mechanical properties, which in turn degrade their electrical properties. "Impurities" also can be morphological in that the melting, extrusion, and re-crystallization processes yield polymers with disparate crystallography. Finally, many film fabricators do not, for economic reasons, take particular care to reduce the influx of contaminants into the films. The conclusion was that no off-the-shelf dielectric film would work in a cryogenic capacitor and provide high energy density. As a result, it became necessary to re-orient the program toward the fabrication of specialized films for our purpose.

We were able to fabricate polymer films with adequate breakdown strengths using the solution casting method, in which a solution of polymer resins and solvent is deposited on a carrier film, UV cured, and then removed as a high purity polymer film. We identified two vendors for this process, General Atomics Advanced Materials Technology (GA-AMT) and TPL, Inc. The films solution-cast by TPL were either pure polymers or were composites of a polymer and a nano-ceramic dispersed in the polymer. Ceramics, such as $BaTiO_3$, can have very high dielectric constants but tend to have very low breakdown strengths. A composite dielectric is thought to possess the high dielectric constant of a ceramic but a breakdown strength in between that of the ceramic or polymer alone. If the material is able to maintain a high dielectric constant at 77 K, the breakdown strength required to achieve high energy density can be lower for the composite compared with a pure polymer.

Table 2-2 shows representative ball and plane breakdown strength data for many of the solution cast films that were tested.

**Table 2-2**
**Breakdown Strength Measurements for Solution Cast Films**

| Material | Thickness (um) | V/um avg | V/um min | V/um max | n |
|---|---|---|---|---|---|
| **PMMA with 2 um SiO2 particles** | **4** | **1463** | **1310** | **1723** | **4** |
| **PMMA without SiO2 particles** | **4** | **1143** | **903** | **1453** | **6** |
| GA-AMT Acrylic WITH Particles | 6 | 572 | 415 | 775 | 5 |
| Chlorinated Polypropylene UV Cured | 6 | 538 | 505 | 583 | 3 |
| Chlorinated Polypropylene Air Cured | 6 | 644 | 495 | 703 | 4 |
| PVA with particles | 3.5 | 505 | 377 | 571 | 3 |
| TrFE(.28) PVDF(.72) | 8 (?) | 1050 | 991 | 1105 | 3 |
| BRF 20% sld E0073-3 rod 22 | 5.6 | 482 | 407 | 557 | 2 |
| BRF 20% sld E0073-4 rod 28 | 10 | 240 | 198 | 282 | 2 |
| BRF 40% sld E0075-2 rod 10 | 6.3 | 470 | 448 | 503 | 3 |
| BRF 40% sld E0075-4 rod 20 | 10.2 | 420 | 410 | 439 | 3 |
| GA-AMT Acrylic No Particles | 10 | 480 | 200 | 675 | 4 |
| GA-AMT Acrylic WITH Particles | 10 | 381 | 365 | 399 | 3 |
| PVA (TPL) | 19 | 301 | 218 | 366 | 4 |
| PMMA (TPL) | 16 | 511 | 464 | 596 | 4 |
| PVCVA (TPL) | 24 | 320 | 296 | 338 | 4 |
| PVCA Composite (TPL) | 22 | 148 | 135 | 164 | 4 |
| TPL PMMA Roll | 20 | 420 | 412 | 423 | 4 |
| TPL-Loaded PMMA 50wt% BSA Roll | 17 | 241 | 211 | 294 | 4 |
| TPL FPE Roll | 13 | 598 | 405 | 728 | 4 |
| TPL Loaded PVCVA 50wt% BSA Roll | 30 | 127 | 124 | 130 | 4 |
| TPL PVCVA Roll | 48 | 236 | 200 | 266 | 4 |
| TPL FPE Sheet | 7.4 | 474 | 288 | 745 | 4 |
| TPL PMMA Sheet | 17.7 | 462 | 437 | 504 | 4 |
| TPL PVCVA Sheet | 14 | 543 | 516 | 588 | 4 |
| TPL PMMA | 6 | 928 | 780 | 1260 | 4 |
| PVCVA (TPL) | 8 | 749 | 558 | 910 | 4 |
| PVCVA (TPL) 50WT% BVA | 7.5 | 358 | 253 | 555 | 4 |

The top three rows show the result that are promising for the target of 8 J /cc.

The table lists the material tested; the thickness of that material; the average, minimum, and maximum breakdown strengths measured in units of Volts per micron; and the final column is the number of data points taken on that particular sample. One material supplied by GA-ATM, a 4 to 5 micron thick film comprised of a PMMA base with additive polymers and 2 μm SiO2 particles, performed better than all others in terms of dielectric breakdown strength, and that material is shaded red in Table 2-2. The TPL materials generally had low breakdown strengths, but most of the composite materials were cast onto a stainless steel foil instead of a polymer film (the idea being that the foil could act as an electrode in ball and plane or stamp capacitor tests). It was later determined that solution casting on metal foils consistently led to much lower breakdown strengths compared with casting onto a polymer film, likely due to the microscopically rough surface morphology of the foils which could serve as electric field concentration and charge injection points. Also, the lack of reliable dielectric constant measurements of the TPL films at 77 K means that the results from the TPL films were inconclusive.

**Table 2-3**
**Electrical performance requirements for 8 J/cc (75% packing fraction)**

| Candidate Material | Dielectric Constant at 77 K | Breakdown Strength (V/μm) |
|---|---|---|
| Polymer | 2 - 3 | 1000 |
| Nano-Ceramic-Polymer Composite | 10 | 490 |
| Acrylic Co-polymer with 2 μm $SiO_2$ particles (baseline material) | 3.5 – 4 measured | 1400 measured (average) |

Table 2-3 summarizes the required values of dielectric constant and breakdown strength to achieve an energy density of 8 J/cc in a capacitor with a 75% packing fraction. Through stamp capacitor testing, we found that all of the polymers tested had dielectric constants near 2 at 77 K, implying that many of the dipoles responsible for high dielectric constant in a polymer at room temperature, get frozen out as the temperature is reduced. Therefore, for a pure polymer, the minimum breakdown strength is 1000 V/μm at 77 K. A higher value of breakdown strength would be required in a practical capacitor to ensure some margin as well as a reasonable capacitor life. An estimated (not measured) dielectric constant of 10 for composite dielectrics would drop the minimum breakdown strength to around 490 V/μm. Most of the TPL composite films had breakdown strengths below this value, but those films had the aforementioned metal foil substrate and were also quite thick, another factor that we found decreases breakdown strength. The last row in Table 2-2 shows data for the GA-AMT film, which offers high average breakdown strength and a dielectric constant that is higher than that for a pure polymer. The latter effect is due to the presence of the SiO2 particles in the film. Both of these values exceed the requirements for 8 J/cc and give us confidence that 8 J/cc in a cryogenic capacitor can be attained.

Most of the samples of the GA-AMT PMMA with additives film were 8 inch x 10 inch sheets made in the laboratory. Near the end of the program, GA-AMT production equipment was used to produce a roll of the material that was 54 inches wide, 600 feet long, and 4.2 microns thick (average). SEMs of the material are shown in Fig. 2-5.

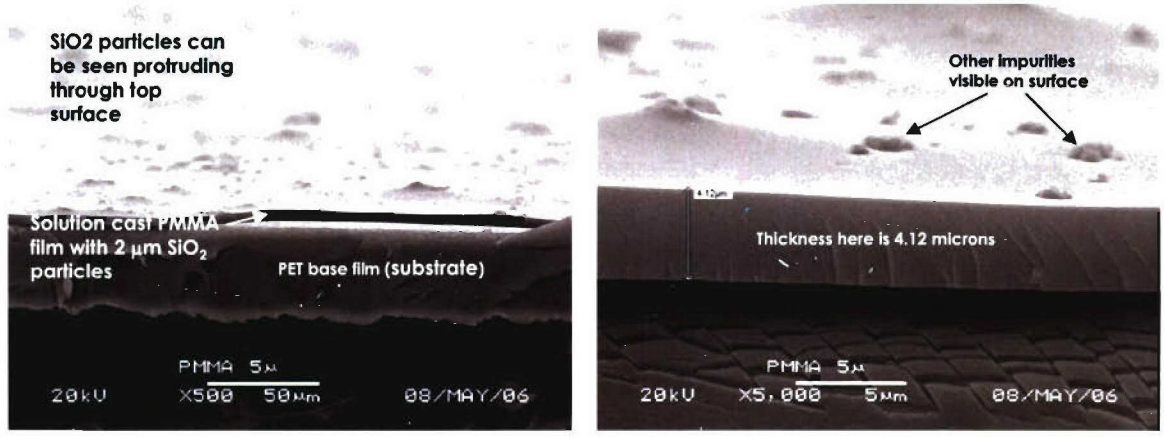


***Fig. 2-5. SEMs of GA-AMT PMMA with additives; first run fabricated on production equipment***

The left SEM is at 500x magnification, and the thin PMMA film can be seen on top of the polyester carrier film. The right SEM is at 5,000x magnification. The SiO2 particles can be seen protruding from the top surface of the film. Given that the film thickness is only twice the average particle size, this is not surprising.

One feature of the films is that the dielectric breakdown strength measurements have considerable scatter. Samples from the roll of film produced on GA-AMT's production equipment were tested with the ball and plane apparatus, and the values of breakdown strength from samples near the right side, middle, and left side of the film are presented in Fig. 2-6. It is clear that many parts of the film exceeded our requirement of 1000 V/micron with considerable margin.

**Results from LEFT sample**

| V/μm |
|---|
| 1602 |
| 2438 |
| 1224 |
| 3155 |
| 1233 |
| 745 |
| 1114 |
| 940 |
| 898 |
| 2655 |
| 2655 |
| 1743 |

| Average |
|---|
| 1700.2 |
| **Standard Deviation** |
| 821.1 |

**Results from CENTER sample**

| V/μm |
|---|
| 1743 |
| 1526 |
| 1145 |
| 2807 |
| 733 |
| 779 |
| 648 |
| 1962 |
| 1967 |
| 995 |
| 2655 |
| 733 |

| Average |
|---|
| 1474.4 |
| **Standard Deviation** |
| 758.5 |

**Results from RIGHT sample**

| V/μm |
|---|
| 1245 |
| 852 |
| 745 |
| 929 |
| 1005 |
| 1917 |
| 2774 |
| 2188 |
| 1624 |
| 1026 |
| 2374 |
| 1938 |

| Average |
|---|
| 1551.4 |
| **Standard Deviation** |
| 678.2 |

***Fig. 2-6. Dielectric breakdown strength measurements on samples of GA-AMT PMMA with additives; first run fabricated with production equipment shows significant variation, but many sections exceed the required operating level with substantial margin***

As seen in Fig. 2-6, the peak and average values of the breakdown strength exceed the values measured on laboratory-made films, but the scatter seen in the laboratory samples remains. We suspect that the size of the $SiO_2$ particles is mostly responsible for this scatter. In the next phase of the program we plan to address this by using smaller, including nano-sized, silica particles.

As part of the effort to investigate the design, fabrication, and operational challenges involved in cryogenic capacitors, we tested COTS capacitors in an LN2 environment. Part of those tests involved DC life tests, to determine if cryogenic operation had an effect on the life of a capacitor. Figure 2-7 shows the results from some of these tests.

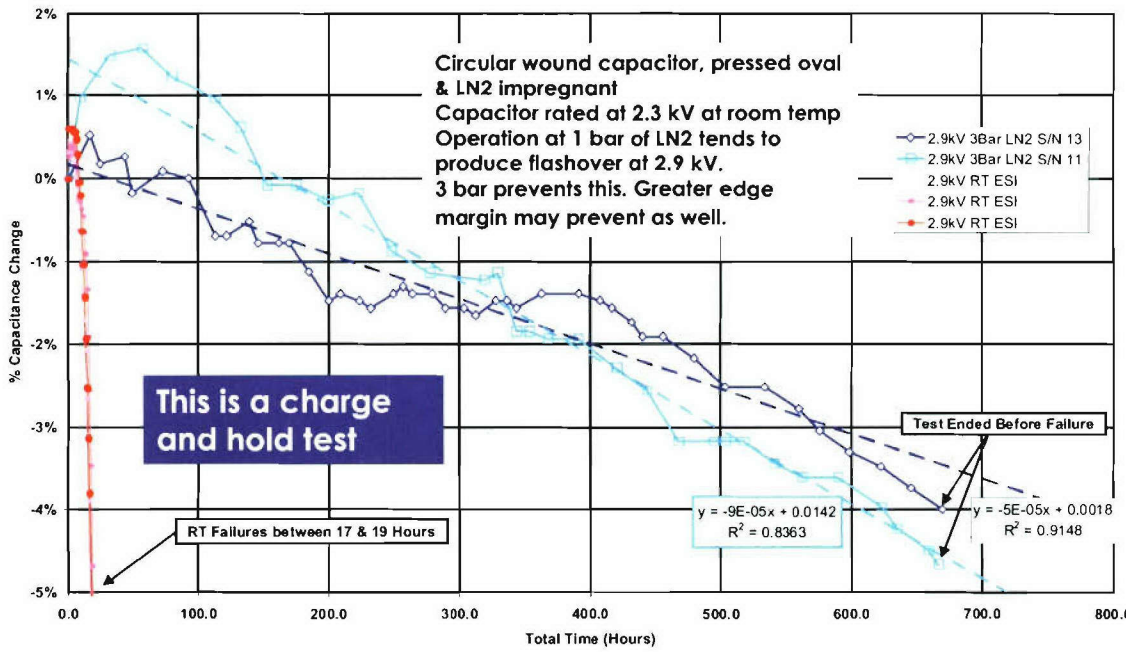


***Fig. 2-7. DC life test of COTS capacitors with metallized polypropylene system shows substantial increase in lifetime (defined as 5% loss in capacitance) when LN2 is used***

In this test, the capacitor is held at a DC voltage until its capacitance drops below 5%, at which time the test is stopped. At room temperature, these capacitors fail after 17 to 18 hours at voltage. At 77 K and in 3 bar of LN2, the capacitors have a life that is 30 times longer. Indications are that with design changes, this could be extended further. This has implications in the ability for a cryogenic capacitor PFN to be held at high voltage for extended periods, for instance in a ship defense application.

A related test is the life cycle test, where the capacitor undergoes many charge / discharge cycles. Results from some of these tests are presented in Fig. 2-8.

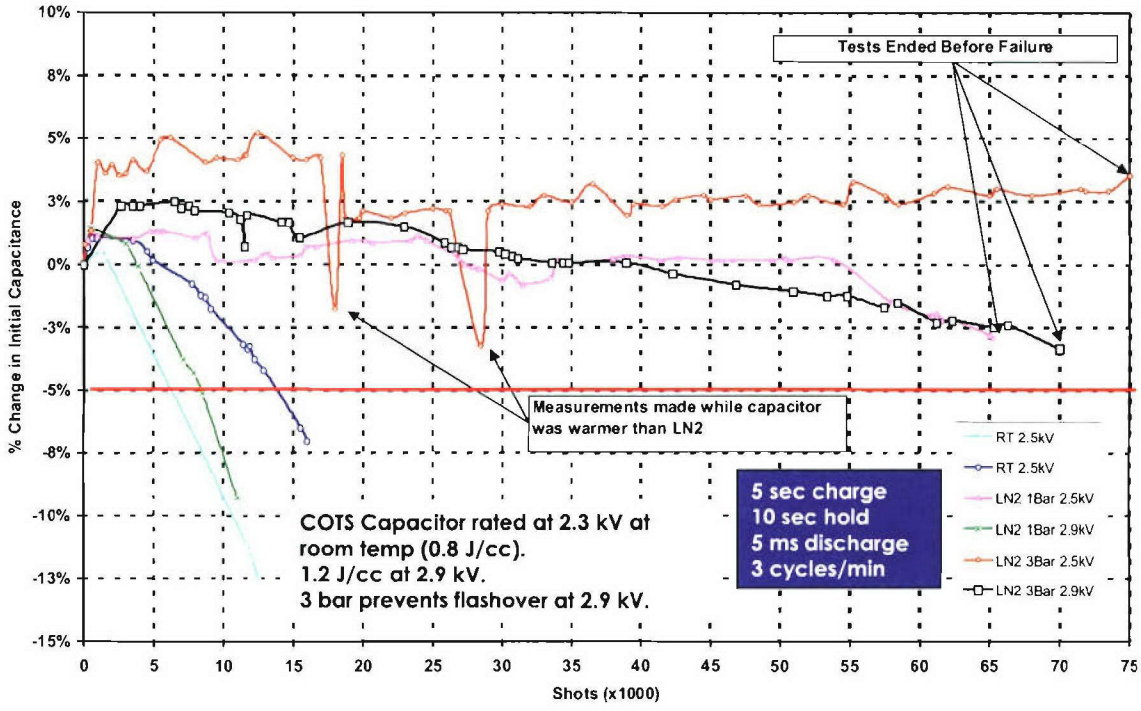


***Fig. 2-8. Life cycle tests of COTS capacitors at room temperature and 77 K shows dramatic improvement in LN2***

Again, the life at 77 K is improved dramatically compared with room temperature. The room temperature capacitors were charged to 2.5 kV and failed after 10,000 to 15,000 cycles. At the same voltage (and 3 bar of LN2 impregnant instead of oil), the capacitor showed no sign of degradation in performance at all at 77 K. The voltage had to be increased to 2.9 kV to see appreciable loss of capacitance.

Significantly more time and resources were spent finding a suitable dielectric material than were planned, therefore no capacitors were fabricated. However, a promising dielectric material and fabrication technique have been identified. The processing steps required to fabricate a cryogenic capacitor have been examined, and there are few steps that are different from conventional capacitor fabrication. The primary difference is that the dielectric film will have to be separated from its carrier film, though in our initial tests, this does not appear to be prohibitive. We see the follow-on phase as being a fairly straight forward process optimization exercise where the dielectric film chemistry and particle size are perfected, the metallization step is tuned with stamp capacitor tests and a few roll coater trials, and 5 kJ-class capacitors are wound and tested. A reasonable goal is the operation of the 5 KJ cryocapacitors in series parallel to demonstrate the scale up process we would expect to use to achieve a 100 KJ cryocapacitor at 8 J/ cc.

## 2.1 Summary of Phase 1 Results

The results of the first phase of the project can be summarized as follows:

1. Conventional polymer films and their fabrication processes do not yield dielectrics that are suitable for use in high energy density cryogenic capacitors.

2. High purity solution cast films have the required breakdown strength. (Results project to 8 J/cc or greater for PMMA with additives at 1000V/μm & K=2.6 projects to 8.7 J/cc )

3. Tests show thinner films (~ 4 micron) perform best. Breakdown strength decreases significantly as film grows from 4 to 6 microns. GA-ESI has used ~ 4 micron films before in capacitor production

4. Most of the fabrication techniques used for conventional capacitors are appropriate for cryogenic capacitors with a few notable but reasonable exceptions

5. LN2 appears to be a good impregnant. Better performance is seen at 3 bar compared with 1 bar, but design changes could relax this.

6. Significant life improvement measured with LN2 impregnated capacitors with standard dielectrics

7. No decrease in capacitance after 75,000 shots at rated voltage vs ~10,000 shots at room temperature

8. A factor of 7 increase seen in cycle life compared with room temperature when operated at 50% above rated energy density (1.2 vs 0.8 J/cc)

9. A factor of 30 increase seen in dc life (at 50% above rated energy density)

10. Custom designs have been started for 5 kJ class, 8 J/cc capacitors

11. Conceptual design has started for 100 KJ cryo-capacitor

# 3 Cryocap Requirements and Applications

The requirements for the sipboard railgun applications were reviewed together with capacitor materials and available data on dielectric materials, to select goals for railgun cryocapacitor parameters, ranges for testing, and the materials to be considered in the development program.

Table 3-1 lists the requirements for a projected application of the Pulsed Power Supply for a Navy shipboard Railgun using the cryocapacitors.

**Table 3-1**
**Requirements for a Projected Application of the Pulsed Power Supply for a Navy Shipboard Railgun**

| | |
|---|---|
| *Total capacitive energy storage* | *~200 MJ* |
| Energy storage per capacitor | >100 kJ |
| Operating voltage | 11 kV |
| Discharge time | 3–4 ms |
| Repetition rate | 6–12 per minute |
| Life expectancy | >10,000 shots at full energy |
| **Energy density per capacitor** | > 8 J/cc |

Table 3-2 indicates the application requirements and the cryogenic capacitor development goals.

**Table 3-2**
**Phase 1 – High Energy Density Cryogenic Pulse Capacitor Requirements and Goals**

| | |
|---|---|
| Capacitor energy storage | >1 kJ |
| Operating temperature | ~80 K |
| Operating environment | Liquid and/or gaseous nitrogen |
| Test operating voltage | 15 kV max |
| Charge time | < 5 s |
| Discharge time | < 5 ms |
| Pulse interval | < 5 s |
| Number of pulses per pulse train | > 100 |
| Time between pulse trains | < 300 s |
| Life expectancy | >10,000 shots at full energy |
| Capacitor losses at liquid nitrogen temperature | < 1% |
| Energy density per capacitor | >8 J/cc |

# 4 Material Review and Selection

Initially this effort was intended to be a survey of available data on the cryogenic properties of potential dielectric materials, followed by the selection of a few candidate materials for ball and plane and stamp capacitor testing, followed by a down-select of two materials for capacitor fabrication and testing. However, we faced great difficulty finding materials that performed adequately, and our search for the appropriate materials and processes came to dominate the effort.

A reprint of Fig. 2-1 is shown in Fig. 4-1 because this figure was fundamental in guiding our materials review and selection.

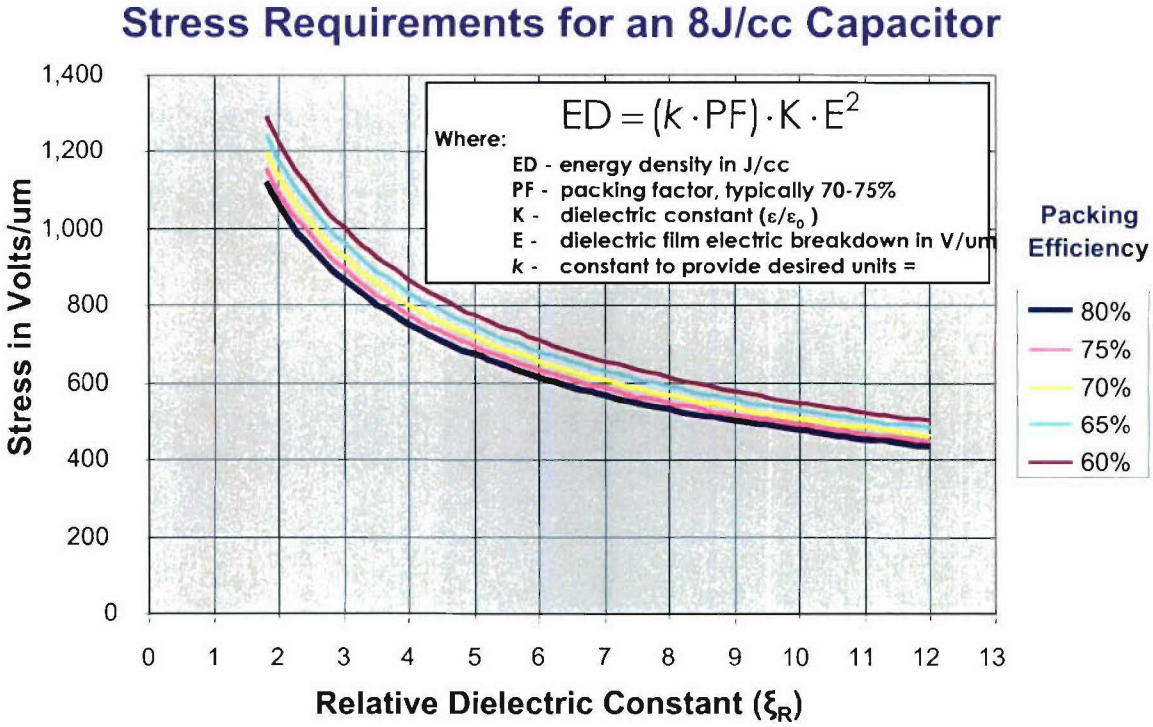


***Fig. 4-1. Dielectric property requirements for 8 J/cc capacitor***

For a given packing factor (75% is conservative), the curve specifies the minimum combination of dielectric constant and breakdown strength (stress) that a material must possess to function in an 8 J/cc capacitor. One message of Fig. 4-1 is that if a polymer has a dielectric constant at 77 K of around 2, as most do, then it must have a high breakdown strength. Breakdown strength, and thus the ball and plane tests, provides a good filter for potential materials. A higher low-temperature dielectric constant helps, but the squared dependency of the breakdown strength is the key performance driver.

A database of dielectric materials was established early in the program for the materials shown in Table 4-1, giving the manufacture's name along with a brief comment.

Selection of materials was based on information gathered in the first part of the program and includes:

a. Common capacitor material that have been used by ESI in COTS capacitor applications and are readily available

b. High dielectric constant material as recommended by consultant to the project, Elizabeth Yen of JPL. Tests are planned for these materials

c. Poly amino ethyl vinyl alcohol

d. Poly (vinylidene fluoride + trifluoroethylene)

e. High energy density material at room temperature (RT)

f. PVDF (polyvinylidene fluoride)

g. Bi-polar materal showing high electric strength at cryogenic conditions based on the 1951 paper by Ball, referenced in Section 2

h. PVA (poly vinyl alcohol)

i. PMMA (polymethyl methacrylate)

j. PVCA (polyvinyl chloride acetate)

k. 55 CPE (55% chlorinated polyethylene)

l. Other Materials

m. Cryoflex proprietary material used in cryo application for high temperature superconductor for voltage transmission lines

n. Other common materials: kapton, nylon

**Table 4-1**
**Polymer Material Master List**

| No. | Film Material | | Manufacture | Comment |
|---|---|---|---|---|
| 1 | PET (Mylar) | Polyethylene terephthalate | Bolmet | Common cap film |
| 2 | OPP | Oriented polypropylene | ExxonMobil | Common cap film |
| 3 | Kraft Paper | | SPO | Common cap film |
| 4 | ETFE (Tefzel) | Ethylene-alt-tetrafluoroethylene | AGC | Common cap film |
| 5 | PEN | Polyethylene naphthalate | Mitsubishi | Common cap film |
| 6 | PEN | Polyethylene naphthalate | Teonex | Common cap film |
| 7 | FPE | Fluorene polyester | Ferrenia | Common cap film |
| 8 | FPE | Fluorene polyester | Brady | Common cap film |
| 9 | PPL | Polypropylene | Terfilm | Common cap film |
| 10 | PEN | Polyethylene naphthalate | Teonex | Common cap film |
| 11 | PEEK | Polyetheretherketone | Mitsui Toatsa TALP | Common cap film |
| 12 | PTFE (Teflon) | Polytetrafluoroethylene | Dupont | Common cap film |
| 13 | SMK | Cellouse | | Common cap film |
| 14 | DLC | Diamond like carbon on foil | K-Systems | Common cap film |
| 15 | PPL-M | Polypropylene | GA Display Products | Common cap film |

| No. | Film Material | | Manufacture | Comment |
|---|---|---|---|---|
| 16 | PVA-M | Polyvinyl alcohol (purified) | GA Display Products | Common cap film |
| 17 | PET (Mylar)-M | Polyethylene terephthalate | GA Display Products | Common cap film |
| 18 | PI (Kapton) | Polyimide | Dupont | Common material |
| 19 | Nylon | | | Common material |
| 20 | PAEVA | Poly amino ethyl vinyl alcohol | TBD | High dielectric constant material |
| 21 | VF2 TrFE | Poly (vinylidene fluoride + trifluoroethylene) | TBD | High dielectric constant material |
| 22 | PVDF | Polyvinylidene fluoride | Terphane | High energy density at RT |
| 23 | PVDF | Polyvinylidene fluoride | Terphane | High energy density at RT |
| 24 | PVDF | Polyvinylidene fluoride | Kureha P-20 | High energy density at RT |
| 25 | PVDF-M | Polyvinylidene fluoride | GA Display Products | High energy density at RT |
| 26 | PVA | Polyvinyl alcohol | Monosol 2000 | Promising from 1951 Tests |
| 27 | PVA | Polyvinyl alcohol | Monosol LXP-6024 | Promising from 1951 Tests |
| 28 | PVA | Polyvinyl alcohol | Monosol A-127 | Promising from 1951 Tests |
| 29 | PVA | Polyvinyl alcohol (purified) | Kuraray | Promising from 1951 Tests |
| 30 | PMMA | Polymethyl methacrylate | Scientfic Polymer | Promising from 1951 Tests |
| 31 | PVCA | Polyvinyl chloride acetate | TBD | Promising from 1951 Tests |

| No. | Film Material | | Manufacture | Comment |
|---|---|---|---|---|
| 32 | 55 CPE | 55% chlorinated polyethylene | TBD | Promising from 1951 Tests |
| 33 | Cryo-Flex #1 3-Ply | Polypropylene | Southwire | Used in cryo applications |
| 34 | Cryo-Flex #2 1-Ply | Polypropylene | Southwire | Used in cryo applications |

M = metallized

Many of the materials listed in Table 4-1, Polymer Material Master List, are available off of the shelf in thin film form ready for testing. Others were procured as resins, and films were manufactured in sufficient film quantities to support ball and plane breakdown, stamp capacitor, and dielectric constant screening tests. As part of the manufacture, a film stretching and surface orientation is performed to enhance performance of the film. A consultant to the project, Thomas Hopkins, assisted in coordinating the manufacture of custom extruded test films. Resins received and processed this quarter are:

- Polymethyl methacrylate (PMMA) normal grade resin for process setup
- Polymethyl methacrylate (PMMA) 95% isotactic resin for final film
- Polyvinyl chloride acetate
- Chlorinated polyethylene

PMMA films were melt extrusion processed at Randcastle under the supervision of Tom Hopkins. Figure 4-2 is a photograph of a film being processed. Initial extrusion results with "normal" material gave poor results. The melt would not flow through the die and required very high extrusion pressure and heater current. The resulting film was of very poor quality.

Polyvinyl chloride acetate material was also cast, resulting in a roll several feet long x 4 in. wide film, 25 to 50 microns thick with a high degree of uncast material impurities.

48% chlorinated polyethylene was also attempted with very poor results.

Isotactic PMMA was extrusion cast; a roll several feet long x 4 in. wide film, 25 to 50 microns thick was made. Again, some embedded impurities and bubbles were visible in the film, which was translucent, a sign of a high degree of crystallinity, scattering light transmitted through the film. The film was very brittle. Test results from these films are reported below.

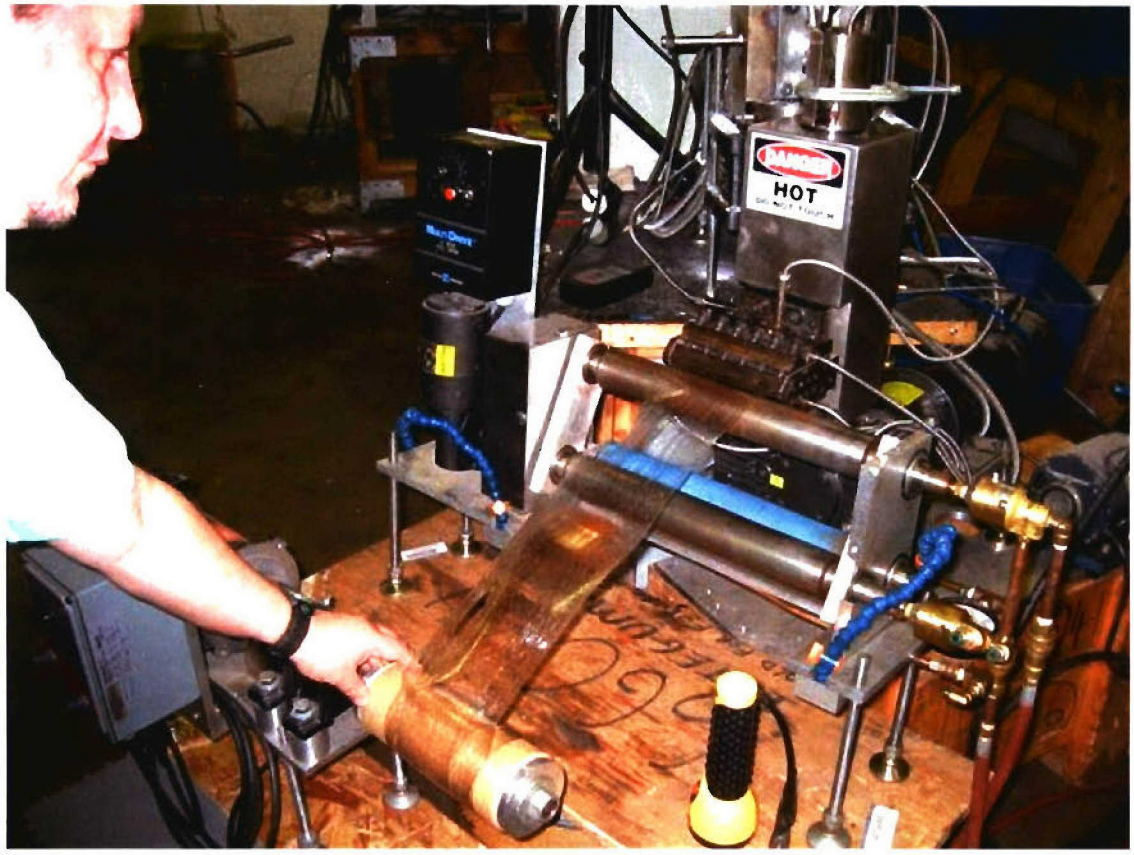


***Fig. 4-2. Melt extrusion casting of a polymer film at Randcastle***

Photographs of the rolls of film fabricated at Randcastle are shown in Fig. 4-3.


***Fig. 4-3. Photographs of, from left to right, isotactic PMMA, polyvinyl chloride acetate, and chlorinated polyethylene fabricated at Randcastle***

During this period we also expanded our materials search beyond traditional dielectric polymers. Some polymers with high room temperature dielectric constants were identified, as shown in Fig. 4-4; however, all polymers evaluated to date have dielectric constants that fall into the 2 to 3 range at $LN_2$ temperatures.

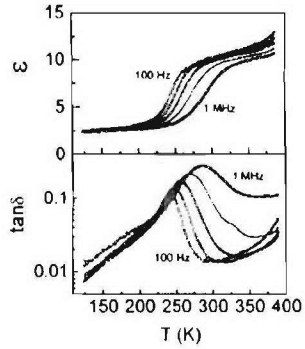


FIG. 2. Temperature dependence of $\epsilon$ and $\tan\delta$ of the P(VDF–TrFE) copolymer at 0.1, 1, 10, 100, and 1000 kHz ($\epsilon$ from top, $\tan\delta$ from bottom).



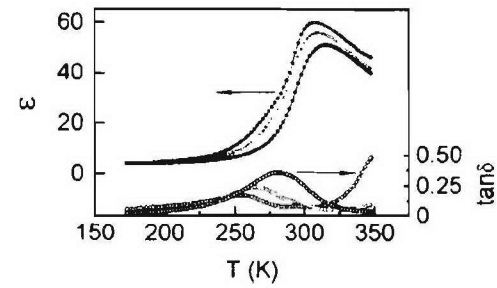


FIG. 1. Temperature dependence of $\epsilon$ and $\tan\delta$ of sample A at 1, 10, and 100 kHz ($\epsilon$ from top to bottom; $\tan\delta$ from bottom to top).

***Fig. 4-4. Dielectric constant for stretched P(VDF-TrFE) copolymer (K ~10) left side and P(VDF:TrFE:CTFE) terpolymer (max. K ~60 near room temperature) in the right panel***

An alternative to pure polymer dielectrics is the family of composite dielectrics where a nano-ceramic is imbedded within the polymer. Ceramics can have high dielectric constants but, especially in polycrystalline forms, low breakdown strengths. Nano-ceramics that are specially processed to prevent agglomeration in the polymer yield higher dielectric constants, and the polymer matrix provides reasonably high breakdown strength.

TPL, Inc. manufactures small-scale composite polymer films with nano-ceramic BaTiO3 particles imbedded in the films. SEM scans of the nano particles and a cross section of the film are shown in Fig. 4-5.

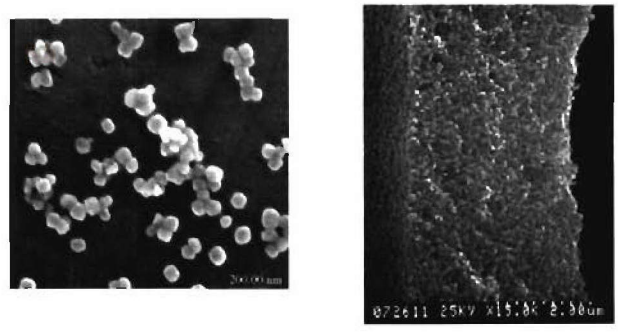

***Fig. 4-5. 50 nm BaTiO3 particles and a nano-ceramic/polymer composite film from TPL***

Composite dielectric films have dielectric constants that remain higher than those for the polymers alone as the temperature is lowered to $LN_2$ levels, as shown in Fig. 4-6. An NDA was signed with TPL and they fabricated several composite dielectric films for evaluation at cryogenic temperatures.

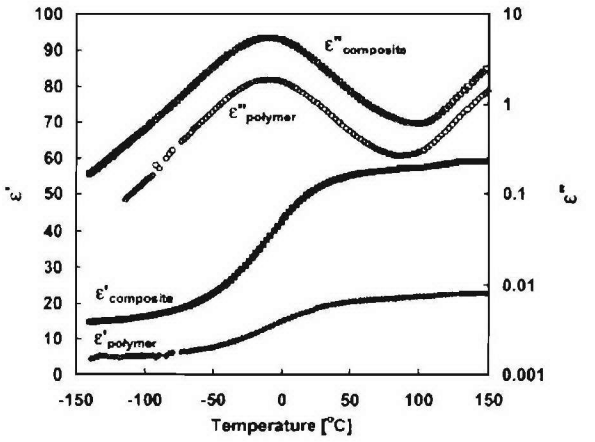


Figure 5. Temperature dependence of the dielectric constant (ε') and dielectric loss factor (ε'') of CR-S polymer and the corresponding 30% $BaTiO_3$ CR-S composite at 100 kHz

***Fig. 4-6. Dielectric constant (lower two curves and left vertical axis) of composite film showing larger dielectric constant for composite than polymer alone***

Finally, most of the COTS dielectric materials tested were melt extrusion cast films. Commercial films have a number of additives to facilitate the extrusion process. The films also have disparate crystal structures and tend to possess other impurities. Purer films can be obtained by solution casting, where the basic resins are mixed in a solvent and spread on a flat surface, being cured in air, at elevated temperature, or under UV light.

We were able to fabricate polymer films with adequate breakdown strengths using the solution casting method, in which a solution of polymer resins and solvent is deposited on a carrier film, UV cured, and then removed as a high purity polymer film. We identified two vendors for this process, General Atomics Advanced Materials Technology (GA-AMT) and TPL, Inc. The films solution-cast by TPL were either pure polymers or were composite dielectrics. Figure 4-7 is a schematic of the solution cast production hardware at GA-AMT, showing the path of the carrier film, how the dielectric film is solution cast onto the carrier film, and finally how the film is cured and taken back up into another roll. Many of these steps are performed in a controlled atmosphere, which limits contamination of the film.

An extensive list of materials that were tested, along with the test results, is listed in the section on ball and plane testing.

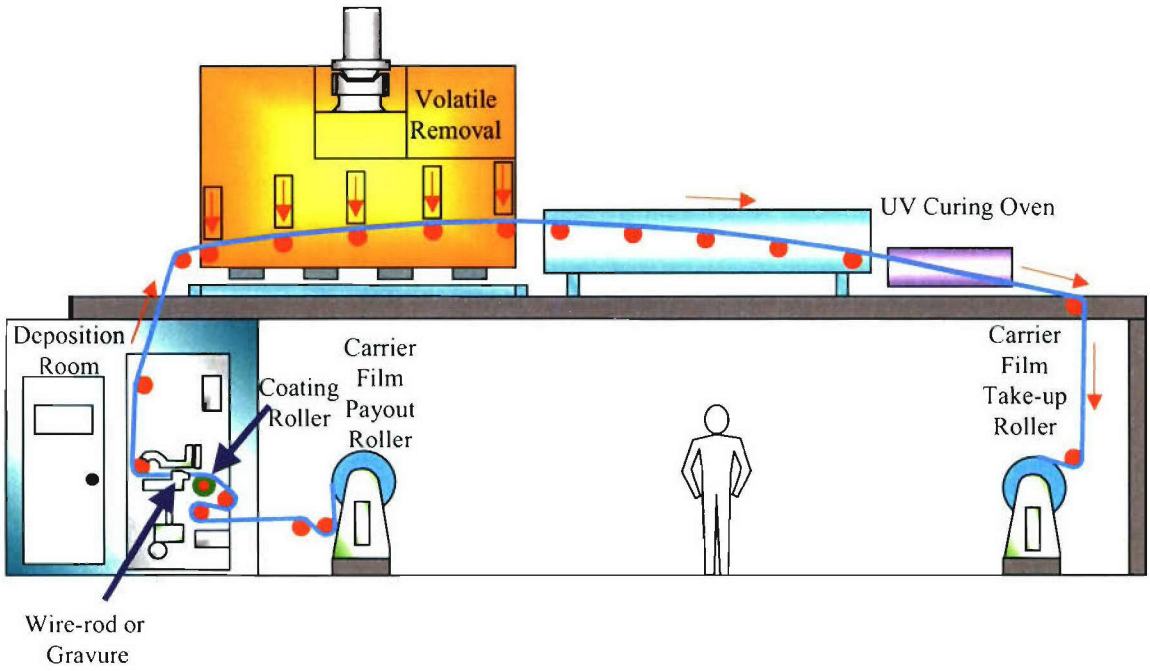


***Fig. 4-7. Film solution cast coating process at General Atomics Advanced Materials Technologies***

# 5 1 KJ Cryocap Design

This section is a summary of the design for a 1KJ cryogenic capacitor as prepared by GA-ESI in Cryogenic Capacitor Design Study, ESI REPORT NUMBER 200-30228-1-A..

## *5.1 Technical Requirements*

The 1-kJ model capacitor will be used to demonstrate the energy density in the dielectric and capacitor winding design that is required to achieve 8 J/cc energy density in the packaged 100-kJ cryocapacitor. Based on a nominal 70% packing factor in the 100-kJ design, this implies a dielectric energy density of 11.4 J/cc. The 1-kJ model capacitor will also be designed to meet the other requirements as specified in Table 3-2.

## *5.2 Assumptions*

Since the dielectric material required to manufacture a wound cryocapacitor at >8 J/cc energy density is not yet fully identified, characterized, tested, and available in quantity, the design makes the assumption that such a material will be available in the future.

### *5.2.1 Dielectric Material*

The probable dielectric material to be selected for the 1-kJ capacitor will be polymethyl methacrylate (PMMA). This material is currently the front-runner in dielectric selection because of previously published data and GA's ball-plane breakdown test results on laboratory samples.

### *5.2.2 Dielectric Constant*

The dielectric constant for PMMA at room temperature and 120 Hz is ~4.0. This material is a polar dielectric and from past experience it has been observed that the dielectric constant of such materials decrease with temperature to a value somewhere between 2 and 3 at cryogenic temperatures. A value of 2.2 is chosen as the expected value of the dielectric constant for PMMA at 77 K.

### *5.2.3 Packing factor*

It is assumed that the packing factor of the 100-kJ cryocapacitor will be about 70%, similar to that of large, room temperature energy storage capacitors. If packaging requirements for cryogenic capacitors result in a lower packing factor, the electric field will need to be increased to reach the same energy density goal. For example, if the packing factor were 50%, the electric field needs to be increased by $(70/50)^{1/2}$ or 18% to achieve 8 J/cc.

## 5.3 General Description

The 1-kJ cryogenic capacitor will represent a single capacitive element used in the construction of a large 100-kJ energy storage capacitor suitable for a railgun application. The objective of the model capacitor testing will be to demonstrate that the dielectric material will operate at the electric field required to achieve 8 J/cc for 10,000 charge/discharge cycles or more.

## 5.4 Electrical Design

The objective of this program is to develop a 100-kJ capacitor at 8 J/cc energy density. The 1KJ capacitor should demonstrate the required electric field in the dielectric material, as well as the energy output per unit volume of winding that is expected.

As specified in Sections 5.1.2.1 and 5.1.2.2, the dielectric material and dielectric constant to be selected for the 1-kJ capacitor will be PMMA based.

The energy density of a capacitor is the energy stored at rated voltage divided by the volume or by the weight. In single-section metallized capacitors in metal cans, where the ratio of dielectric thickness to total dielectric plus electrode thickness is approximately 100%, the PF is typically 70–75%.

For purposes of the 1-kJ model capacitor design calculations here, the packing factor in the winding itself is assumed to be about 90%. This factor will be mainly determined by the ratio of the active width to the total width of the film. The width of the edge margins is dictated by the surface flashover characteristics of the film and impregnant. For room temperature capacitors impregnated with oil, a 5 mm edge margin on each edge is sufficient for operation at 5.65 kV, so a 100mm-wide film yields a packing factor of about 90%.

These assumptions indicate that the ratio of the winding volume to the total 100-kJ capacitor volume needs to be 77%.

Based on the energy density goal, assumed packing factor, and estimated dielectric constant, the required electric field in the polymer film dielectric is 1082 V/μm. For comparison, the highest electric fields currently being achieved by GA-ESI in room temperature capacitors with lifetimes in the thousands of cycles is in the 500–600 V/μm range. These capacitors are made with high purity, high crystallinity, polypropylene film developed over the past 40 years.

The breakdown strength of the polymer dielectric film needs to be greater than the operating stress by a ratio that depends on the required lifetime. For a 10,000 shot self-healing capacitor at room temperature, the dielectric strength needs to be greater than 143% of the operating stress. If the same rule applies at cryogenic temperature, the dielectric strength needs to be greater than 1546 V//μm. It is quite possible that a smaller ratio will yield the required life at cryogenic temperature, however.

The thickness of the selected dielectric will be determined by experiments that yield the highest dielectric strength, as long as it results in a manufacturable film. The target voltage of 11 kV will be achieved by putting capacitor elements in series. For a single capacitance, the film needs to be 10.2 μm, whereas for two capacitances in series the film thickness would be 5.1 μm, and so on. In reality, the single element design is probably not practical due to the size of edge margins required to hold off 11.0 kV from surface flashover in $LN_2$. Two or three series capacitances would be preferable, at 5.65 or 3.67 kV per element, at film thickness values of 5.1 or 3.4μm.

The best breakdown strength results on PMMA so far have been with 4.5 μm films, so it is likely that the final 100-kJ, 11-kV capacitor would contain two series-connected groups of elements rated at 5.65 kV and made using 5.1-micron thick film. (If the available film for the 1-kJ model capacitor is not exactly this value, it will still be possible to demonstrate the critical metrics.)

The impregnant for the 1-kJ capacitor will be liquid nitrogen. Other materials that have been considered as impregnants solidify at temperatures of less than 90 K and could possibly damage the film due to crystalline structures that form during the freezing process.

The 1-kJ model capacitor winding will be cylindrical. This will minimize the size and weight of the pressure vessel required to enclose the capacitor and maintain the $LN_2$ under pressure. It will also minimize thermo-mechanical stresses in the winding that result from cooling to 77 K. The specific dimensions of the winding are calculated in Section 5.1.4.2.

The dimensions of the reusable vessel used for testing the capacitor winding are not critical to the demonstration of energy density. The critical metric will be the electric field in the dielectric film, as determined by the applied voltage and the measured film thickness. Confirmation of the energy density in the dielectric itself will also be performed by measuring the electrical energy discharged from the capacitor and the winding volume. This data will be used together with the measured film thickness and active area of the capacitor to determine the effective dielectric constant of the film as well.

The design of the 1-kJ capacitor is based on the requirements and the assumptions described previously. The resulting values are shown in Table 5-1.

**Table 5-1**
**Design Values for 1-kJ Capacitor Winding**

| | Value | Units |
|---|---|---|
| Energy | 1000 | Joules |
| Energy density | 8 | J/cc |
| Packing factor | 77 | % |
| Winding volume | 96 | cc |
| Dielectric constant | 2.2 | |
| Electric field | 1082 | V/μm |
| Film thickness | 5.1 | μm |
| Element voltage | 5650 | volts |
| Capacitance | 62.7 | uF |
| Active area | 16.36 | $m^2$ |
| Film width | 100 | mm |
| Edge margin | 5 | mm |
| Active width | 90 | mm |
| Active length | 90.9 | M |
| Core diameter | 9 | mm |
| Outside diameter | 35.5 | mm |
| Number of turns | 1299 | turns |

The energy and charge storage capability of a capacitor are directly proportional to the capacitance and will be determined by the requirement of 1000 Joules delivered energy at 5650 V.

## *5.5 Mechanical Design*

The most probable dielectric material to be selected for the 1-kJ capacitor will be PMMA.

The best breakdown strength results on PMMA so far have been with 4.5 μm films, so it is likely that the final 100-kJ, 11-kV capacitor would contain two series-connected groups of elements rated at 5.65 kV and made using 5.1-micron thick film.

The ideal width of the film for this application is 150 mm, as this would give the highest packing factor while still fitting on the best winding equipment. Calculations performed assume that 100 mm film width to be conservative.

Two layers of metallized film will be laminated and wound together as shown in Fig. 5-1 to form the capacitor. The green rectangles represent the cross-section of the film, and the black lines are the metallized electrodes.

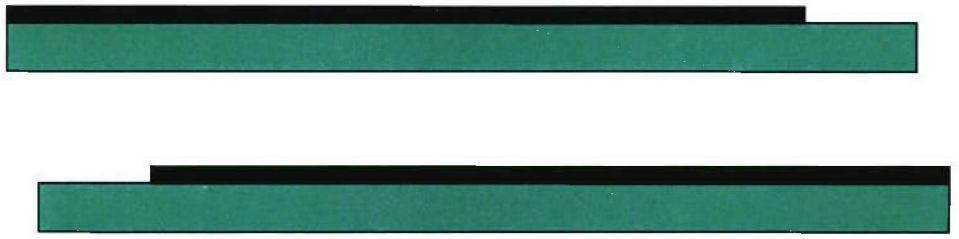

***Fig. 5-1. Cross-section showing dual-metallized films positioning of two films to be laminated and wound into a capacitor (not to scale)***

The winding will be started on a glass-fiber-reinforced-plastic core of 9mm outside diameter and will be wound to the calculated length required for the specified capacitance value.

The winding edges will be arc-sprayed with zinc to make electrical contact to the metallized electrodes. The zinc forms about a 1 mm thick porous layer on each end of the winding. A small stripe across each end of the winding will be masked to allow an opening in each turn of the winding for vacuum drying and impregnation.

The best candidates for insulation at liquid nitrogen temperatures are relatively soft plastics like polypropylene and polyethylene. The plan is to use many layers of capacitor-grade polypropylene film of 12–25 micron thickness as insulation between the winding and the test vessel in the 1-kJ capacitor. The nominal electric field in this major insulation should be kept below 40 V/micron, based on room temperature design criteria, indicating that at least 140 microns total thickness should be used to insulate the 5650 volt winding. This conservative approach accounts for any field enhancements from sharp edges, defects in the layers, etc. These recommended thermoplastics can also be thermally spot-welded to themselves to prevent unwrapping.

Manufacturing cylindrical windings on hard cores as shown in Fig. 5-2 will minimize problems associated with the brittleness of PMMA as well as thermo-mechanical stresses from cryo-cooling.

*Fig. 5-2. Cylindrical capacitor winding*

The capacitance is calculated between 2 parallel plates separated by a dielectric with a dielectric constant value. High voltage film capacitors are often manufactured with capacitive elements like sections, windings, or groups of windings connected in series. In large capacitors, the capacitive elements may also be connected in parallel to produce the target terminal capacitance.

The total width of the film to be wound into capacitors should nominally be between 75 and 150 mm in order to fit on the best winding equipment. The wider the film, the better the packing factor. Assuming a 100 mm width and using the same 5 mm edge margin dimension used on room temperature capacitors at this operating voltage, an active width of 90 mm is obtained, where the two electrodes overlap and a packing factor close to 90%.

The active length is calculated as the length of the winding over which the two electrodes overlap, and is determined from the active area and width. In the case where the film width is 100 mm and the active width is 90 mm, the length of 90.0 m is calculated to produce a 62.7 uF capacitor.

At the start and end of the winding, the metallization of one electrode (i.e., the anode) on both films will be removed by an electrical discharge process on the winding machine, known as "burn-off." This will provide a margin on these ends that will hold off the high voltage.

In order to calculate the winding dimensions, it is assumed that the space factor (also known as film factor), which is the average gap between the surfaces of the films expressed as a percentage of the film thickness, will be zero. This is typical of "hard wound" capacitors wound on solid cores at high tension and/or using a compression roller to eliminate air from the winding.

For flattened windings, the space factor is typically 3–5% and the winding is made on a removable arbor or crushable hollow core.

A tinned copper wire or flat ribbon will then be soldered to the zinc arc spray layer.

The ceramic feedthrough bushing, Ceramtech PN 4275-17-W has been recommended.

The insulated winding will be inserted in a reusable cryogenic test vessel and the wires soldered to the feedthrough bushing terminals. The top cover of the reusable vessel will be bolted to the flange of the body. The unit is then ready for vacuum drying.

Figures 5-3 and 5-4 show the reusable vessels that will be used.

Liquid-impregnated film capacitors generally have higher energy density than either unimpregnated or solid-impregnated film capacitors. This is due to the higher breakdown strength and dielectric constant of liquids compared to gases. Even in solid-impregnated capacitors, such as mica-epoxy constructions, thermal contraction and expansion results in gas-filled voids that determine the dielectric strength of those capacitors.

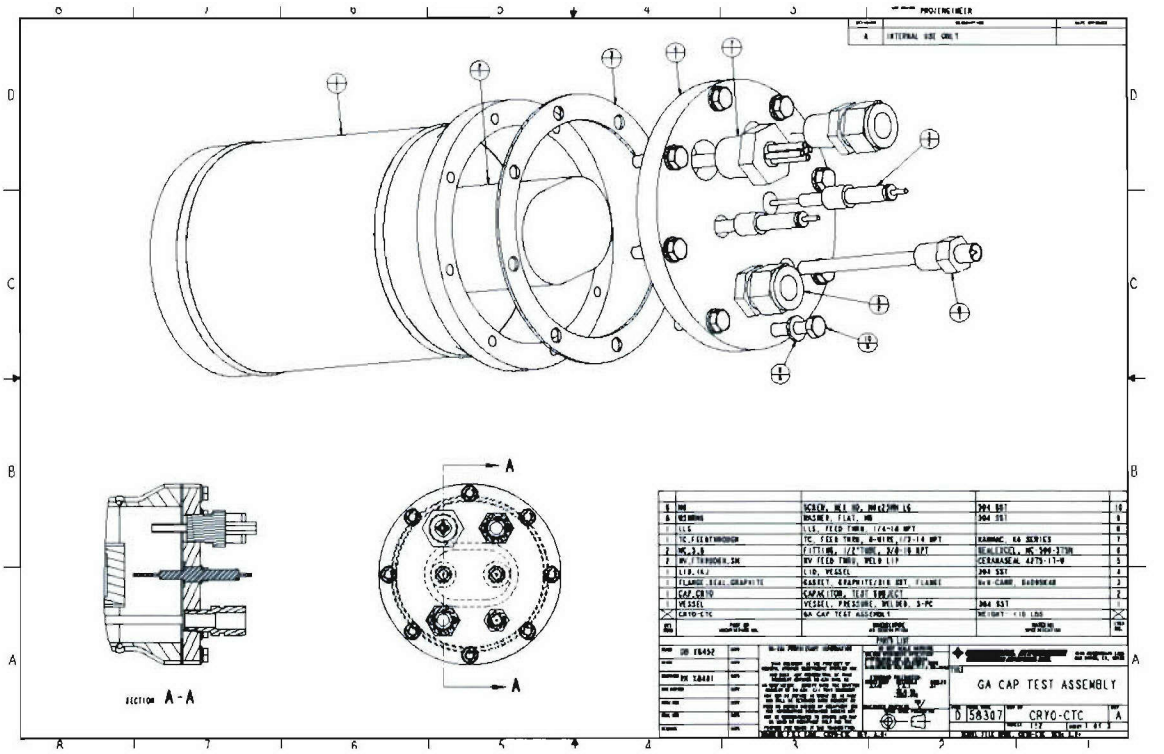


***Fig. 5-3. Reusable cryogenic capacitor test vessel***

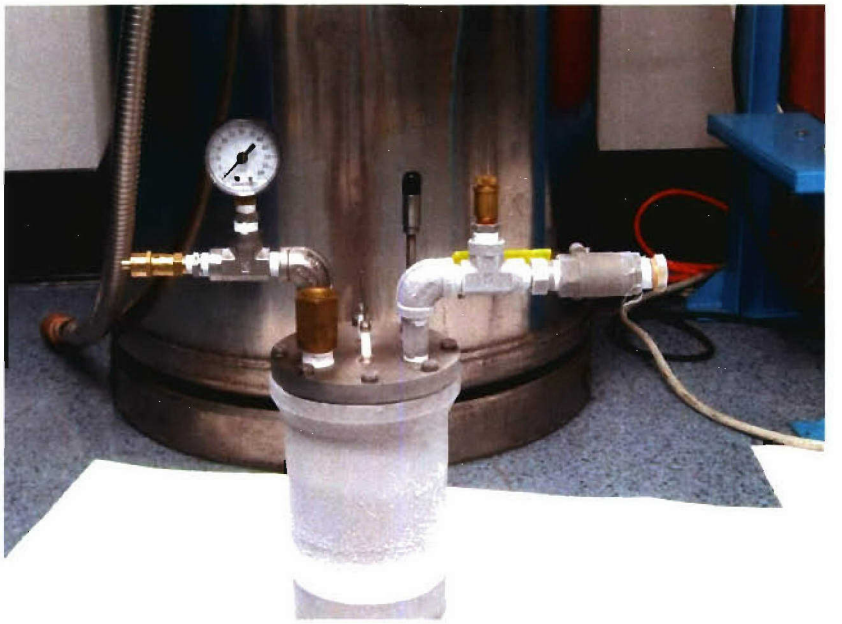

*Fig. 5-4. Photograph of a reusable cryogenic test vessel being pressure-tested*

At 77 K and within a reasonable pressure range, only nitrogen was found to be a liquid. All of the materials normally used as liquid impregnants at room temperature are solids at 77 K.

COTS capacitors supplied by GA-ESI indicated that liquid nitrogen was a suitable impregnant provided it was pressurized to at least 3 bars. Higher pressure might improve performance further, but at the cost of energy density due to lower packing factor as the result of more robust packaging requirements.

Figure 5-5 shows the proposed options being investigated for packaging the cylindrical capacitors.

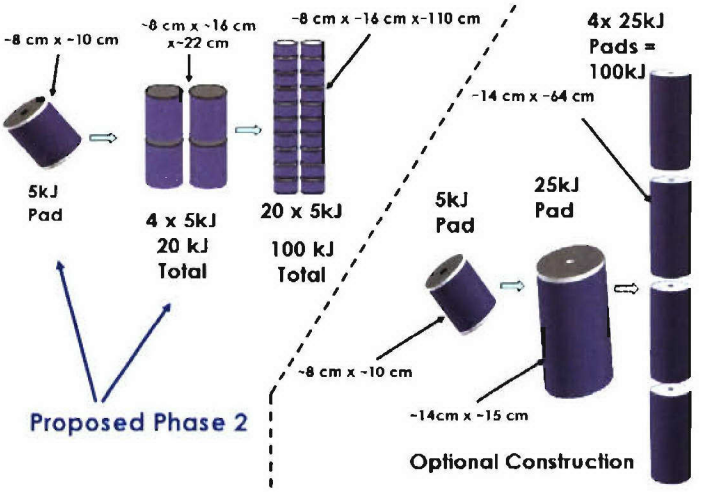


*Fig. 5-5. Scale-up to 100 KJ by Series/Parallel Modules*

## 5.6 Life Expectancy

The life of a high energy density capacitor is generally limited by dielectric aging mechanisms that eventually result in electrical breakdown of the dielectric.

Metallized electrode capacitors generally have self-healing capability. In these components, the electrode is very thin (~10 nm) compared to the dielectric thickness. In the event of a dielectric breakdown, the current density in the electrode immediately surrounding the arc contact point reaches high enough values to cause fusing action, vaporizing the metal, extinguishing the arc, and leaving a small "clearing" surrounding the breakdown point. Some of the substrate for the metallization is pyrolized, and it is critical for successful self-healing that this process does not result in carbonization of the organic material. Carbon is conductive and leads to a thermal runaway failure mode.

It is also possible to pattern the metallization, dividing the electrode into segments that are connected via fusible links. This approach is suitable for lower energy density, longer life, high power density units, such as DC Link capacitors in inverters on electric trains.

Metallized capacitor failure is usually defined by a 5% loss in capacitance, which evolves gradually over the life of the component, whereas discrete foil capacitor failure is usually defined by a sudden short-circuit event.

The life of a high energy density capacitor is generally limited by dielectric mechanism factors that eventually result in electrical breakdown of the dielectric. The primary dielectric factors are partial discharges, ionic conduction, and temperature-dependent chemical reactions and morphological changes. It is generally not possible to predict capacitor lifetime from first principles. Instead, life of a new design or a new application is scaled from the life of similar capacitors under similar conditions. The empirical scaling equations are developed from years of life testing and are proprietary to each manufacturer.

## 5.7 Thermal Analysis

A transient thermal analysis was performed for two potential operating conditions for the high energy density capacitor. The results were compared to empirical data from temperature measurements taken of actual cool down testing. One analysis simulated a cryogenically cooled capacitor, while the other simulated cooling with dry ice. The purpose of the modeling was to obtain temperature profiles throughout the volume of a capacitor as function of cooldown time. With this information further mechanical analysis could be performed with the temperature data as input to determine relative deflections of the capacitor dielectric materials. This could lead to understanding possible material wrinkling that was experienced during capacitor cryo testing. See Section 7.1.1.1.1 for discussion about wrinkling.

### *5.7.1 Model Assumptions and Parameters*

The thermal model was based on the configuration of a typical COTS capacitor. It consisted of oval wound Mylar dielectric pad with a 1.1-in. minor dimension and a 3-in. major dimension. The large temperature range between room temperature (270 K) and the cooling medium temperature (80 K) has a major affect on the thermal properties of the Mylar dielectric. Also, because the Mylar film is in layers, the thermal conductivity across the capacitor is not the same as the thermal conductivity in the axial direction. To accommodate these differences the following procedure was followed.

1. Thermal data for thermal conductivity and specific heat were obtained for both room temperature and for 77 K. These values are shown in Table 5-2.
2. It was assumed that linear curve fits of the thermal data would simulate the actual thermal properties.
3. The radial conductivity was multiplied by a factor selected so that the calculated temperature profile would match nearly as possible the experimental results. The radial conductivity factor was found to be 0.33 long. Therefore the radial conductivity used in the model is 1/3 of that shown in Table 5-2.

**Table 5-2**
**RT and 77 K Thermal Properties Used in Model (Axial Direction)**

| | Room Temperature | 77 K |
|---|---|---|
| Conductivity (watt/m/K)) | 0.20 | 1.17 |
| Specific Heat (joule/gm/K) | 0.18 | 0.56 |

The geometric properties used in the model are shown in Fig. 5-6.

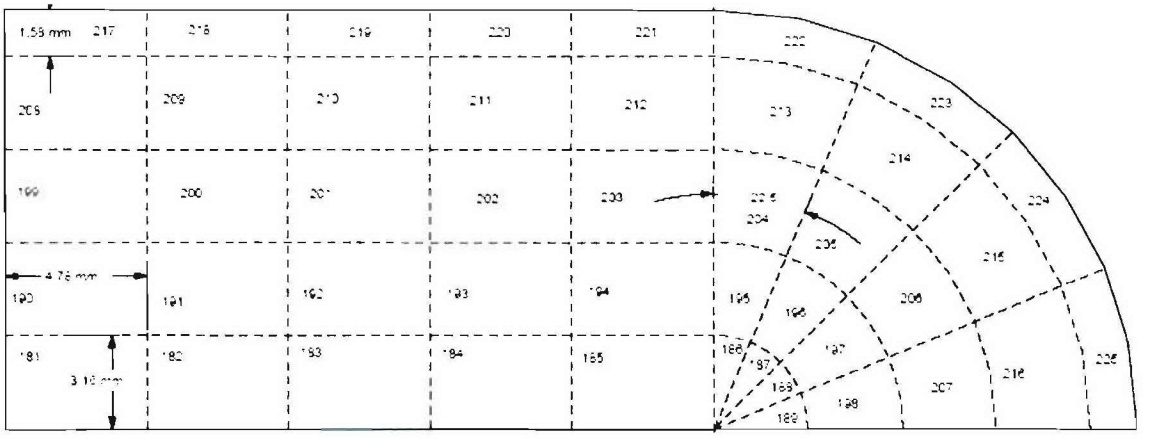


***Fig. 5-6. Thermal model geometry***

With this thermal data, the model calculated the temperature profiles at various locations within the capacitor. It was assumed that the heat transfer coefficient at the

outer surface was sufficiently large to keep the outer surface at the temperature of the cooling bath.

### *5.7.2 Thermal Model Results*

Figure 5-7 shows the transient response for the two cases. From these two sets of results the following conclusions can be made.

1. The calculated results for cryogenic cool down with $LN_2$ approximate the measured centerline temperatures for that case.
2. It is also clear from these results that the faster cryogenic cool down results in a larger temperature gradient in the capacitor. This in turn results in larger thermal stresses.

### *5.7.3 Comparison of Test Results*

In comparing the thermal cool down test results with the models, it was determined that the cool down rate of a capacitor could have a significant affect on its performance. Since a capacitor consists of many windings of metallized plastic on a core, there will be a temperature gradient across the capacitor. This will result in uneven rates of thermal contraction and could cause excessive stresses as the outer windings shrink down on the inner windings. This temperature gradient is shown in Figures 5-7 and 5-8.

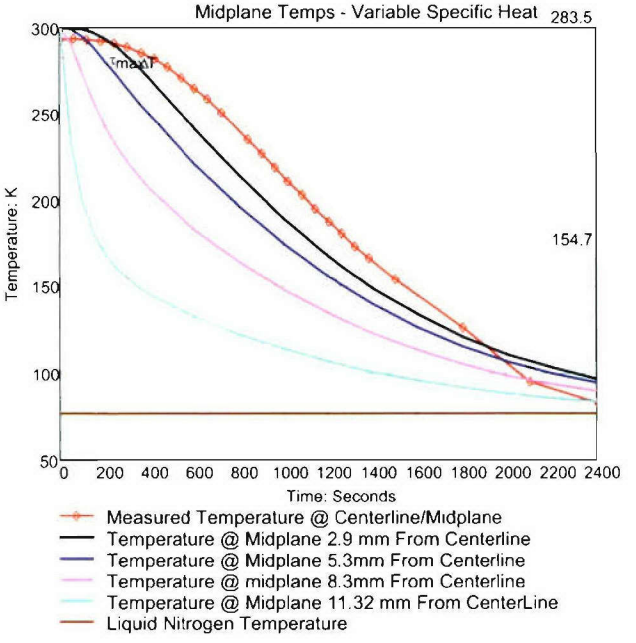


***Fig. 5-7. Model of capacitor pad cooling by immersion in liquid nitrogen***

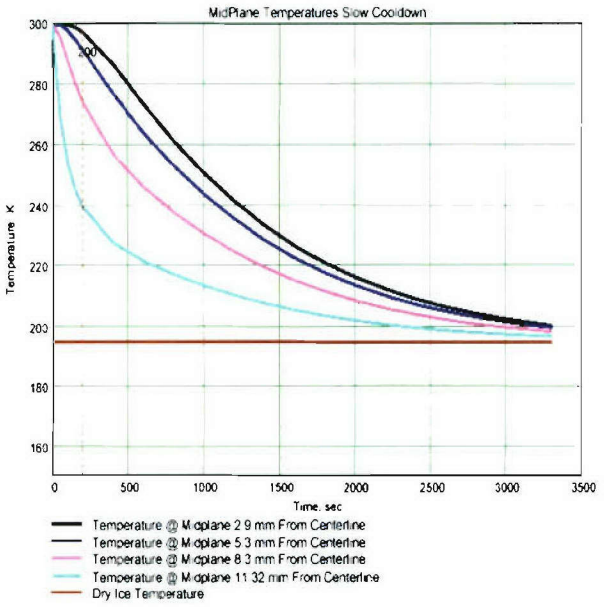


***Fig. 5-8. Model of capacitor pad cooling by packing in dry ice***

Figure 5-7 shows the temperature as a function of time of a capacitor pad immersed in liquid nitrogen. Figure 5-8 shows the same capacitor pad packed in dry ice ($CO_2$) to provide a slower cool down rate. The results show that the difference in temperature from the center to the outer layers is much less for a slower cooldown rate.

The centerline curves of Figs. 5-7 and 5-8 can be compared with actual measurements made of a capacitor pad being cooled down. To make the measurements, a thermocouple was inserted into the windings as shown in Fig. 5-9.

***Fig. 5-9. Capacitor pad with inserted thermocouple for cooldown measurements***

The data from the cool down measurements is shown in Fig. 5-10. Note that there are three curves shown in Fig. 5-9. The "fast" curve is the measurement from a pad

immersed in $LN_2$. The "2-step" curve is the measurement from a pad that was first packed in dry ice. Once the center of the pad reached dry ice temperature, it was then immersed in $LN_2$. The "vapor cool" curve resulted from a third way of cooling that is described later.

Comparing the fast curve of Fig. 5-10 with the midplane-centerline curve of Fig. 5-8 shows good agreement. For example both curves reach 200° at about 100 seconds and 150° at about 1500 seconds. Thus we can assume that the model is a fairly accurate representation of the cooldown of the pad. In the same way, the 2.9mm curve of Fig. 5-8 can be compared to the first part of the "2-step" curve of Fig. 5-10. While the agreement is not quite as good (possibly because of the difficulty of getting good thermal contact between the dry ice and the capacitor pad), the model shows the reduced temperature differences resulting from slower cooling. Indeed, the model shows faster cooling than was actually measured so the reduction in delta T should be even greater for the slower cooling actually measured.

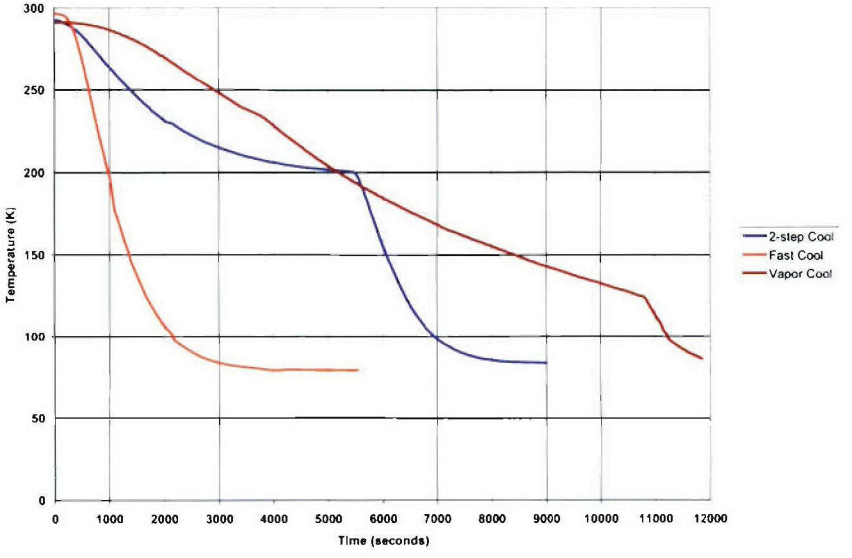


***Fig. 5-10. Measured cool down of capacitor pads***

Based on these results, a method to provide a more constant but slow cooling rate was devised. A small amount of $LN_2$ was placed in a large Dewar. The capacitor to be cooled was suspended above the Dewar and slowly lowered into the Dewar. A programmable stepper motor was used to control the rate of descent into the Dewar. Measurement of the cool down using this method is shown in the "vapor cool" curve of Fig. 5-10. Figure 5-11 shows a dynamic vapor cooled system. While this method of cooling was not modeled, it is anticipated that the delta T across the pad would be considerably small.


*Fig. 5-11. Dynamic cool down system*

# 6 Cryocap Test Facilities

## *6.1 GA Test Facilities*

GA has built a cryo-capacitor test facility that can do dc and charge/discharge testing of capacitors. GA also has ball-plane test equipment to conduct dielectric breakdown strength testing of thin films.

The capacitor test facility is shown in Fig. 6-1. The test area is enclosed by a fence for safety. Control and monitoring equipment is located outside the fence for convenience. The key components of the test facility are the high voltage power supply, the Programmable Logic Comtroller (PLC), the data acquisition system (DAS), the high voltage switch, the load, the liquid nitrogen Dewar, and the pressure vessel. Each of these is described in more detail below.

***Fig. 6-1. The capacitor test facility at GA. The control and monitoring are located just outside the left edge of the photograph***

Figure 6-2 is a simplified schematic diagram of the test facility showing the connections of the power supply, high power switch and diagnostics.

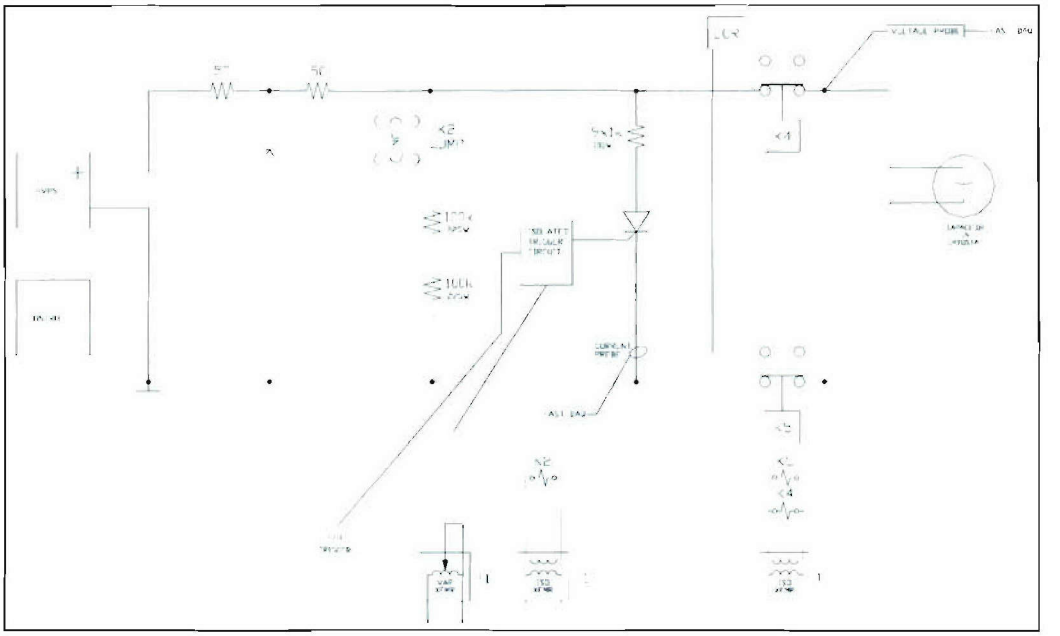

*Fig. 6-2. Simplified schematic diagram of the test facility*

### *6.1.1 High Voltage Power Supply*

The high voltage power supply (HVPS), shown in Fig. 6-3, is used to charge the capacitor under test. The power supply is a Spellman MODEL rated at 15 kV and 400 mA. The power supply has automatic crossover so that it can be set to charge to a predetermined voltage at a constant current. This allows the charge time to be controlled. The power supply can be remotely set, controlled and monitored by the PLC.

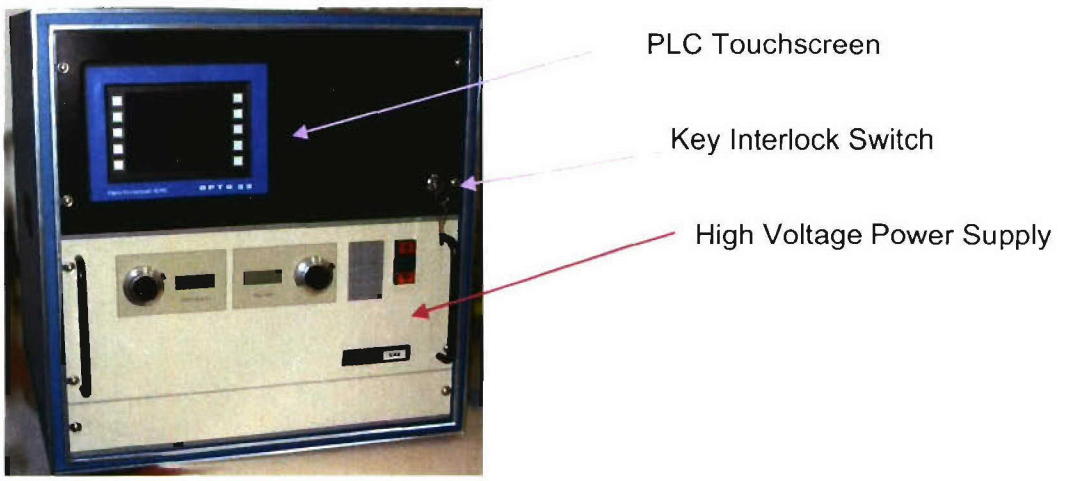


*Fig. 6-3. The high voltage power supply and PLC controller are integrated into a single bench-top cabinet*

### 6.1.2 PLC

The PLC is an OPTO 22 Snap-I/O. Integrated with a touch screen, shown in Fig. 6-3, the PLC provides for control and monitoring of the test stand. Different test scenarios can be programmed into the PLC giving the test stand good versatility.

### 6.1.3 Data Acquisition System (DAS)

The DAS consists of an HP MODEL LCR bridge and a LeCroy MODEL digital oscilloscope. The LCR bridge is connected to the capacitor terminals using high voltage relays for isolation. During the time that high voltage is applied to the capacitor, the relays are open protecting the LCR meter. When a measurement is desired, the capacitor is discharged and then the relays close connecting the meter to the capacitor. This particular meter does not have remote reading capability so readings have to be taken by hand.

The oscilloscope is used to monitor and record voltages and currents associated with the capacitor tests. A Tektronix MODEL high voltage probe is used to record the voltage on the capacitor. A Pearson MODEL current transformer is used to record the capacitor discharge current.

The LCR meter and oscilloscope are shown in Fig. 6-4.

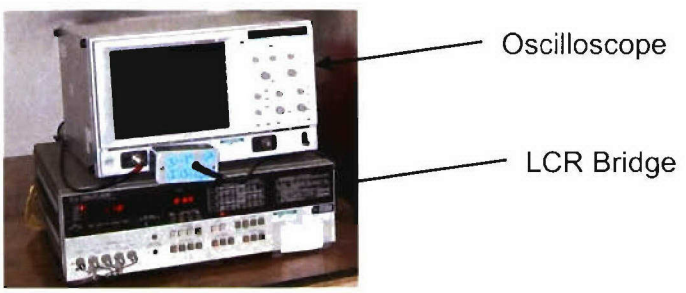


***Fig. 6-4. The data acquisition system consisting of an oscilloscope and a LCR bridge***

### 6.1.4 High Voltage Switch

The high voltage switch, shown in Fig. 6-5, is an ABB MODEL. The switch is a stack of 6 silicon-controlled-rectifiers (SCRs) providing a voltage rating of 15kV and a current rating of 3.7kA. The switch was sized to be able to handle the testing of a 100 kJ capacitor. Fiber optic triggering isolates the switch from the controls. A portion of the Pearson current transformer, used to measure the discharge current, is also visible in the figure.

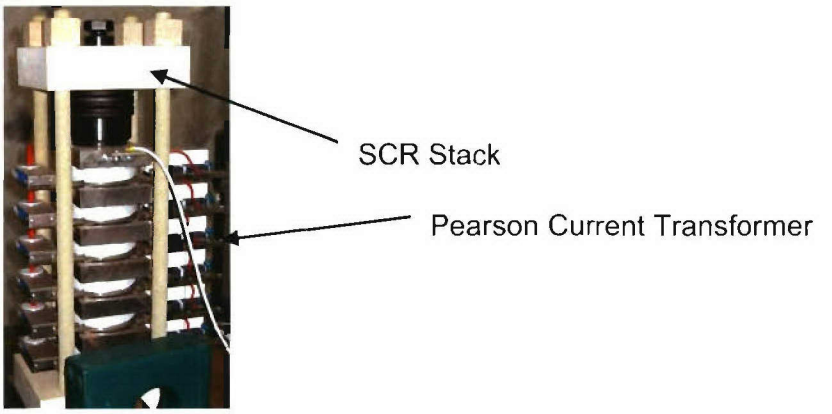


*Fig. 6-5. ABB high power switch*

### *6.1.5 Load*

When the high voltage switch closes, it discharges the capacitor into the load. The load consists of an array of high power carbon rod resistors. Up to 9 resistors can be paralleled in the load to provide variability in the power and resistance value. In Fig. 6-6, shows the 3 resistors that are installed.

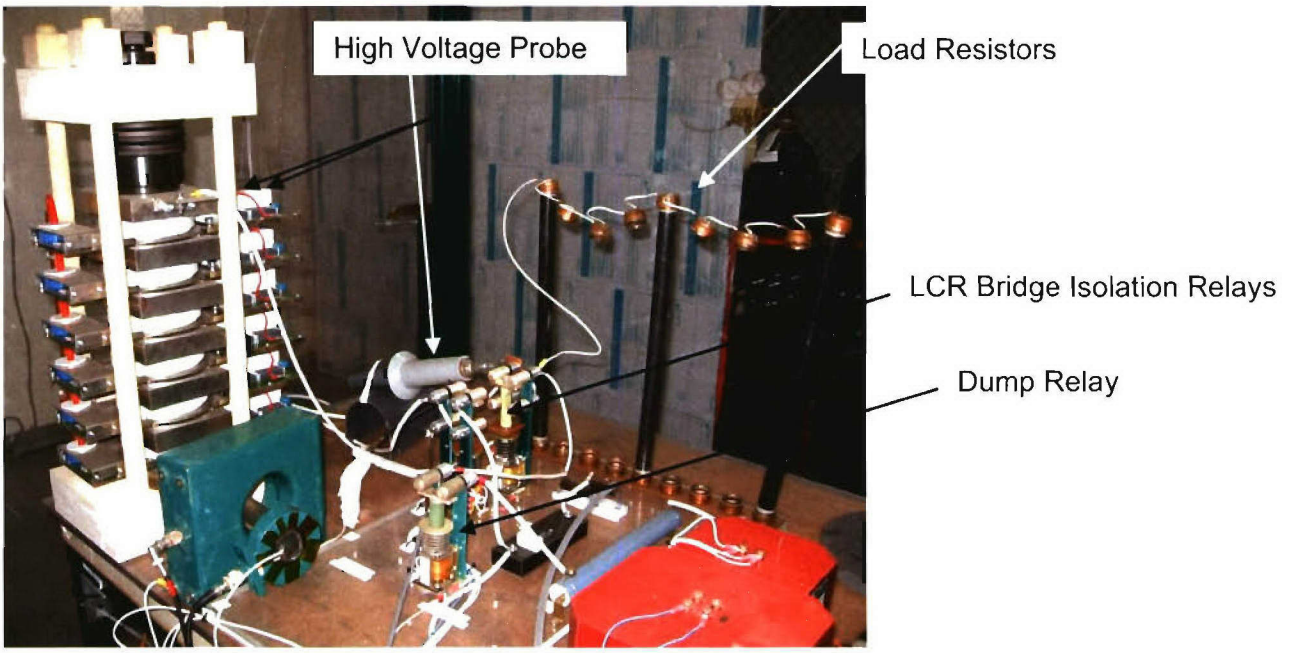


*Fig. 6-6. The high voltage circuitry showing the load resistors*

### *6.1.6 Liquid Nitrogen Dewar*

The test stand includes two Dewars. The large one is used for the pressurized capacitor testing and the smaller one is used for testing capacitors at atmospheric pressure. Figure 6-7 shows the larger Dewar with the pressure vessel installed for testing.

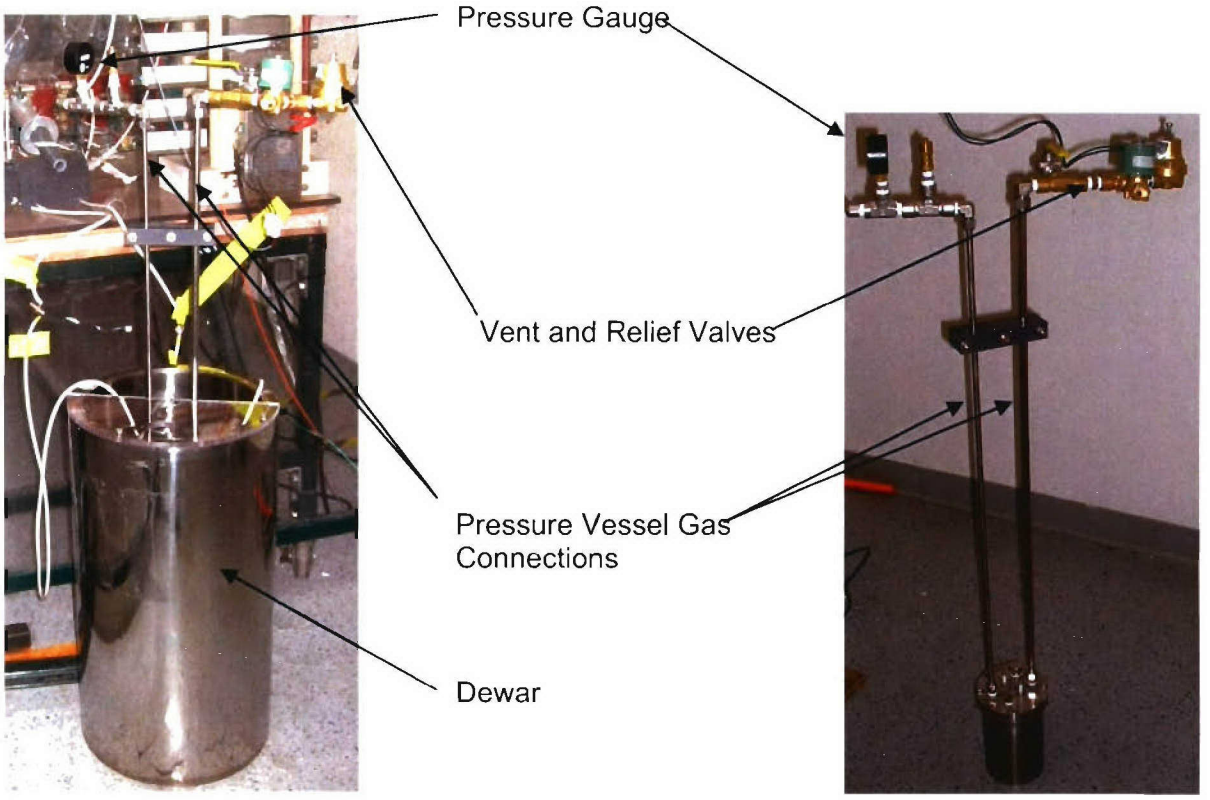


*Fig. 6-7. Large Dewar and pressure vessel*

### *6.1.7 Pressure Vessel*

The pressure vessel shown in Fig. 6-8 was designed by GA-ESI to allow testing of capacitor pads in different environments including pressurized $LN_2$. The vessel is rated for operation at up to 3 bar and includes feedthroughs for filling, venting, temperature and pressure gauges, and liquid level sensors. Ceramic feedthrough bushings provide electrical connections at up to 15 kV.

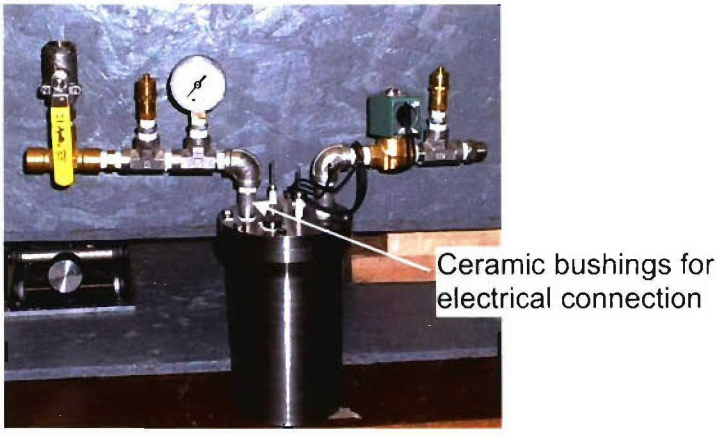


*Fig. 6-8. Pressure vessel*

### *6.1.8 Ball-Plane Test Facility*

The ball-plane test facility is used for rapid screening of materials. Its simple construction and ease of use permit a large number of samples to be tested under the same conditions in a minimum amount of time. The sample to be tested is placed between two electrodes; one a 2.25-in. diameter sphere and the other a flat plate. High voltage is then applied to the sphere using a hi-pot test unit. The voltage is increased steadily until the sample breaks down. The voltage at which this break down occurs is recorded on an oscilloscope. This break down voltage is an indicator of the relative dielectric strength of the material.

Figure 6-9 shows the ball-plane test device. Figure 6-10 is a photograph of the hi-pot test device. Figure 6-11 shows the entire system assembled and ready to test. Room temperature testing can be done quickly. For cyrogenic testing, the ball-plane device is placed in a small dewar full of liquid nitrogen as shown in Fig. 6-12. The small size of the device allows for rapid cooling and quick turn-around of samples.

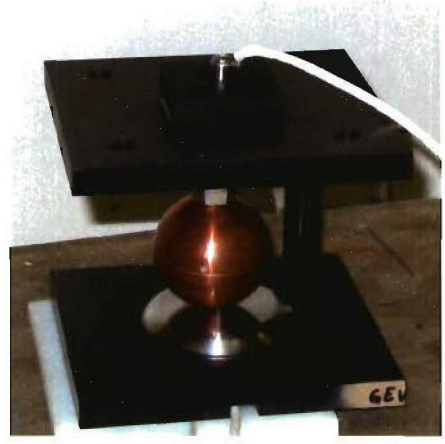

***Fig. 6-9. The ball-plane test rig***

***Fig. 6-10. Hi-pot test device***


*Fig. 6-11. Ball plane test assembly*

*Fig. 6-12. Ball-plane test rig installed into a small dewar*

## 6.2 ESI Test Facilities

### 6.2.1 Stamp Capacitor Testing

Using the ESI standard room temperature stamp capacitor testing technique for testing in cryogenic conditions resulted in broken glass slides due to the pressure being used to hold them together. A typical broken slide can be seen in Fig. 6-13

*Fig. 6-13. Broken glass slide*

To overcome this problem, the glass slides, which are normally used for stamp capacitor testing, were replaced with thicker polycarbonate slides. These thicker slides can be seen in Fig. 6-14 in a sideways configuration. ESI had several dozen of these custom slides manufactured to the dimension and thickness levels that were deemed necessary for successful cryogenic testing.

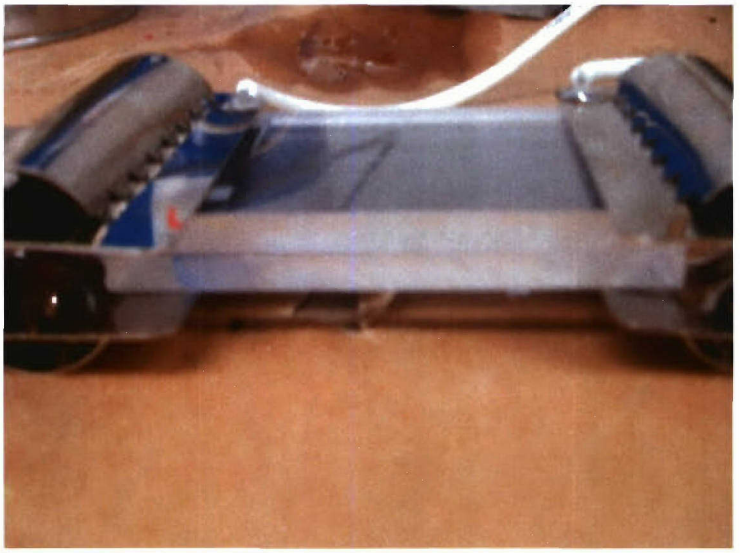

***Fig. 6-14. Stamp capacitor with polycarbonate slides***

The stamp capacitors were clamped in such a way as to keep constant pressure of approximately 300 psi on the dielectric. This insures that test results will be consistent from batch. to batch. Figure 6-15 shows the clamps used to hold the stamp capacitor and the open top dewar used for testing. The open top dewar was chosen because it allowed for the quick loading and removal of stamp capacitors from the test set.

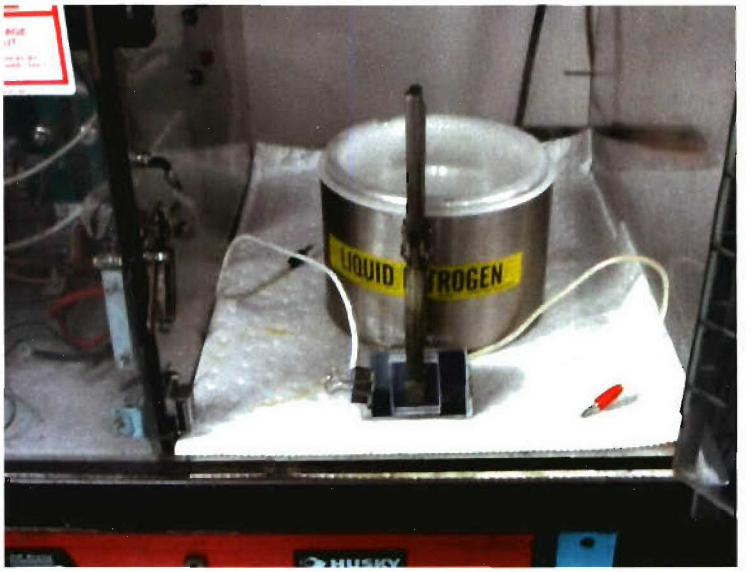


***Fig. 6-15. Stamp capacitor clamping and test dewar***


*Fig. 6-16. Stamp capacitor tester*

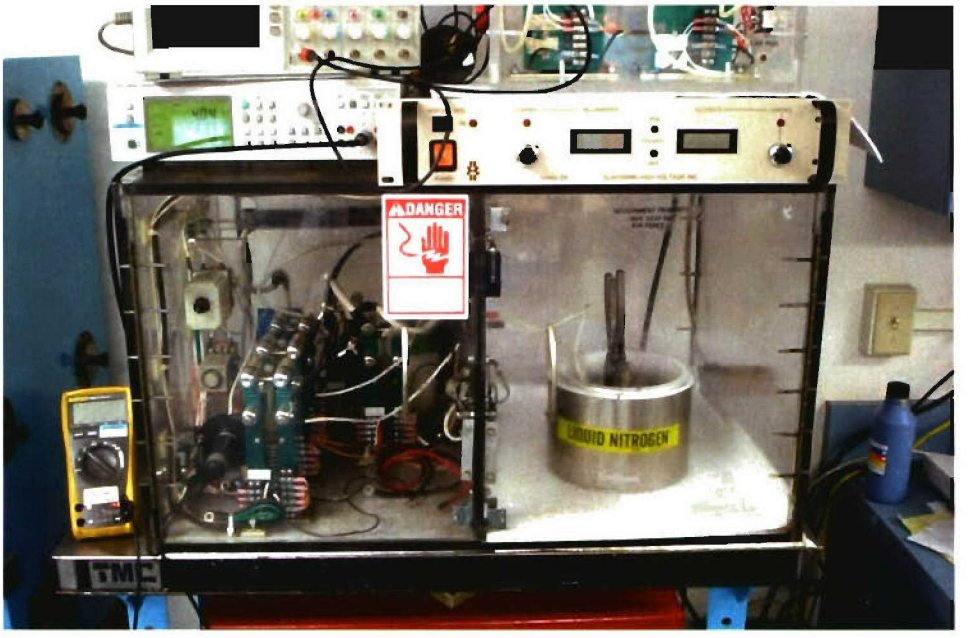


*Fig. 6-17. Stamp capacitor test setup with dewar for cryogenic testing*

### 6.2.2 *Model Size Capacitor Testing*

ESI has several large test chambers available for testing at cryogenic temperatures. Pictured in **Error! Reference source not found.**6-18 is one of the test cells with a supply dewar and cryostat after testing. No modification was needed to the test cell other than the addition of the supply dewar.

***Fig. 6-18. Test cells with a supply dewar and cryostat after testing***

## 6.3 *MTech Test Facilities*

### 6.3.1 *Stamp Capacitor Fabrication*

MTECH has fabricated a special holder, shown in Fig. 6-19, used to mask dielectric films to form a stamp capacitor. A typical metallized film holds three individual capacitors, as shown in Fig. 6-20.

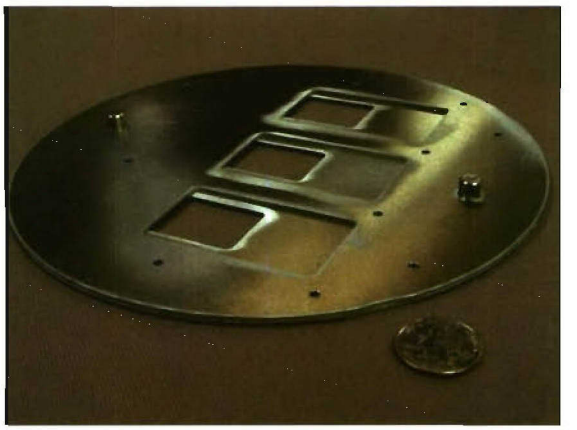

***Fig. 6-19. Special holder fabricated by MTECH for metallization of dielectric materials***

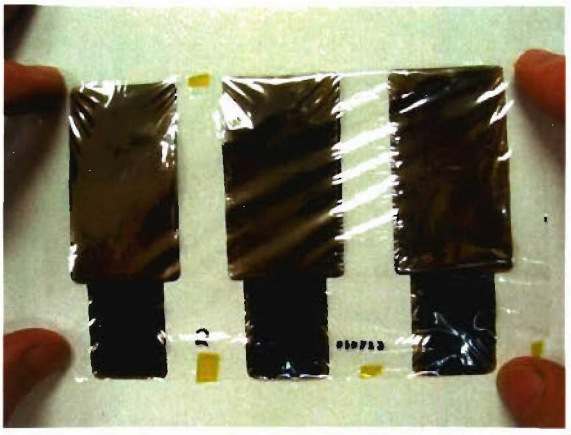

***Fig. 6-20. Metallized film showing three individual stamp capacitors***

The dielectric films are supplied by General Atomics or MTECH. MTECH mounts the films in the holders shown in Fig. 6-19 and sends them to Albany NanoTech (ANT) for metallization. ANT's equipment, shown in Fig. 6-21, consists of a Varian 980 E-Beam Evaporator, which can evaporate a variety of metals, including aluminum, which was used to metallize the films. The evaporator is calibrated to deposit metallization layers with thicknesses from 20 Å to 5 µm. ANT also owns a Scanning Electron Microscope (SEM) and a Focused Ion Beam (FIB) imaging system, which were used to analyze the thicknesses of both the polymer film and the deposited metal layers. An example of the images produced is shown in Fig. 6-22.

***Fig. 6-21. Albany NanoTech's metal evaporation equipment, which can deposit metallization thickness between 20 Å and 5 µm***

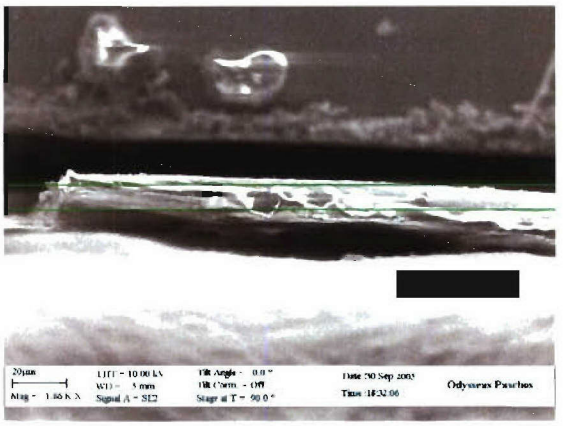

*Fig. 6-22. SEM image of a cross section of the metallized film*

The metallized films are tested by MTECH using specially fabricated film holders, similar to those shown in Fig. 6-23.

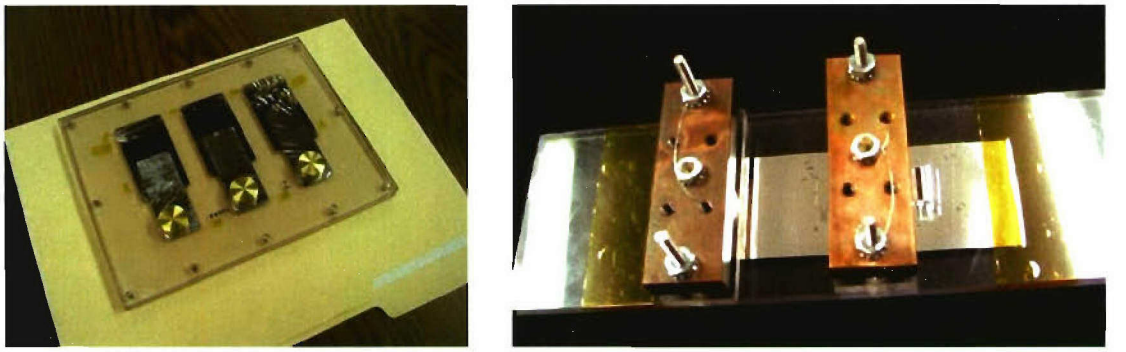

*Fig. 6-23. Two of the test fixtures used by MTECH to test the breakdown voltages, capacitances, and dissipation factors of the metallized films*

### *6.3.2 Stamp Testing*

The samples are tested in MTECH's high-voltage capacitor test unit, shown in Fig. 6-24. The test setup consists of a large clear polycarbonate housing for the high-voltage equipment, and a smaller insulated enclosure containing the control electronics. The voltages are scanned and data is recorded and logged by a computer using software developed at MTECH. Relays are used to isolate the user from the high voltage, and to reduce leakage from the capacitor through the measurement equipment (probes, etc.).

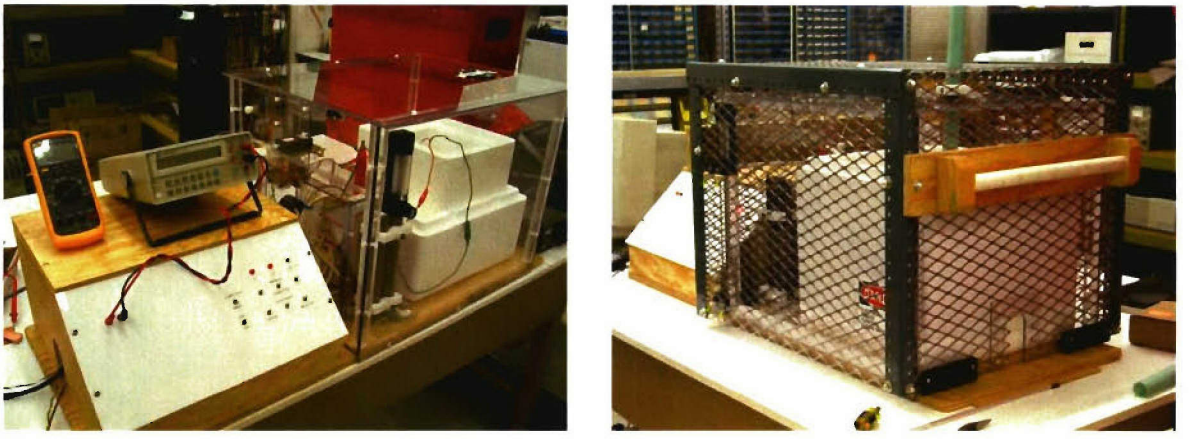

***Fig. 6-24. High-voltage test equipment built at MTECH to test voltage breakdown of the stamp capacitors***

The high-voltage box also provides for a dry nitrogen gas environment. The dry nitrogen atmosphere inside the box is used to minimize frost formation on the DUT and its leads during cryogenic testing. All tests are performed with the capacitor housed in a Styrofoam container, which can be filled with liquid nitrogen via a G-10 fill pipe.

Other parameters, such as capacitance, dissipation factor (D), and equivalent series resistance (ESR) were measured using an HP 4284A LCR meter. This precision meter can scan frequencies from 20 Hz to 1 MHz. The device under test is connected to the meter using a special test fixture, fabricated at MTECH and consisting of four 1-meter long Teflon-coated, single-conductor shielded cables. These cables are terminated at one end with BNC connectors, and are soldered at the other end to one of two copper blocks. This allows for very precise, four-point probe measurements. The shields of all four cables are stripped back and are soldered to a copper grounding sheet, mounted on an insulator, which provides the ground plane. The shielding also helps increase noise immunity during testing. The test setup, including the Dewar and the LCR meter, is shown in Fig. 6-25.

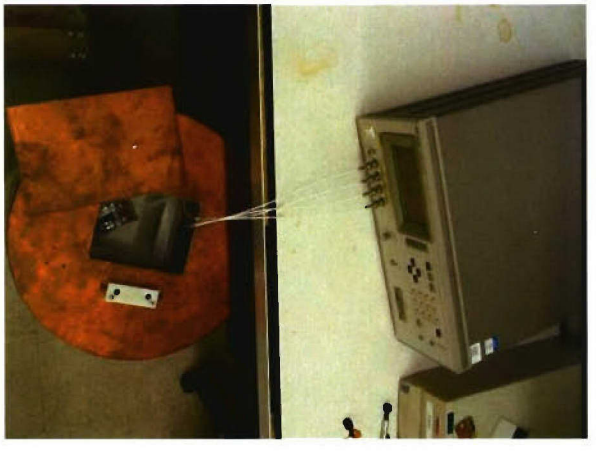

***Fig. 6-25. Top view of the LCR meter setup used to measure factors such as capacitance and dissipation factor***

# 7 Cryocap Testing Results

## *7.1 GA Testing*

### *7.1.1 COTS Capacitor Testing*

Initial test efforts in the program focused on the testing of COTS capacitors. The purpose of these tests was to:

1. Determine if operation at cryogenic temperatures could increase the energy density of existing capacitor materials.
2. Determine if COTS designs were suitable for operation at cryogenic temperatures.
3. Develop test methodologies for testing of future designs.

Several types of tests were conducted over the course of the program. These tests and the results are presented in the following sections.

Preliminary tests were conducted with a power supply limited to an output current of about 6 mA. This limited output current meant that the charge time would be much longer than desired for testing. However, it was felt that relative measurements could be made initially to compare room temperature performance to cold performance under the same charge conditions.

Testing was also performed with an improved ower supply that allowed rapid charging of the capacitors. This permitted conventional test methods in which the capacitor is charged to a given voltage in five seconds and then held at that voltage for sixty seconds. It is then discharged and the capacitance measured. The cycle is then repeated at a higher voltage until failure. The initial charge voltage was the capacitor's rated voltage and failure was defined as a 5% loss of capacitance. This test method is preferred because it uses a quantifiable determination of failure and it more closely represents the conditions under which a capacitor would actually be used.

#### *7.1.1.1 Charge to Failure Tests*

These tests were conducted by charging the capacitors at a constant rate until the clearing losses were great enough to change the constant-charge voltage slope. The voltage at which the slope changes is defined as the failure voltage.

Figure 7-1 shows the typical data obtained from this test. In this figure, the red colored lines are the data from capacitors tested at room temperature. The blue colored lines are the capacitors tested at cryogenic temperature. The test was conducted using a constant-current power supply. Charging a capacitor at constant current results in a linear increase in voltage that is seen during the initial part of the test. As the voltage increases, the dielectric begins to fail and clearing events begin to take place. At some

point the clearing rate exceeds the capacity of the power supply to charge the capacitor and the slope changes. This is the point that is defined as the failure point indicated by the arrows in Fig. 7-1.

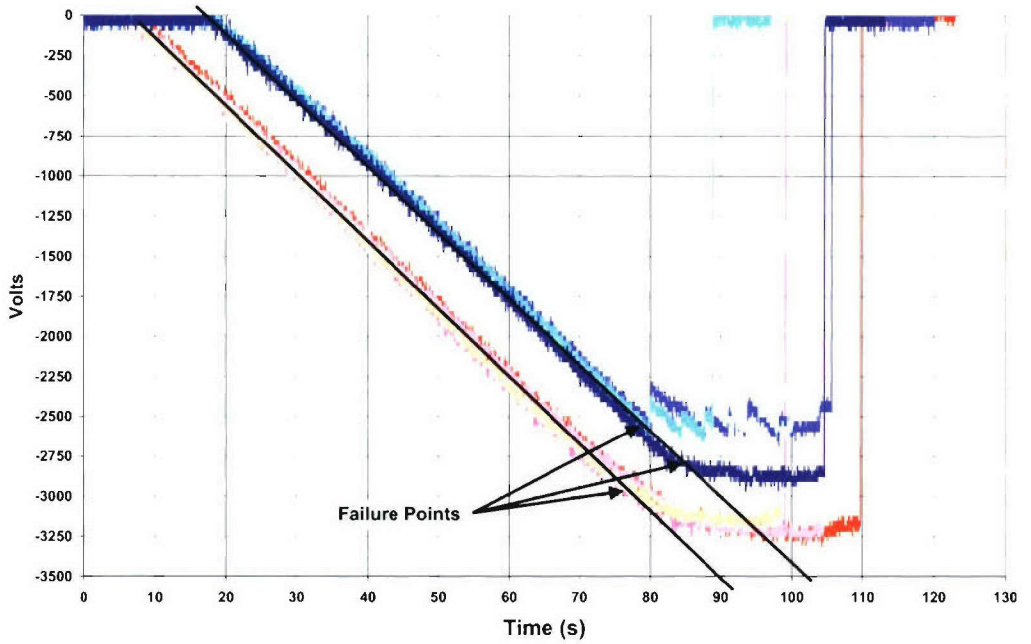


***Fig. 7-1. Typical charge to failure waveform***

It must be noted here that because of the different values of capacitance and the limitations of the power supply available at the time, the test conditions from one model to the next were not identical. A smaller value capacitor will have a higher charge rate (dV/dt) than a larger value capacitance. The time a capacitor spends at high voltage can significantly affect its lifetime. The ideal operation for this type of capacitor is to charge as quickly as possible and then discharge immediately. Therefore it is reasonable to think that the slower dV/dt may result in a higher failure voltage than would be observed at a higher charge rate. Table 7-1 is a list of the capacitors tested by this method including their ratings and materials.

**Table 7-1**
**Capacitors Tested Using the Charge-to-Failure Method**

| Model | 30922 | 30932 | 30786 | 30937 | 30957 | 30956 |
|---|---|---|---|---|---|---|
| Ratings | 35uF, 5.2kV | 100uF, 2.2kV | 32uF, 5.5kV | 115uF, 2.3kV | 115uF, 2.3kV | 115uF, 2.2kV |
| Material | MHPPL, 11μm, $e_r$=2.2 | MPPL, 4.5μm, $e_r$=2.2 | MP, 8μm, $e_r$=4.5 PET, 12μm, $e_r$=3.2 | MPPL, 4.8μm, $e_r$=2.2 | MPPL, 4.8μm, $e_r$=2.2 | MPPL, 4.8μm, $e_r$=2.2 |
| Impregnant | Rapeseed Oil | Rapeseed Oil | Castor Oil | Rapeseed Oil | Rapeseed Oil | None (LN2) |

Since different capacitors have different dielectrics of different thickness, it is useful for comparison purposes to convert the failure voltage to the energy density in the dielectric. Note that this is different than the energy density of the capacitor which must include the packing factor and derating for lifetime considerations.

Voltage can be converted to an equivalent dielectric energy density by the equation:

$$ED = 0.5\varepsilon_r\varepsilon_0\left(\frac{V}{t}\right)^2 \cdot 10^6$$

where:

ED is the energy density of the dielectric in J/cc
$\varepsilon_r$ is the relative dielectric constant (unitless)
$\varepsilon_0$ is the permittivity of free space (8.85 x $10^{-12}$ coul$^2$/n·m$^2$)
V is the voltage across the dielectric
t is the dielectric thickness in microns
$10^6$ is for units conversion

#### *7.1.1.1.1 Charge to Failure Test Results*

The results of the various models of capacitors are compared in Fig. 7-2.

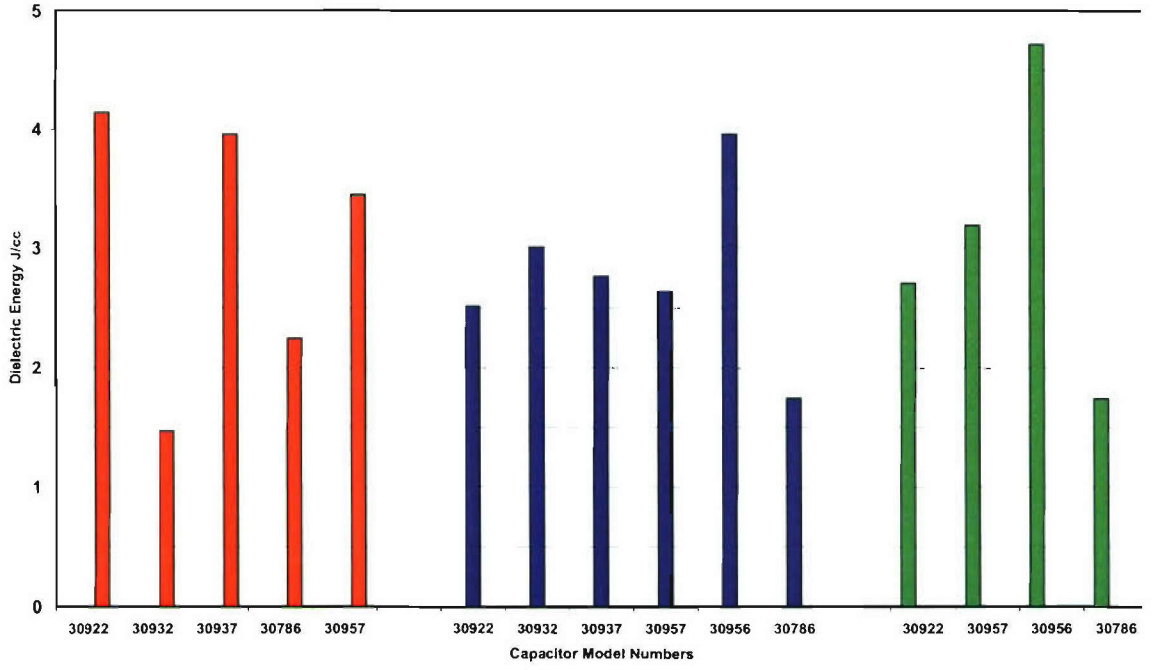


***Fig. 7-2. Compares the results of this testing for various models of COTS capacitors***

Several conclusions can be drawn from the data shown in Fig. 7-2 :

1. COTS capacitors will not obtain the desired energy density.

   When packing factor and lifetime derating are taken into account, a dielectric energy density of 10-15 J/cc or more is required. The best obtained in the testing was just slightly over 4.5 J/cc. Note that the model 30956 is technically not a COTS capacitor since it is not impregnated. However, it is the same construction as the model 30957. Capacitors with oil impregnation all fared worse with the exception of a model 30932. This, along with autopsy results, leads to the second conclusion.

2. Oil impregnation is not desirable for cryogenic capacitors.

   The model 30956 is the same construction as the model 30957 with the exception that the 30956 is not impregnated. The non-impregnated model 30956 capacitors at cryogenic temperatures outperform the model 30957 capacitors at both cryogenic and room temperatures. Tests on the oils used in capacitor impregnation showed that they become solid at 77 K. It is hypothesized that the solidification of the oil, coupled with the thermal contraction of the dielectric material, causes damage to the dielectric film. It is also possible that the oil freezes into a crystalline structure resulting in sharp points that may damage the film.

3. A cylindrical geometry is better for cryogenic operation.

   The model 30932, a cylindrical geometry, fared better than the other models which all have an oval geometry. The oval capacitors are manufactured as cylinders and then flattened to yield an oval geometry. This may lead to much higher mechanical stresses at certain points in the dielectric films. These stress points would then be further aggravated by the thermal contraction, especially if the impregnant were a solid.

   It may be noticed that even though a cylindrical geometry is better, later testing due to implementation of dynamic cool down was done with oval capacitors. This was because of the easy availability of oval capacitors. Even though the cylindrical capacitor fared better than the oval capacitors when compared to room temperature operation, it still did not perform adequately at cryogenic temperatures and, indeed, did not perform as well as the oval 30956. Therefore it was decided that further testing could be done on oval capacitors with the knowledge that any improvements could possibly be further helped by using a cylindrical geometry.

4. A (slow) cooling process is better than a fast one.

   Comparing the data for capacitors cooled rapidly by immersion into $LN_2$ with capacitors cooled in two steps to keep the dT/dt smaller it can be seen that there was some improvement in three of four cases. In the fourth case, the results were about the same.

5. Wrinkling

Examination of failed capacitors indicated significant wrinkling of the film. An example is shown in Fig. 7-3. This could lead to degraded performance due to localized enhancement of the electric field or weakening of the film due to mechanical stress. Several theories were put forth as to the possible cause of this wrinkling including:

- the high rate of change in temperature (high dT/dt)
- the long charge time and the extended time of clearing
- leakage of $LN_2$ into the case

***Fig. 7-3. Wrinkling of the capacitor film***

A series of tests were conducted on a model 30957 capacitor to try and determine the cause of the wrinkling.

**Table 7-2**
**Wrinkling Observations**

| Conditions | Wrinkling |
|---|---|
| No cooling – No charge | None |
| Fast cooling – No charge | Light to moderate |
| Two-step cooling – No charge | Light |
| Fast cooling – Charge to failure | Severe |
| Two-step cooling – Charge to failure | Moderate |
| Dynamic Cooling – No Charge | None |
| Dynamic Cooling – Charge | None |

The results though not entire conclusive, indicate that slow cooling may be preferable. They also indicate that allowing the capacitor to endure constant clearing (charge to failure) has an affect. Tests continued with the slow cooling method. Automation of the continuous cooling method to minimize any possible effects from high dT/dt was also done.

The 1-kJ capacitor will be manufactured based on cylindrical windings on hard core for purposes of the demonstration. This minimizes the problems associated with the brittleness of PMMA as well as thermo-mechanical stresses from cryo-cooling.

#### *7.1.1.2 Step-Charge Testing*

The acquisition of a new power supply allowed rapid charging of the capacitors. This made possible the use of a more conventional test method in which the capacitor is charged to a voltage and held for a given time. It is then discharged and the capacitance is measured. The voltage is then raised by 100 V and the test repeated until the capacitor fails. The initial voltage used for each test was the capacitor's rated voltage. The hold time at voltage was either 60 seconds or 10 seconds depending on the test. A typical capacitor charging waveform is shown in **Error! Reference source not found.** 7-4.

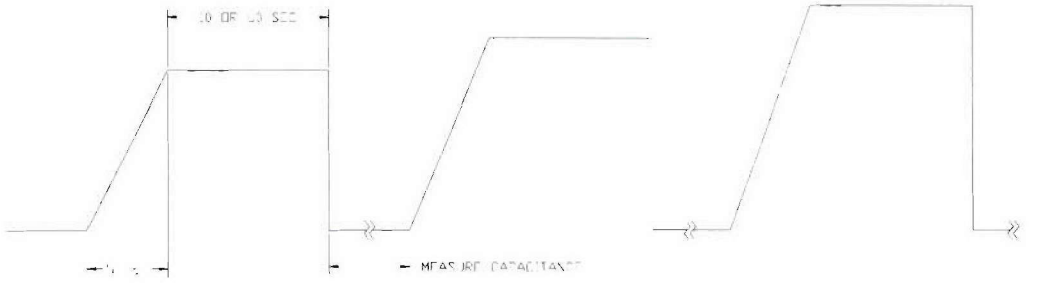

***Fig. 7-4. Typical step-charge voltage waveform***

Two versions of this test were conducted. The first compared oil filled model 30957 capacitors at room temperature and at cryogenic temperatures. (Note that one of the capacitors tested was a model 30937 which is the same as the 30957 except for the external lead configuration). The second version was conducted on non-impregnated model 30956 capacitors. All these capacitors have a voltage rating of 2.3 kV.

##### *7.1.1.2.1 Step-Charge Testing Results*

A total of ten oil filled capacitors were tested: three at room temperature, three after being fast cooled, and four after being slow cooled. The slow cool method for these tests was the continuous cooling method. The results for oil filled capacitors are shown in Fig. 7-5. Each of the slow cooled and fast cooled capacitors had one sample where no improvement was seen while the room temperature capacitors had one sample that showed the greatest improvement. This scatter of the data makes it difficult to draw

conclusions. However, even if some improvement is granted, it is not enough to provide confidence that COTS capacitors will obtain the energy density goal.

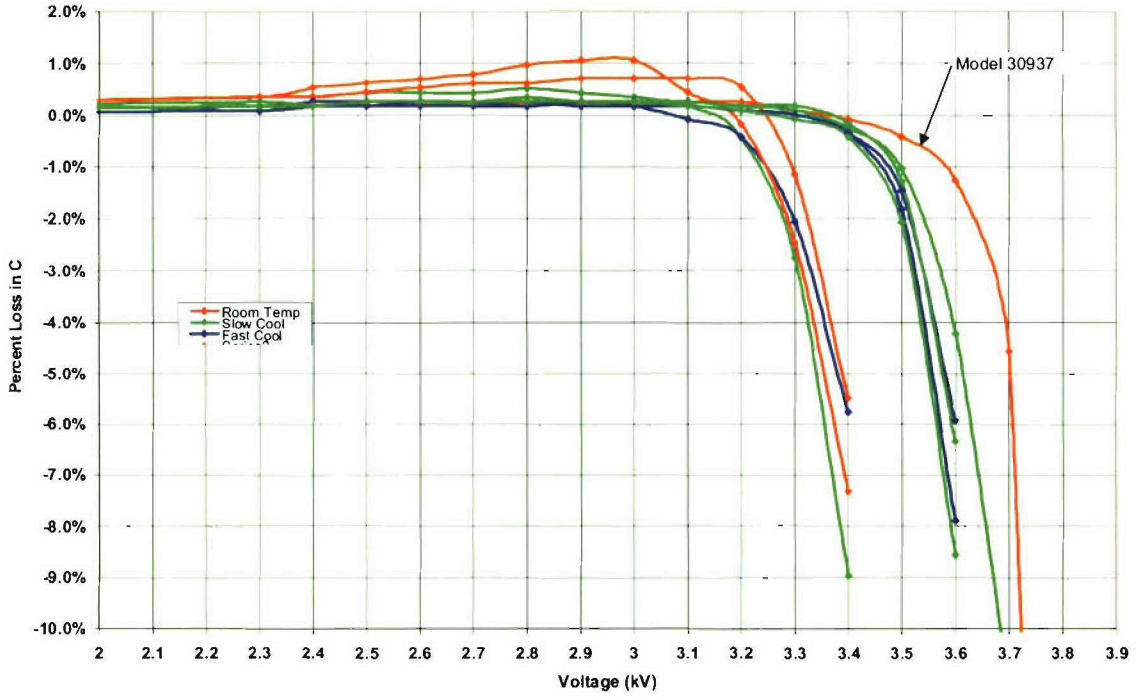


***Fig. 7-5. Step-charge test results for oil filled capacitors***

The increase in capacitance seen for the room temperature capacitors is normal and is due to electrostatic forces causing the windings to become tighter. This is not seen for the cooled capacitors possibly because the oil has frozen and cannot be squeezed out from between the windings when the charge is applied.

A total of seven, non-impregnated model 30956 capacitors were also tested using the step charge method. Two configurations of this capacitor were tested. The first configuration was not sealed in the can and did not undergo any vacuum-baking process. The second configuration used capacitors that underwent the same manufacturing processes as a normal capacitor except that they were not impregnated. They were, however, subjected to a vacuum-baking process.

Initial tests were conducted with the capacitors in the unsealed cans. The first capacitor was fast cooled and a 60 second hold time was used. After the catastrophic failure of this capacitor, it was thought that the can and/or outer insulation wrapping may have been impeding the flow of $LN_2$ into the capacitor pad so tests were done with just the capacitor pad. Again the pads had not undergone any factory drying process but they were baked out in an oven at 65°C for 12–24 hours before testing. Both fast cool and vapor cool methods were tested and both also failed catastrophically.

After consultation with ESI, it was decided to reduce the hold time from 60 seconds to 10 seconds. If the failures were related to gas generation, the shorter hold time would result in less gas and hence higher failure voltages. The capacitor pad tested with the

10-second hold time did not fail catastrophically, but by a sudden drop in capacitance of greater than 5%. Typically, a gradual decrease in capacitance is seen.

Testing of the factory dried, sealed-can, capacitors was next. The sealed cans were vapor cooled. During the vapor cooling process, once the cans were completely immersed in the $LN_2$ vapor, the can lids were punctured using a can opener. Four punctures were made in each lid. At the completion of the vapor cooling cycle the can to be tested was transferred to the test dewar. While care was taken to make the transfer quickly, it is possible that air, and therefore moisture, was able to enter the can. However, it is doubtful that this moisture could pass the outer insulation wrap and reach the pad.

These three capacitors all also failed catastrophically with no change in capacitance beforehand. A failed capacitor is shown in Fig. 7-6. The punctures in the lid to allow the entrance of $LN_2$ are also visible in this photograph. Due the catastrophic failure mechanism, additional step-charge testing was not attempted. A summary of the tests and results is shown in 3 below.

One explanation for the catastrophic failures may be that they were caused by a margin flashover. Oil impregnation plays a significant role in providing margin insulation and replacing the oil with nitrogen may reduce the voltage hold-off capability of the margin. Alternatively, the nitrogen may not be completely filling all the edge gaps. It was proved later that the $LN_2$ pressurization provided flashover margins similar to oil.

The step-charge testing on the oil filled capacitors was not consistent due to the scatter in the data, but was sufficient to indicate that oil filled COTS capacitors would not reach the program goal for energy density. With one exception, every non-impregnated capacitor tested by the step-charge method failed catastrophically.

***Fig. 7-6. Catastrophic failure of a Model 30956 capacitor during step-charge testing***

**Table 7-3**
**Step Charge Testing of Model 30956 Non-Impregnated Capacitors**

| Test Configuration | Cooling Method | Hold Time | Failure |
|---|---|---|---|
| In can with open lid | Fast cool | 60 | Catastrophic failure at 3.2 kV |
| Pad only | Fast cool | 60 | Catastrophic failure at 3.3 kV |
| Pad only | Vapor cool | 60 | Catastrophic failure at 3.3 kV |
| Pad only | Vapor cool | 10 | >5% capacitance loss after charge to 3.3 kV |
| Punctured can | Vapor cool | 10 | Catastrophic failure at 3.1 kV |
| Punctured can | Vapor cool | 10 | Catastrophic failure at 3.2 kV |
| Punctured can | Vapor cool | 10 | Catastrophic failure at 3.1 kV |

#### *7.1.1.3 Life Testing*

Typical capacitor design rules indicate a decrease in life when the capacitor is operated at higher voltages. Higher energy density operation will require higher voltage operation and so the effect on life at cryogenic temperatures needs to be found. Towards this end, two types of life tests were conducted on COTS capacitors. The first was a cyclic life test where the capacitor was repeatedly charged and discharged. The second was a dc life test where the capacitor was left charged for extended periods of time. Details of each of these tests are described below.

All cryogenic life testing was performed with non-oil impregnated model 30956 capacitors. The capacitors were not dried prior to testing. The testing was done in the reusable pressure vessel shown in **Error! Reference source not found.** 7-7. The capacitor pad was removed from the can and all external insulation was removed. The pad was then attached to the feedthroughs in the lid of the pressure vessel as shown in **Error! Reference source not found.**-7-8. The lid was then bolted to the canister with a gas tight seal.

*Fig. 7-7. Pressure vessel ready for testing*

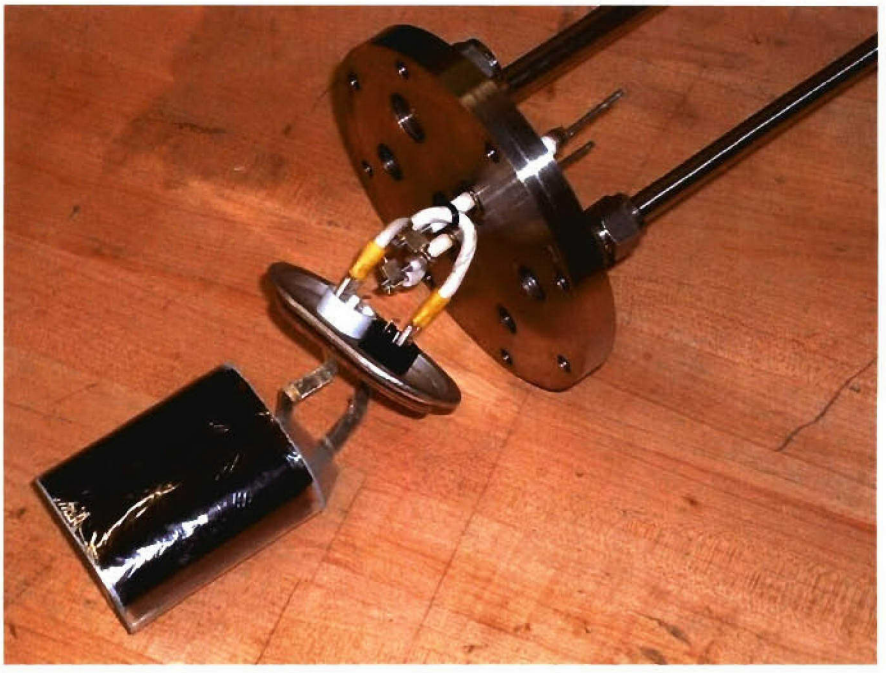

*Fig. 7-8. Capacitor pad suspended from lid of pressure vessel*

Long tubes were attached to the lid to allow the introduction and exhaust of gaseous nitrogen into the pressure vessel. The long tubes allow the entire pressure vessel to be immersed in a dewar of $LN_2$.

Once the capacitor was sealed inside the pressure vessel, it was pressurized with nitrogen gas. The entire assembly was then immersed in a dewar of $LN_2$. As the nitrogen in the pressure vessel began to cool and contract, additional gaseous nitrogen was supplied to maintain the pressure. The gas in the pressure vessel was considered to be liquefied once the flow of gaseous nitrogen ceased. At this point the capacitor would be immersed in liquid nitrogen at the set pressure. The pressure is maintained by keeping a source of pressurized gaseous nitrogen on the pressure vessel. Fig. 7-9 and Fig. 7-10 are diagrams of the electrical and test set-up.

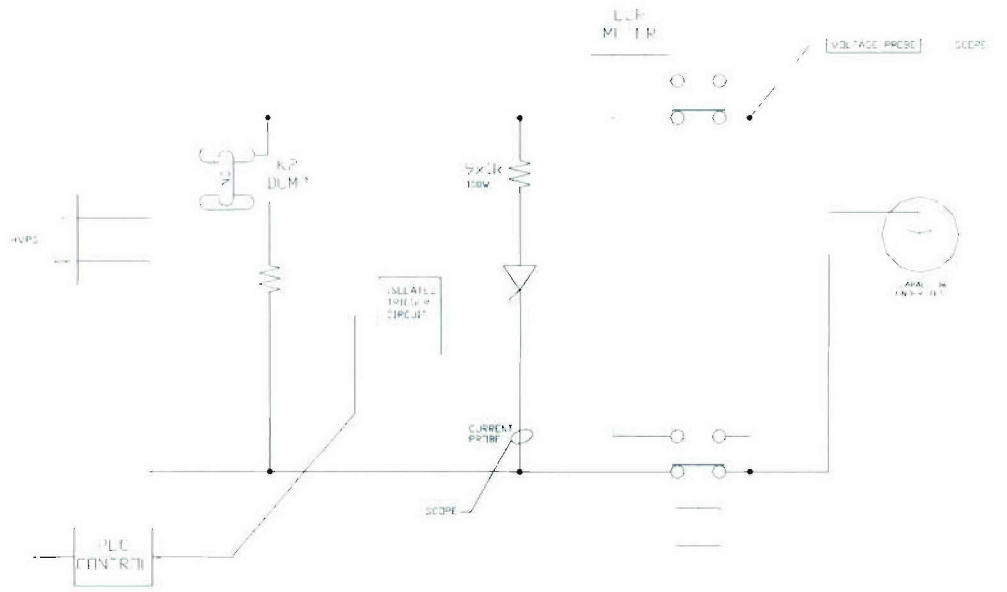


***Fig. 7-9. Simplified electrical diagram***

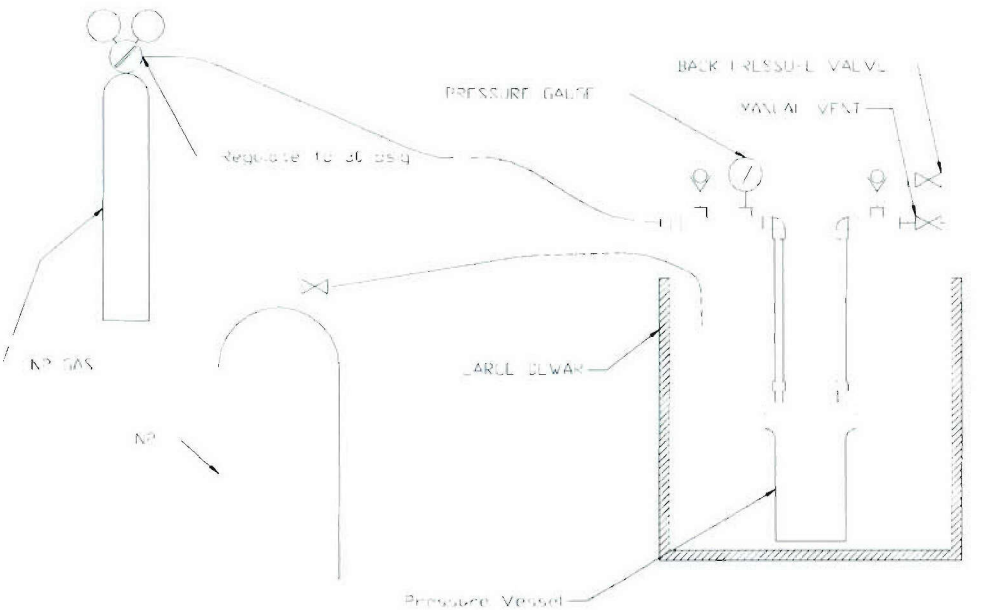


***Fig. 7-10. Test set-up diagram***

A PLC controlled the timing of the charge cycles. The power supply was set to a constant current that would charge the capacitor to either 2.5 kV or 2.9 kV, depending on the test, in approximately 5 seconds. The capacitors were tested at a rate of approximately three charge/discharge cycles per minute. Once the capacitor was charged, it was held at voltage for 10 seconds and then discharged into a 60 ohm resistive load. Five seconds after discharging, the cycle was restarted. Figure 7-11 shows a typical series of charge voltage waveforms. A careful look at the chart will show

that the charge, hold, and dwell times are slightly different from the nominal values. Table 7-4 shows the nominal and measured parameters of the test.

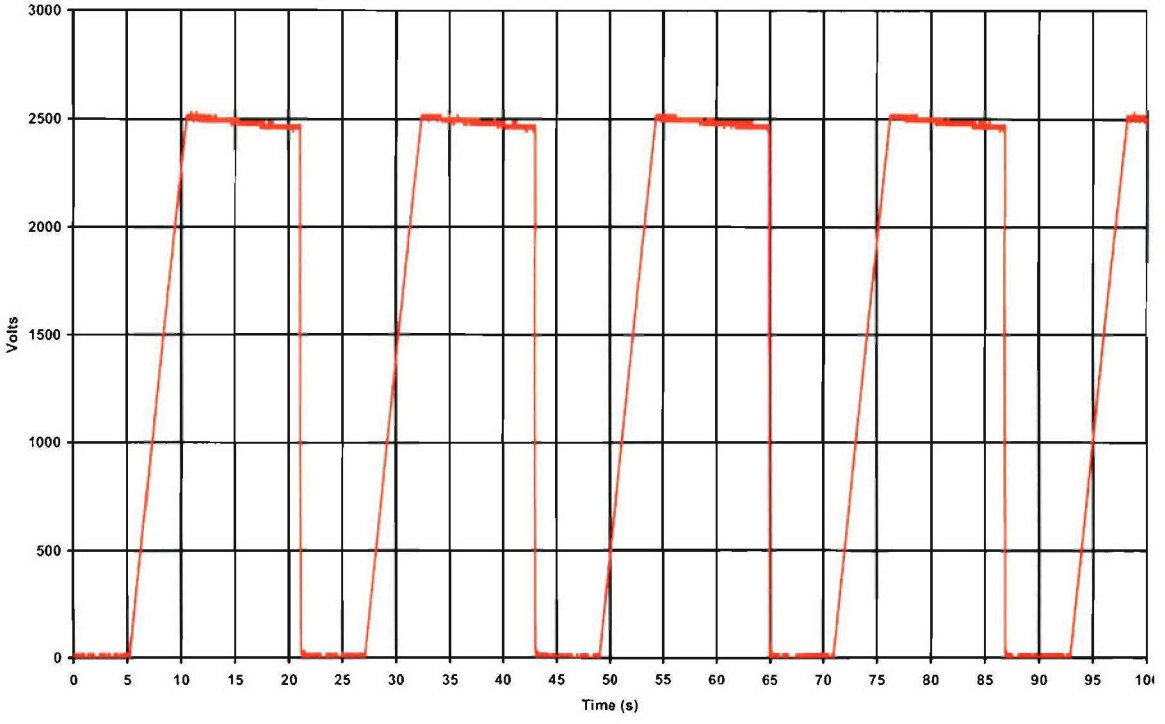


*Fig. 7-11. Charge voltage waveforms*

**Table 7-4**
**Nominal and Measured Parameters**

| Parameter | Nominal Values | Measured Values |
|---|---|---|
| Charge voltage | 2.5 kV | 2.47 kV |
| Charge current | 58 mA | 58 mA |
| Time to charge | 5 sec | 5.6 sec |
| Hold time | 10 sec | 10.1 sec |
| Time between cycles | 5 sec | 6.1 sec |
| Peak discharge current | 42 amps | 43.1 amps |
| Discharge waveform | Exponential decay | Exponential decay |
| Decay time (1/e) | 7.1 ms | 7.19 ms |
| Cycles per minute | 3 | 2.75 |

Figure 7-12 shows the discharge voltage and current waveforms from a typical cycle near the end of the test. Note that the current waveform is not accurate in late time due to droop in the sensor at these long pulse widths. However, the peak current reading is accurate. The figure shows a peak current of 43.1 amps. At the charge voltage of 2,470 V this would require a 57.3 ohm load which is consistent with the nominal 60 ohms of the test setup.

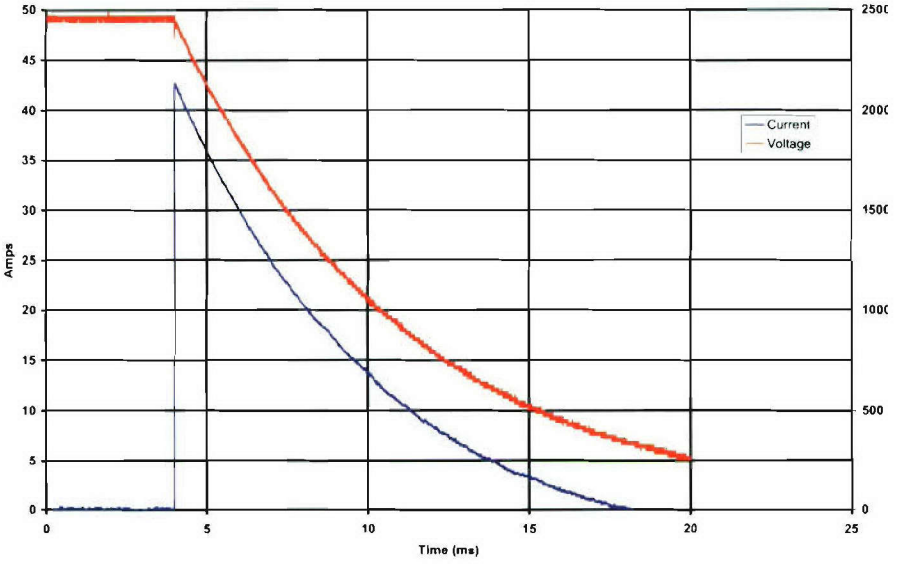


***Fig. 7-12. Discharge voltage and current waveforms***

Periodically during the cycling the tests would be stopped and the capacitance measured using an LCR meter. The measurements were made at 120 Hz. The capacitor would be considered at end-of-life when the capacitance had decreased by 5% from its original value. This is typically expected at around 20,000 cycles of normal operation.

A total of four capacitors were tested at cryogenic temperatures. For comparison, two ESI model 30957 standard oil-filled capacitors were tested at room temperature. The model 30956 and model 30957 are essentially the same construction, only the lead terminations are different. The room-temperature tests were conducted by connecting the capacitors to the test apparatus and applying a large number of charge and discharge cycles. The capacitors were charged to 2.5 kV, slightly in excess of their 2.3 kV rating.

#### *7.1.1.3.1 Life testing Results*

The results of this testing are summarized in Table 7-5 below and in the graph of Fig. 7 13.

**Table 7-5**
**Summary of Cyclic Life Test Data**

| Voltage | Temperature | Pressure | # Shots |
|---|---|---|---|
| 2.5 kV | Room temp | 1 bar | ≈ 6000 |
| 2.5 kV | Room temp | 1 bar | ≈ 14,000 |
| 2.5 kV | 77 K | 1 bar | > 65,000 |
| 2.5 kV | 77 K | 3 bar | > 75,000 |
| 2.9 kV | 77 K | 1 bar | ≈ 8000 |
| 2.9 kV | 77 K | 3 bar | > 70,000 |

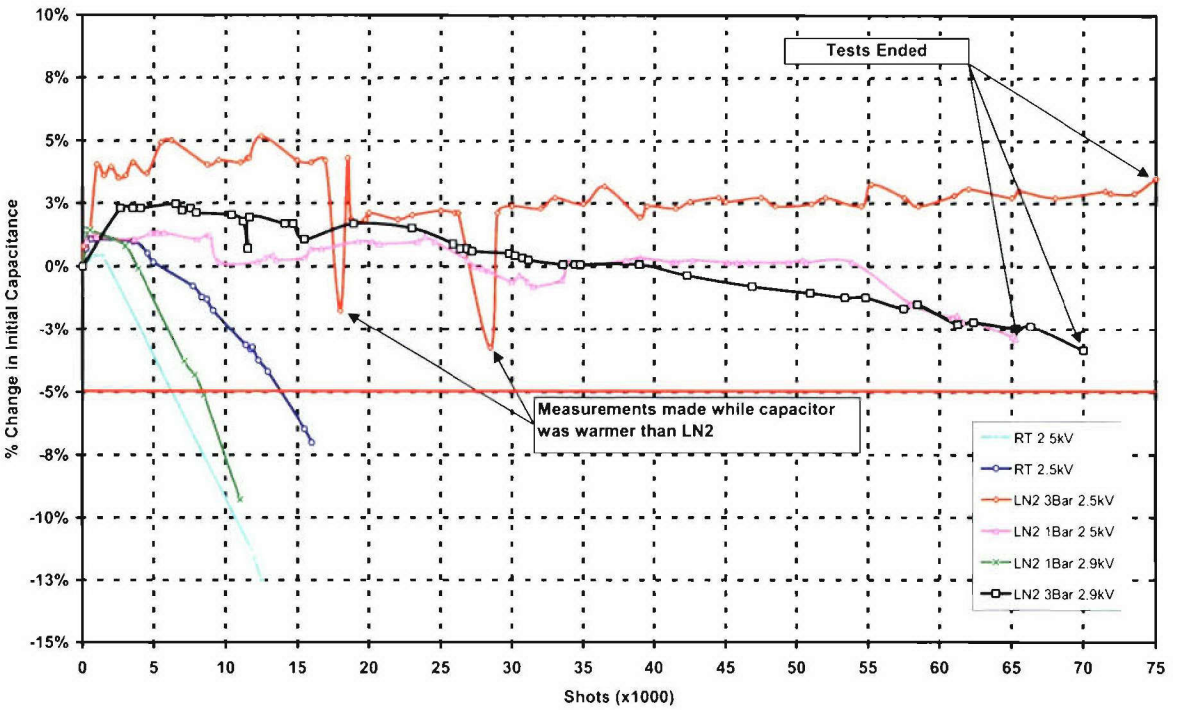


***Fig. 7-13. Results of cyclic life testing***

It is useful to consider the data in two groups defined by the test voltage. The first group consists of the four capacitors tested at 2.5 kV. The two room temperature capacitors both failed at less than 15,000 shots, which is normal. Typical life for this model capacitor is 20,000 shots at the rated voltage of 2.3 kV. Operation at higher voltage results in a decrease in life.

The two capacitors tested at cryogenic temperatures at 2.5 kV both exceeded 65,000 shots. In both cases the test was stopped because of time constraints; the capacitors had not yet reached the failure point of a 5% loss. In fact, as can be seen in Fig. 7-13, the capacitor tested at 3 bar pressure was not even showing signs of capacitance loss at 75,000 shots. Thus it is safe to say that cryogenic operation can provide at least a factor of 4 increase in life.

Note also that the capacitor tested at 3 bar and 2.5 kV has two points where its measured value was significantly lower than would be expected. After reviewing the raw data it was discovered that these particular measurements were made after a weekend when the liquid nitrogen was allowed to evaporate and the capacitor was allowed to warm up. It is likely that in warming up, the windings became looser than when cold and thus the capacitance change. Note also that when the capacitor was cooled back down, the capacitance returned to its expected value.

Two capacitors tested at 2.9 kV, 26% above the rated voltage displayed an 50% increase in energy density. Experience has shown that operating this far above the rated voltage will significantly shorten the life of the capacitor. With 1 bar pressure, this decrease in life is seen even at cryogenic temperature. However, by increasing the

pressure to 3 bar, significant improvement in life is seen. While there is no data for comparison with a standard room temperature capacitor, it is reasonable to expect this to be a factor of ten or more improvement in lifetime based on ESI experience.

To achieve the high energy densities that are the goal of this program, it will almost certainly be necessary to operate at higher voltages and higher dielectric stresses than normal. This would normally indicate a significantly reduced lifetime for the capacitors. However, this data indicates that the cryogenic temperature, especially when coupled with a small amount of pressurization, will allow for normal or perhaps even extended life.

Pressurization may be advantageous for a number of reasons:

1. It forces the nitrogen between the windings preventing voids from forming as the inter-winding air cools.
2. It improves the quality of the liquid nitrogen by reducing the size of micro-bubbles.
3. It minimizes or prevents the formation of gas bubbles due to clearing events.

#### *7.1.1.4 DC Life Testing at Cryo Temperatures*

Another method of testing capacitors, besides the cycle testing described in the previous section, is to charge the capacitors to a given voltage and determine how many hours pass before the capacitor loses 5% of its value. This test is conducted with the same set-up as the cycle testing. The control software was changed to provide a fixed dc charge. The capacitor is discharged once or twice a day to allow the capacitance to be measured and to refill the nitrogen. To mitigate charging and discharging heating affects, the charge and discharge rates were kept low. The charge current was held at 35 mA and the discharge into a 500-ohm load. To accelerate the life testing, the tests were conducted at 2.9 kV.

The dc life testing was conducted using model 30957 oil-filled capacitors for the room temperature tests and model 30956 "dry" $LN_2$ unimpregnated capacitors for the cryogenic tests. The cryogenic tests were conducted at 3 Bar pressure in the same manner as the cyclic testing.

##### *7.1.1.4.1 DC Life Testing Results at Cryo Temperatures*

A total of five capacitors were tested for dc life. The results are shown in Fig. 7-14. The three capacitors tested at room temperature all failed in less than 20 hours. Linear regression trend lines are shown for the capacitors tested at cryogenic temperatures. These trend lines project lifetimes in excess of 700 hours, a factor of 35 times the room temperature life.

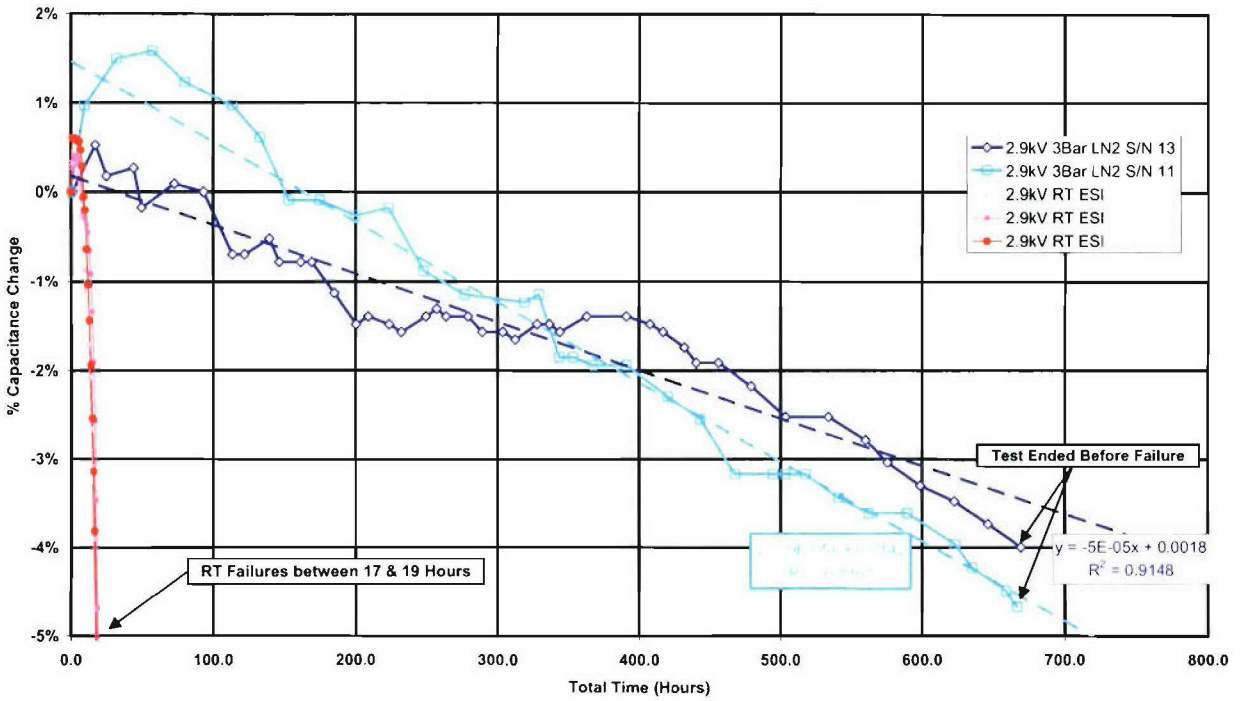


***Fig. 7-14. DC life test results***

The dc life test results support the cyclic test conclusions that cryogenic operation, especially with a slight pressurization, can significantly increase the life of capacitors.

### *7.1.1.5 Thermal Life Testing*

Operation of cryogenically cooled capacitors will almost certainly entail some thermal cycling where the capacitors are allowed to warm up to room temperature and then recooled. A test was conducted to determine if there would be any adverse affects due to thermal cycling.

The thermal cycling test was conducted on two model 30956 capacitors. The first capacitor to be tested was the same capacitor used for the dc life testing and had already been at dc charge for 667 hours. The second capacitor tested was a new one. The test procedure was the same for both capacitors. The capacitor pad was placed in the pressure vessel and pressurized to 3 bar with dry nitrogen. The pressure vessel was then immersed in liquid nitrogen. A gaseous nitrogen supply was maintained on the vessel to keep the pressure at 3 bar as the gas in the vessel cooled and liquefied. Once the gas in the pressure vessel was liquefied, the capacitor was charged to 2.9 kV with constant current of 35 mA and held at voltage for up to several hours. The capacitor was then discharged and the capacitance measured.

Following the capacitance measurement, the pressure vessel was removed from the liquid nitrogen and allowed to warm up. A vent valve was opened to allow the expanding gas to escape. The capacitor pad was kept in a nitrogen atmosphere throughout the tests. The time allowed for the capacitor to warm up varied from cycle to cycle.

### *7.1.1.5.1 Thermal Life Testing Results*

There were no adverse affects seen on either capacitor. The first capacitor underwent three thermal cycles, not counting the initial cooldown. The measured capacitance varied from 107.5 μF to 108.0 μF, well within the normal variation for this measurement.

The second capacitor underwent a total of 20 thermal cycles where the warm-up time varied. The results are summarized in Table 7-6 below.

**Table 7-6**
**Results of Thermal Cycle Testing**

| Cycle | Warming Time (hr) | Total time at charge (hr) | C μF |
|---|---|---|---|
| 0 | -- | 2.4 | 114.9 |
| 1 | 75.3 | 3.1 | 114.4 |
| 2 | 14.9 | 5.3 | 114.9 |
| 3 | 19.1 | 9.2 | 115.0 |
| 4 | 17.5 | 14.8 | 115.6 |
| 5 | 17.8 | 15.6 | 114.8 |
| 6 | 20.6 | 47.0 | 115.4 |
| 7 | 17.3 | 47.9 | 115.3 |
| 8 | 16.0 | 53.1 | 115.4 |
| 9 | 16.0 | 54.7 | 115.9 |
| 10 | 20.8 | 61.6 | 115.8 |
| 11 | 18.7 | 62.9 | 115.5 |
| 12 | 66.3 | 67.4 | 115.8 |
| 13 | 16.5 | 75.3 | 115.9 |
| 14 | 15.7 | 80.4 | 116.0 |
| 15 | 17.8 | 86.0 | 116.2 |
| 16 | 15.5 | 92.6 | 115.6 |
| 17 | 63.1 | 97.6 | 116.2 |
| 18 | 15.8 | 104.3 | 116.3 |
| 19 | 17.4 | 109.9 | 116.4 |
| 20 | 17.2 | 114.9 | 116.5 |

The capacitor shows no signs of degradation and a trend towards increasing capacitance. This is normal behavior for this type of capacitor and is seen in the dc life test results shown in Fig. 7-14 where the early trend is to increasing capacitance. This would indicate that the thermal cycling has no adverse affects on the capacitor.

### *7.1.2 Ball-Plane Materials Testing*

Ball and plane testing is used to measure the relative breakdown strengths of different dielectric materials under nearly identical conditions. As mentioned above, a sample of the dielectric of interest is placed between the ball electrode and plate electrode. The entire assembly is then immersed in liquid nitrogen. An increasing potential is applied to the electrodes (done by manually rotating the voltage knob on a Hi-pot tester power

supply from 0 to as high as 20 kV in approximately 1 second) until the dielectric breaks down, and current conducts between the electrodes. The breakdown voltage is recorded from a stored digital oscilloscope trace, and the dielectric strength is calculated as the measured value of the breakdown voltage divided by the film thickness. The dielectric breakdown strength is then reported in units of Volts per micrometer. Ball and plane testing is used primarily as a screening tool determine if a dielectric material has adequate breakdown strength for use in high energy density cryogenic capacitors.

Results for ball-plane tests conducted during the period 30 June through 30 September are shown Tables 7-7 through 7-10. All data are shown for completeness. The film material, thickness, temperature, breakdown voltage, and dielectric strength (V/μm) are shown. The earliest materials tested were commercially available polymer films. Some are "capacitor grade" and are used in room temperature capacitors. These materials include polypropylene (PPL), polyester or polyethylterphthalate (PET), and polyvinylidene di-fluoride (PVdF). Commercially available polyvinyl alcohol (PVA) of various grades was also tested as were a number of common polymer films (e.g., Saran wrap), which were used primarily to characterize the test apparatus and to inexpensively compare results with other test measurements.

Stamp capacitor tests showed that the dielectric constants of the polymer films in the table dropped from their room temperature levels to a value between 2 and 3 at liquid nitrogen temperatures. Therefore the required breakdown strength for these materials to achieve 8 J/cc is 1000 V/μm or greater. The measured breakdown strengths in Tables 7-7 through 7-10 are mostly below the required breakdown strength. The exception seems to be some PET tests, samples 255-260 taken on 11 August 2005. However, other sets of PET test (samples 121-125, 148-151,159-160, 165-168, and 227-229) did not show this superior performance, making the results suspect. After noticing this discrepancy, we began to use a baseline film (8 micron PVdF) for ball and plane tests before and after each data set to check for instrument drift. One last observation of this data set is that the PVA films all performed significantly below the expected values, based on the high breakdown strengths shown in the 1951 Ball paper.

## Table 7-7
## Results from Ball and Plane Breakdown Tests

| Sample | Date | Material | Thickness (um) | Temp | Breakdown Voltage (V) | Dielectric Strength (V/um) |
|---|---|---|---|---|---|---|
| 111 | 6/29/2005 | PPL | 8 | LN2 | 6400 | 800 |
| 112 | 6/29/2005 | PPL | 8 | LN2 | 6820 | 853 |
| 113 | 6/29/2005 | PPL | 8 | LN2 | 6000 | 750 |
| 114 | 6/29/2005 | PPL | 8 | LN2 | 6680 | 835 |
| 115 | 6/30/2005 | PPL | 8 | Room | 5920 | 740 |
| 116 | 6/30/2005 | PPL | 8 | Room | 5550 | 694 |
| 117 | 6/30/2005 | PPL | 8 | Room | 3930 | 491 |
| 118 | 6/30/2005 | PPL | 8 | Room | 3910 | 489 |
| 119 | 6/30/2005 | PVdF | 8 | Room | 2200 | 275 |
| 120 | 6/30/2005 | PVdF | 8 | Room | 5320 | 665 |
| 121 | 6/30/2005 | PET | 4.8 | Room | 3090 | 644 |
| 122 | 6/30/2005 | PET | 9.6 | Room | 2300 | 240 |
| 123 | 7/1/2005 | PET | 4.8 | Room | 3260 | 679 |
| 124 | 7/1/2005 | PET | 4.8 | Room | 2050 | 427 |
| 125 | 7/1/2005 | PET | 4.8 | Room | 2600 | 542 |
| 126 | 7/1/2005 | PVdF | 8 | Room | 4030 | 504 |
| 127 | 7/1/2005 | PPL | 8 | Room | 4460 | 558 |
| 128 | 7/1/2005 | PPL | 8 | Room | 5010 | 626 |
| 129 | 7/1/2005 | PPL | 8 | Room | 5390 | 674 |
| 130 | 7/1/2005 | PPL | 8 | Room | 4570 | 571 |
| 131 | 7/1/2005 | Saran Cling Plus | 12.7 | Room | 5070 | 399 |
| 132 | 7/1/2005 | Saran Cling Plus | 12.7 | Room | 5550 | 437 |
| 133 | 7/1/2005 | Saran Cling Plus | 12.7 | Room | 5440 | 428 |
| 134 | 7/1/2005 | Saran Cling Plus | 12.7 | Room | 5050 | 398 |
| 135 | 7/1/2005 | Saran Cling Plus | 12.7 | Room | 4300 | 339 |
| 136 | 7/1/2005 | Saran Cling Plus | 12.7 | LN2 | 8600 | 677 |
| 137 | 7/1/2005 | Saran Cling Plus | 12.7 | LN2 | 8550 | 673 |
| 138 | 7/1/2005 | Saran Cling Plus | 12.7 | LN2 | 7320 | 576 |
| 139 | 7/1/2005 | Saran Cling Plus | 12.7 | LN2 | 7870 | 620 |
| 140 | 7/1/2005 | PVdF | 8 | LN2 | 5500 | 688 |
| 141 | 7/1/2005 | PVdF | 8 | LN2 | 5270 | 659 |
| 142 | 7/1/2005 | PVdF | 8 | LN2 | 5270 | 659 |
| 143 | 7/1/2005 | PVdF | 8 | LN2 | 4950 | 619 |
| 144 | 7/1/2005 | PPL | 8 | LN2 | 7000 | 875 |
| 145 | 7/1/2005 | PPL | 8 | LN2 | 6180 | 773 |
| 146 | 7/1/2005 | PPL | 8 | LN2 | 5730 | 716 |
| 147 | 7/1/2005 | PPL | 8 | LN2 | 6050 | 756 |
| 148 | 7/1/2005 | PET | 4.8 | LN2 | 4300 | 896 |
| 149 | 7/1/2005 | PET | 4.8 | LN2 | 4050 | 844 |
| 150 | 7/1/2005 | PET | 4.8 | LN2 | 1720 | 358 |
| 151 | 7/1/2005 | PET | 4.8 | LN2 | 4190 | 873 |

## Table 7-8
## Results from Ball and Plane Breakdown Tests

| Sample | Date | Material | Thickness (um) | Temp | Breakdown Voltage (V) | Dielectric Strength (V/um) |
|---|---|---|---|---|---|---|
| 152 | 7/8/2005 | Purified PVA | 40 | LN2 | 12500 | 313 |
| 153 | 7/8/2005 | Purified PVA | 40 | LN2 | 11600 | 290 |
| 154 | 7/8/2005 | Purified PVA | 40 | LN2 | 11600 | 290 |
| 155 | 7/8/2005 | Purified PVA | 40 | LN2 | 10700 | 268 |
| 156 | 7/8/2005 | Purified PVA | 40 | LN2 | 12100 | 303 |
| 157 | 7/8/2005 | Purified PVA | 40 | LN2 | 15400 | 385 |
| 158 | 7/8/2005 | Purified PVA | 40 | LN2 | 14700 | 368 |
| 159 | 7/11/2005 | PET | 4.8 | LN2 | 4000 | 833 |
| 160 | 7/11/2005 | PET | 4.8 | LN2 | 2090 | 435 |
| 161 | 7/11/2005 | Purified PVA | 40 | LN2 | 11300 | 283 |
| 162 | 7/11/2005 | Purified PVA | 40 | LN2 | 11600 | 290 |
| 163 | 7/11/2005 | Purified PVA | 40 | LN2 | 12800 | 320 |
| 164 | 7/11/2005 | Purified PVA | 40 | LN2 | 12100 | 303 |
| 165 | 7/11/2005 | PET | 4.8 | LN2 | 1470 | 306 |
| 166 | 7/11/2005 | PET | 4.8 | LN2 | 4140 | 863 |
| 167 | 7/11/2005 | PET | 4.8 | LN2 | 4460 | 929 |
| 168 | 7/11/2005 | PET | 4.8 | LN2 | 4030 | 840 |
| 169 | 7/11/2005 | Saran Premium | 12.7 | LN2 | 5730 | 451 |
| 170 | 7/11/2005 | Saran Premium | 12.7 | LN2 | 9280 | 731 |
| 171 | 7/11/2005 | Saran Premium | 12.7 | LN2 | 10740 | 846 |
| 172 | 7/11/2005 | Saran Premium | 12.7 | LN2 | 10280 | 809 |
| 173 | 7/11/2005 | Glad Clingwrap | 12.7 | LN2 | 10700 | 843 |
| 174 | 7/11/2005 | Glad Clingwrap | 12.7 | LN2 | 10790 | 850 |
| 175 | 7/11/2005 | Glad Clingwrap | 12.7 | LN2 | 4950 | 390 |
| 176 | 7/11/2005 | Glad Clingwrap | 12.7 | LN2 | 5500 | 433 |
| 177 | 7/12/2005 | Saran Premium | 12.7 | Room | 5920 | 466 |
| 178 | 7/12/2005 | Saran Premium | 12.7 | Room | 5940 | 468 |
| 179 | 7/12/2005 | Saran Premium | 12.7 | Room | 2090 | 165 |
| 180 | 7/12/2005 | Saran Premium | 12.7 | Room | 4050 | 319 |
| 181 | 7/12/2005 | Glad Clingwrap | 12.7 | Room | 4340 | 342 |
| 182 | 7/12/2005 | Glad Clingwrap | 12.7 | Room | 2000 | 157 |
| 183 | 7/12/2005 | Glad Clingwrap | 12.7 | Room | 5530 | 435 |
| 184 | 7/12/2005 | Glad Clingwrap | 12.7 | Room | 5690 | 448 |
| 185 | 7/12/2005 | Reynolds Green | 12.7 | Room | 1970 | 155 |
| 186 | 7/12/2005 | Reynolds Green | 12.7 | Room | 4300 | 339 |
| 187 | 7/12/2005 | Ralphs plastic | 12.7 | Room | 5690 | 448 |
| 188 | 7/12/2005 | Ralphs plastic | 12.7 | Room | 3360 | 265 |
| 189 | 7/12/2005 | Ralphs plastic | 12.7 | Room | 3110 | 245 |
| 190 | 7/12/2005 | Saran Premium | 12.7 | LN2 | 8830 | 695 |
| 191 | 7/12/2005 | Saran Premium | 12.7 | LN2 | 9780 | 770 |
| 192 | 7/12/2005 | Saran Premium | 12.7 | LN2 | 10380 | 817 |
| 193 | 7/12/2005 | Saran Premium | 12.7 | LN2 | 10560 | 831 |
| 194 | 7/12/2005 | Glad Clingwrap | 12.7 | LN2 | 9240 | 728 |
| 195 | 7/12/2005 | Glad Clingwrap | 12.7 | LN2 | 8920 | 702 |
| 196 | 7/12/2005 | Glad Clingwrap | 12.7 | LN2 | 9510 | 749 |

## Table 7-9
## Results from Ball and Plane Breakdown Tests

| Sample | Date | Material | Thickness (um) | Temp | Breakdown Voltage (V) | Dielectric Strength (V/um) |
|---|---|---|---|---|---|---|
| 197 | 7/12/2005 | Reynolds Green | 12.7 | LN2 | 5000 | 394 |
| 198 | 7/12/2005 | Reynolds Green | 12.7 | LN2 | 5320 | 419 |
| 199 | 7/12/2005 | Reynolds Green | 12.7 | LN2 | 4810 | 379 |
| 200 | 7/12/2005 | Reynolds Green | 12.7 | LN2 | 5320 | 419 |
| 201 | 7/12/2005 | Ralphs plastic | 12.7 | LN2 | 6680 | 526 |
| 202 | 7/12/2005 | Ralphs plastic | 12.7 | LN2 | 8460 | 666 |
| 203 | 7/12/2005 | Ralphs plastic | 12.7 | LN2 | 9100 | 717 |
| 204 | 7/12/2005 | Ralphs plastic | 12.7 | LN2 | 9830 | 774 |
| 205 | 7/25/2005 | Saran Premium | 12.7 | Room | 5330 | 420 |
| 206 | 7/25/2005 | Saran Premium | 12.7 | Room | 5410 | 426 |
| 207 | 7/25/2005 | Saran Premium | 12.7 | Room | 4020 | 317 |
| 208 | 7/25/2005 | Saran Premium | 25.4 | Room | 10660 | 420 |
| 209 | 7/25/2005 | Saran Premium | 25.4 | Room | 9750 | 384 |
| 210 | 7/25/2005 | Saran Premium | 12.7 | LN2 | 6280 | 494 |
| 211 | 7/25/2005 | Saran Premium | 12.7 | LN2 | 10620 | 836 |
| 212 | 7/25/2005 | Saran Premium | 12.7 | LN2 | 9520 | 750 |
| 213 | 7/25/2005 | Saran Premium | 12.7 | GN2 | 9590 | 755 |
| 214 | 7/25/2005 | Saran Premium | 12.7 | GN2 | 8620 | 679 |
| 215 | 7/25/2005 | Saran Premium | 12.7 | GN2 | 9300 | 732 |
| 216 | 7/28/2005 | Purified PVA | 40 | Room | 880 | 22 |
| 217 | 7/28/2005 | Purified PVA | 40 | Room | 813 | 20 |
| 218 | 7/29/2005 | Purified PVA | 40 | LN2 | 12430 | 311 |
| 219 | 7/29/2005 | Purified PVA | 40 | LN2 | 12250 | 306 |
| 220 | 8/1/2005 | PPL | 8 | LN2 | 5720 | 715 |
| 221 | 8/2/2005 | PPL | 8 | LN2 | 6000 | 750 |
| 222 | 8/2/2005 | PPL | 8 | LN2 | 7370 | 921 |
| 223 | 8/2/2005 | PPL | 8 | LN2 | 7090 | 886 |
| 224 | 8/2/2005 | PVdF | 8 | LN2 | 6000 | 750 |
| 225 | 8/2/2005 | PVdF | 8 | LN2 | 6680 | 835 |
| 226 | 8/2/2005 | PVdF | 8 | LN2 | 6810 | 851 |
| 227 | 8/2/2005 | PET | 4.8 | LN2 | 3720 | 775 |
| 228 | 8/2/2005 | PET | 4.8 | LN2 | 4780 | 996 |
| 229 | 8/2/2005 | PET | 4.8 | LN2 | 3930 | 819 |
| 230 | 8/4/2005 | PVdF | 8 | LN2 15PSI( | 4530 | 566 |
| 231 | 8/8/2005 | PPL | 8 | LN2 30psig | 5250 | 656 |
| 232 | 8/8/2005 | PPL | 8 | LN2 30psig | 7180 | 898 |
| 233 | 8/9/2005 | PMMA-im | 50 | Room | 28450 | 569 |
| 234 | 8/9/2005 | PMMA-im | 50 | LN2 | 1384 | 28 |
| 235 | 8/9/2005 | PMMA-im | 50 | LN2 | 1580 | 32 |
| 236 | 8/10/2005 | Teflon | 50 | Room | 14160 | 283 |
| 237 | 8/10/2005 | Teflon | 50 | Room | 13920 | 278 |
| 238 | 8/10/2005 | FEP | 25 | Room | 11340 | 454 |
| 239 | 8/10/2005 | FEP | 25 | Room | 12840 | 514 |
| 240 | 8/10/2005 | PFA | 25 | Room | 12290 | 492 |
| 241 | 8/10/2005 | PFA | 25 | Room | 12520 | 501 |

## Table 7-10
## Results from Ball and Plane Breakdown Tests

| Sample | Date | Material | Thickness (um) | Temp | Breakdown Voltage (V) | Dielectric Strength (V/um) |
|---|---|---|---|---|---|---|
| 242 | 8/10/2005 | Teflon | 50 | LN2 | 13070 | 261 |
| 243 | 8/10/2005 | Teflon | 50 | LN2 | 14710 | 294 |
| 244 | 8/10/2005 | Teflon | 50 | LN2 | 13930 | 279 |
| 245 | 8/10/2005 | Teflon | 50 | LN2 | 14170 | 283 |
| 246 | 8/11/2005 | PFA | 25 | LN2 | 12930 | 517 |
| 247 | 8/11/2005 | PFA | 25 | LN2 | 11370 | 455 |
| 248 | 8/11/2005 | PFA | 25 | LN2 | 10900 | 436 |
| 249 | 8/11/2005 | FEP | 25 | LN2 | 9730 | 389 |
| 250 | 8/11/2005 | FEP | 25 | LN2 | 9570 | 383 |
| 251 | 8/11/2005 | FEP | 25 | LN2 | 8480 | 339 |
| 252 | 8/11/2005 | FEP | 25 | LN2 | 9730 | 389 |
| 253 | 8/11/2005 | PMMA-im | 50 | LN2 | 15980 | 320 |
| 254 | 8/11/2005 | PMMA-im | 50 | LN2 | 13480 | 270 |
| 255 | 8/11/2005 | PET | 4.8 | LN2 | 8080 | 1683 |
| 256 | 8/11/2005 | PET | 4.8 | LN2 | 5000 | 1042 |
| 257 | 8/11/2005 | PET | 4.8 | LN2 | 8420 | 1754 |
| 258 | 8/11/2005 | PET | 4.8 | LN2 | 3670 | 765 |
| 259 | 8/11/2005 | PET | 4.8 | LN2 | 4360 | 908 |
| 260 | 8/11/2005 | PET | 4.8 | LN2 | 4390 | 915 |
| 261 | 9/7/2005 | PVA VF-J | 18 | Room | 400 | 22 |
| 262 | 9/7/2005 | PVA VF-J | 19 | Room | 380 | 20 |
| 263 | 9/7/2005 | PVA VF-J | 20 | Room | 380 | 19 |
| 264 | 9/7/2005 | PVA VF-J | 21 | Room | 415 | 20 |
| 265 | 9/7/2005 | PVA VF-H | 35 | Room | 471 | 13 |
| 266 | 9/7/2005 | PVA VF-H | 35 | Room | 387 | 11 |
| 267 | 9/7/2005 | PVA VF-H | 35 | Room | 387 | 11 |
| 268 | 9/7/2005 | PVA VF-H | 35 | Room | 412 | 12 |
| 269 | 9/15/2005 | K PVA | 18 | LN2 | 4210 | 234 |
| 270 | 9/15/2005 | K PVA | 18 | LN2 | 1210 | 67 |
| 271 | 9/15/2005 | K PVA | 35 | LN2 | 11800 | 337 |
| 272 | 9/15/2005 | K PVA | 35 | LN2 | 12640 | 361 |
| 273 | 9/28/2005 | Kureha PVdF | 8 | LN2 | 6020 | 753 |
| 274 | 9/28/2005 | PVA VF-H | 35 | LN2 | 12700 | 363 |
| 275 | 9/28/2005 | PVA VF-H | 35 | LN2 | 10300 | 294 |
| 276 | 9/28/2005 | PVA VF-H | 35 | LN2 | 11230 | 321 |
| 277 | 9/28/2005 | PVA VF-H | 35 | LN2 | 8340 | 238 |
| 278 | 9/28/2005 | PVA VF-J | 18 | LN2 | 7950 | 442 |
| 279 | 9/28/2005 | PVA VF-J | 18 | LN2 | 8800 | 489 |
| 280 | 9/28/2005 | PVA VF-S | 25 | LN2 | 8960 | 358 |
| 281 | 9/28/2005 | PVA VF-S | 25 | LN2 | 8880 | 355 |
| 282 | 9/28/2005 | PVA VF-S | 25 | LN2 | 10370 | 415 |
| 283 | 9/28/2005 | PVA VF-S | 25 | LN2 | 10990 | 440 |
| 284 | 9/28/2005 | PET metalized | 4.5 | LN2 | 1330 | 296 |
| 285 | 9/28/2005 | PET metalized | 4.5 | LN2 | 2960 | 658 |
| 286 | 9/28/2005 | PET metalized | 4.5 | LN2 | 1610 | 358 |
| 287 | 9/28/2005 | PET metalized | 4.5 | LN2 | 1270 | 282 |
| 288 | 9/28/2005 | PET metalized | 4.5 | LN2 | 3330 | 740 |

Table 7-11 shows more ball and plane breakdown test results. In these tests, the baseline PVdF material was employed at the beginning and end of each test series. The first tests were with an isotactic PMMA that had been specially extrusion cast at Randcastle films. PMMA and PVA are the materials with the highest measured breakdown strengths in the 1951 Ball paper and were thus of great interest. However, this material demonstrated very low breakdown strengths.

**Table 7-11**
**Results from Ball and Plane Breakdown Tests**

| Sample | Date | Material | Thickness (um) | Temp | Breakdown Voltage (V) | Dielectric Strength (V/um) |
|---|---|---|---|---|---|---|
| 290 | 9/28/2005 | Kureha PVdF | 8 | LN2 | 5610 | 701 |
| 291 | 9/28/2005 | Kureha PVdF | 8 | LN2 | 5630 | 704 |
| 292 | 9/28/2005 | PMMA Isotactic | 44.45 | LN2 | 12630 | 284 |
| 293 | 9/28/2005 | PMMA Isotactic | 44.45 | LN2 | 7780 | 175 |
| 294 | 9/28/2005 | PMMA Isotactic | 44.45 | LN2 | 12860 | 289 |
| 295 | 9/28/2005 | PMMA Isotactic | 44.45 | LN2 | 9500 | 214 |
| 296 | 9/28/2005 | PMMA Isotactic | 44.45 | LN2 | 9740 | 219 |
| 297 | 9/28/2005 | PMMA Isotactic | 44.45 | LN2 | 9580 | 216 |
| 298 | 9/28/2005 | PMMA with 2 um SiO2 particles | 4 | LN2 | 5600 | 1400 |
| 299 | 9/28/2005 | PMMA with 2 um SiO2 particles | 4 | LN2 | 5240 | 1310 |
| 300 | 9/28/2005 | PMMA with 2 um SiO2 particles | 4 | LN2 | 5680 | 1420 |
| 301 | 9/28/2005 | PET substrate only | 75 | LN2 | 11300 | 151 |
| 302 | 9/28/2005 | PVA on PET | 79 | LN2 | 14030 | 178 |
| 303 | 9/28/2005 | PMMA with 2 um SiO2 particles | 4 | LN2 | 6890 | 1723 |
| 304 | 9/29/2005 | PMMA without SiO2 particles | 4 | LN2 | 3780 | 945 |
| 305 | 9/29/2005 | PMMA without SiO2 particles | 4 | LN2 | 4750 | 1188 |
| 306 | 9/29/2005 | PMMA without SiO2 particles | 4 | LN2 | 3860 | 965 |
| 307 | 9/29/2005 | PMMA without SiO2 particles | 4 | LN2 | 5610 | 1403 |
| 308 | 9/29/2005 | PMMA without SiO2 particles | 4 | LN2 | 3610 | 903 |
| 309 | 9/29/2005 | PMMA without SiO2 particles | 4 | LN2 | 5810 | 1453 |
| 310 | 9/30/2005 | Kureha PVdF | 8 | Room | 4160 | 520 |
| 311 | 9/30/2005 | Kureha PVdF | 8 | Room | 4040 | 505 |
| 312 | 9/30/2005 | PMMA with 2 um SiO2 particles | 4 | Room | 1960 | 490 |
| 313 | 9/30/2005 | PMMA with 2 um SiO2 particles | 4 | Room | 1080 | 270 |
| 314 | 9/30/2005 | PMMA with 2 um SiO2 particles | 4 | Room | 1870 | 468 |
| 315 | 9/30/2005 | Chlorinated Polypropylene Air cured | 6 | Room | 948 | 158 |
| 316 | 9/30/2005 | Chlorinated Polypropylene Air Cured | 6 | Room | 840 | 140 |
| 317 | 9/30/2005 | Chlorinated Polypropylene UV Cured | 6 | Room | 538 | 90 |
| 318 | 9/30/2005 | Chlorinated Polypropylene UV Cured | 6 | Room | 778 | 130 |
| 319 | 9/30/2005 | Chlorinated Polypropylene UV Cured | 6 | Room | 432 | 72 |
| 320 | 9/30/2005 | Kureha PVdF | 8 | Room | 3410 | 426 |
| 321 | 9/30/2005 | Kureha PVdF | 8 | LN2 | 6000 | 750 |
| 322 | 9/30/2005 | Kureha PVdF | 8 | LN2 | 5500 | 688 |
| 323 | 9/30/2005 | Chlorinated Polypropylene UV Cured | 6 | LN2 | 3160 | 527 |
| 324 | 9/30/2005 | Chlorinated Polypropylene UV Cured | 6 | LN2 | 3500 | 583 |
| 325 | 9/30/2005 | Chlorinated Polypropylene UV Cured | 6 | LN2 | 3030 | 505 |
| 326 | 9/30/2005 | Chlorinated Polypropylene Air Cured | 6 | LN2 | 2970 | 495 |
| 327 | 9/30/2005 | Chlorinated Polypropylene Air Cured | 6 | LN2 | 4220 | 703 |
| 328 | 9/30/2005 | Chlorinated Polypropylene Air Cured | 6 | LN2 | 4130 | 688 |
| 329 | 9/30/2005 | Chlorinated Polypropylene Air Cured | 6 | LN2 | 4130 | 688 |
| 330 | 9/30/2005 | PVA with particles | 3.5 | LN2 | 2000 | 571 |
| 331 | 9/30/2005 | PVA with particles | 3.5 | LN2 | 1980 | 566 |
| 332 | 9/30/2005 | PVA with particles | 3.5 | LN2 | 0 | 0 |
| 333 | 9/30/2005 | PVA with particles | 3.5 | LN2 | 1320 | 377 |
| 334 | 9/30/2005 | Kureha PVdF | 8 | LN2 | 5000 | 625 |
| 335 | 9/30/2005 | Kureha PVdF | 8 | LN2 | 5430 | 679 |

Nearly all melt extrusion cast films have additives that facilitate their manufacture but reduce the chemical purity. Further, the melt extrusion process does not provide for a uniform morphological structure in the resultant polymer film. Finally, most commercial

film manufactures do not control particulate and other contamination to any degree, primarily because it is not in their economic interest to do so.

Polymer films of higher purity (chemical, morphological, and contaminant) can be made by solution casting instead of melt extrusion casting. We found two sources for solution cast films: TPL Inc. of Albuquerque and General Atomics Advanced Materials Technology division (GA-AMT). Table 7-11 shows the first results from the GA-AMT solution cast films. The films were cast to a thickness of 3.5 to 4 microns, with the thickness measured by optical interferometry. The PMMA films were cast on 75 micron thick sheets of PET, and the PMMA films were peeled off the PET for the experiments. Some of the PMMA films had silica ($SiO_2$) particles added (5% by mass), ostensibly to aid in the release of the PMMA films from the PET substrates. The PMMA films reproduced the high breakdown strengths (1000 to 1500 V/μm) shown in the 1951 Ball paper. In particular, the films with the silica particles had consistently high breakdown strengths, averaging 1463 V/μm. The films without the particles had considerably more scatter but still performed well. The films all showed significantly higher breakdown strengths at 77 K than at room temperature, again repeating the observations in the Ball paper. The breakdown strengths of the baseline film (Kureha PVdF) were in a range that was consistent but with a significant amount of scatter, likely indicating the magnitude of variability to be expected from ball and plane breakdown tests.

GA-AMT also solution cast films of chlorinated polypropylene (CPP) which again showed higher breakdown strengths at cryogenic temperatures than at room temperature. Their breakdown strength was not high enough to be of interest. CPP is not a material that was being considered but was merely a prototype film for chlorinated polyethylene (CPE), which is one of the four highest breakdown strength materials reported in Ball.

Additional ball and plane test data are shown in Table 7-12. The interesting results are for the GA-AMT PMMA films showing that increasing the film thickness from 4 to 6 microns resulted in a larger scatter in the breakdown strength data and a lower average value. Further increasing the thickness to 10 microns reduced the measured breakdown strength to levels that are quite low. This trend was observed in general: **thinner films have higher dielectric stress capability than thicker films.**

The test of samples 339-348 were of the same GA-AMT PMMA but with varying percentages of silica additive and varying film thickness. In all of these cases, however, the polymer films were cast on an aluminum sheet instead of a PET sheet, and in all cases the breakdown strengths were unacceptably low. Later tests on aluminum substrates revealed the same behavior including poor performance in stamp capacitor tests. It is hypothesized that the microscopically rough aluminum surface asperities act as charge injection centers that degrade the ability of the dielectric to hold off an applied voltage.

## Table 7-12
## Results from Ball and Plane Breakdown Tests

| Sample | Date | Material | Thickness (um) | Temp | Breakdown Voltage (V) | Dielectric Strength (V/um) |
|---|---|---|---|---|---|---|
| 336 | 11/17/2005 | Kureha PVdF | 8 | LN2 | 4680 | 585 |
| 337 | 11/17/2005 | Kureha PVdF | 8 | LN2 | 11560 | 1445 |
| 338 | 11/17/2005 | Kureha PVdF | 8 | LN2 | 5310 | 664 |
| 339 | 11/17/2005 | BRF 20% sld E0073-3 rod 22 | 5.6 | LN2 | 3120 | 557 |
| 340 | 11/17/2005 | BRF 20% sld E0073-3 rod 22 | 5.6 | LN2 | 2280 | 407 |
| 341 | 11/17/2005 | BRF 20% sld E0073-4 rod 28 | 10 | LN2 | 1980 | 198 |
| 342 | 11/17/2005 | BRF 20% sld E0073-4 rod 28 | 10 | LN2 | 2820 | 282 |
| 343 | 11/17/2005 | BRF 40% sld E0075-2 rod 10 | 6.3 | LN2 | 2820 | 448 |
| 344 | 11/17/2005 | BRF 40% sld E0075-2 rod 10 | 6.3 | LN2 | 3170 | 503 |
| 345 | 11/17/2005 | BRF 40% sld E0075-2 rod 10 | 6.3 | LN2 | 2890 | 459 |
| 346 | 11/17/2005 | BRF 40% sld E0075-4 rod 20 | 10.2 | LN2 | 4480 | 439 |
| 347 | 11/17/2005 | BRF 40% sld E0075-4 rod 20 | 10.2 | LN2 | 4180 | 410 |
| 348 | 11/17/2005 | BRF 40% sld E0075-4 rod 20 | 10.2 | LN2 | 4180 | 410 |
| 349 | 11/17/2005 | Kureha PVdF | 8 | LN2 | 5600 | 700 |
| 350 | 11/17/2005 | Kureha PVdF | 8 | LN2 | 6700 | 838 |
| 351 | 12/13/2005 | Kureha PVdF | 8 | LN2 | 5100 | 638 |
| 352 | 12/13/2005 | Kureha PVdF | 8 | LN2 | 6030 | 754 |
| 353 | 12/13/2005 | GA-AMT Acrylic No Particles | 6 | LN2 | 4050 | 675 |
| 354 | 12/13/2005 | GA-AMT Acrylic WITH Particles | 6 | LN2 | 11180 | 1863 |
| 355 | 12/13/2005 | GA-AMT Acrylic WITH Particles | 6 | LN2 | 13990 | 2332 |
| 356 | 12/13/2005 | GA-AMT Acrylic WITH Particles | 6 | LN2 | 2490 | 415 |
| 357 | 12/13/2005 | GA-AMT Acrylic WITH Particles | 6 | LN2 | 13900 | 2317 |
| 358 | 12/13/2005 | GA-AMT Acrylic WITH Particles | 6 | LN2 | 3060 | 510 |
| 359 | 12/13/2005 | GA-AMT Acrylic WITH Particles | 6 | LN2 | 3990 | 665 |
| 360 | 12/13/2005 | GA-AMT Acrylic WITH Particles | 6 | LN2 | 6120 | 1020 |
| 361 | 12/13/2005 | GA-AMT Acrylic WITH Particles | 6 | LN2 | 2990 | 498 |
| 362 | 12/13/2005 | GA-AMT Acrylic WITH Particles | 6 | LN2 | 4650 | 775 |
| 363 | 12/13/2005 | GA-AMT Acrylic No Particles | 10 | LN2 | 5050 | 505 |
| 364 | 12/13/2005 | GA-AMT Acrylic No Particles | 10 | LN2 | 2000 | 200 |
| 365 | 12/13/2005 | GA-AMT Acrylic No Particles | 10 | LN2 | 5400 | 540 |
| 366 | 12/13/2005 | GA-AMT Acrylic WITH Particles | 10 | LN2 | 3990 | 399 |
| 367 | 12/13/2005 | Kureha PVdF | 8 | LN2 | 4150 | 519 |
| 368 | 12/13/2005 | GA-AMT Acrylic WITH Particles | 10 | LN2 | 3650 | 365 |
| 369 | 12/13/2005 | GA-AMT Acrylic WITH Particles | 10 | LN2 | 3800 | 380 |
| 370 | 12/13/2005 | Kureha PVdF | 8 | LN2 | 5830 | 729 |
| 371 | 12/20/2005 | Kureha PVdF | 8 | LN2 | 4900 | 613 |
| 372 | 12/20/2005 | Kureha PVdF | 8 | LN2 | 3490 | 436 |
| 373 | 12/20/2005 | PVA | 19 | LN2 | 5400 | 284 |

Tables 7-13 and 7-14 show ball and plane test results for films cast by TPL. All films were solution cast and include polymer films and polymer films with various ceramics loaded in the polymer matrices. In all cases, the films are thick compared with the GA-AMT films that were successful, which were 4 to 6 microns thick. All of these films had breakdown strengths that are below the range of interest for high energy density dielectrics. Thinner films were fabricated, but they were nearly impossible to remove from their substrates. Also, many of the TPL films were cast onto stainless steel or aluminum foil, which yielded poor results for all films. Though the TPL results were all negative, the fact that they were not deposited on a polymer substrate film or at thickness levels similar to more successful films means that these materials should not yet be ruled out for use in cryogenic capacitors. Subsequent efforts should reexamine TPL composite films for this application under appropriate conditions.

## Table 7-13
## Results from Ball and Plane Breakdown Tests of TPL films

| Sample | Date | Material | Thickness (um) | Temp | Breakdown Voltage (V) | Dielectric Strength (V/um) |
|---|---|---|---|---|---|---|
| 376 | 1/9/2006 | Kureha PVdF | 8 | LN2 | 2490 | 311 |
| 377 | 1/9/2006 | Kureha PVdF | 8 | LN2 | 5800 | 725 |
| 378 | 1/9/2006 | Kureha PVdF | 8 | LN2 | 4620 | 578 |
| 379 | 1/9/2006 | PVA (TPL) | 19 | LN2 | 5470 | 288 |
| 380 | 1/9/2006 | PVA (TPL) | 19 | LN2 | 6330 | 333 |
| 381 | 1/9/2006 | PVA (TPL) | 19 | LN2 | 6950 | 366 |
| 382 | 1/9/2006 | PVA (TPL) | 19 | LN2 | 4140 | 218 |
| 383 | 1/9/2006 | PMMA (TPL) | 16 | LN2 | 7420 | 464 |
| 384 | 1/9/2006 | PMMA (TPL) | 16 | LN2 | 9530 | 596 |
| 385 | 1/9/2006 | PMMA (TPL) | 16 | LN2 | 7580 | 474 |
| 386 | 1/9/2006 | PMMA (TPL) | 16 | LN2 | 8120 | 508 |
| 387 | 1/9/2006 | PVCVA (TPL) | 24 | LN2 | 8120 | 338 |
| 388 | 1/9/2006 | PVCVA (TPL) | 24 | LN2 | 7110 | 296 |
| 389 | 1/9/2006 | PVCVA (TPL) | 24 | LN2 | 7420 | 309 |
| 390 | 1/9/2006 | PVCVA (TPL) | 24 | LN2 | 8120 | 338 |
| 391 | 1/9/2006 | PVCA Composite (TPL) | 22 | LN2 | 2970 | 135 |
| 392 | 1/9/2006 | PVCA Composite (TPL) | 22 | LN2 | 3610 | 164 |
| 393 | 1/9/2006 | PVCA Composite (TPL) | 22 | LN2 | 3240 | 147 |
| 394 | 1/9/2006 | PVCA Composite (TPL) | 22 | LN2 | 3180 | 145 |
| 395 | 1/9/2006 | Kureha PVdF | 8 | LN2 | 5550 | 694 |
| 396 | 1/9/2006 | Kureha PVdF | 8 | LN2 | 5080 | 635 |
| 397 | 1/19/2006 | Kureha PVdF | 8 | LN2 | 5140 | 643 |
| 398 | 1/19/2006 | Kureha PVdF | 8 | LN2 | 6440 | 805 |
| 399 | 1/19/2006 | TPL PMMA Roll | 20 | LN2 | 8230 | 412 |
| 400 | 1/19/2006 | TPL PMMA Roll | 20 | LN2 | 8460 | 423 |
| 401 | 1/19/2006 | TPL PMMA Roll | 20 | LN2 | 8420 | 421 |
| 402 | 1/19/2006 | TPL PMMA Roll | 20 | LN2 | 8460 | 423 |
| 403 | 1/19/2006 | TPL-Loaded PMMA 50wt% BSA Roll | 17 | LN2 | 4040 | 238 |
| 404 | 1/19/2006 | TPL-Loaded PMMA 50wt% BSA Roll | 17 | LN2 | 5000 | 294 |
| 405 | 1/19/2006 | TPL-Loaded PMMA 50wt% BSA Roll | 17 | LN2 | 3810 | 224 |
| 406 | 1/19/2006 | TPL-Loaded PMMA 50wt% BSA Roll | 17 | LN2 | 3580 | 211 |
| 407 | 1/19/2006 | TPL FPE Roll | 13 | LN2 | 7190 | 553 |
| 408 | 1/19/2006 | TPL FPE Roll | 13 | LN2 | 5270 | 405 |
| 409 | 1/19/2006 | TPL FPE Roll | 13 | LN2 | 9150 | 704 |
| 410 | 1/19/2006 | TPL FPE Roll | 13 | LN2 | 9460 | 728 |
| 411 | 1/19/2006 | TPL Loaded PVCVA 50wt% BSA Roll | 30 | LN2 | 3900 | 130 |
| 412 | 1/19/2006 | TPL Loaded PVCVA 50wt% BSA Roll | 30 | LN2 | 3810 | 127 |
| 413 | 1/19/2006 | TPL Loaded PVCVA 50wt% BSA Roll | 30 | LN2 | 3710 | 124 |
| 414 | 1/19/2006 | TPL Loaded PVCVA 50wt% BSA Roll | 30 | LN2 | 3800 | 127 |
| 415 | 1/19/2006 | Kureha PVdF | 8 | LN2 | 5170 | 646 |
| 416 | 1/19/2006 | Kureha PVdF | 8 | LN2 | 4980 | 623 |

**Table 7-14**
**Results from Ball and Plane Breakdown Tests of TPL Films**

| Sample | Date | Material | Thickness (um) | Temp | Breakdown Voltage (V) | Dielectric Strength (V/um) |
|---|---|---|---|---|---|---|
| 417 | 1/20/2006 | Kureha PVdF | 8 | LN2 | 3520 | 440 |
| 418 | 1/20/2006 | Kureha PVdF | 8 | LN2 | 6600 | 825 |
| 419 | 1/20/2006 | Kureha PVdF | 8 | LN2 | 4270 | 534 |
| 420 | 1/20/2006 | TPL PVCVA Roll | 48 | LN2 | 11060 | 230 |
| 421 | 1/20/2006 | TPL PVCVA Roll | 48 | LN2 | 12790 | 266 |
| 422 | 1/20/2006 | TPL PVCVA Roll | 48 | LN2 | 9600 | 200 |
| 423 | 1/20/2006 | TPL PVCVA Roll | 48 | LN2 | 11800 | 246 |
| 424 | 1/20/2006 | TPL FPE Sheet | 7.4 | LN2 | 2500 | 338 |
| 425 | 1/20/2006 | TPL FPE Sheet | 7.4 | LN2 | 2130 | 288 |
| 426 | 1/20/2006 | TPL FPE Sheet | 7.4 | LN2 | 3890 | 526 |
| 427 | 1/20/2006 | TPL FPE Sheet | 7.4 | LN2 | 5510 | 745 |
| 428 | 1/20/2006 | Kureha PVdF | 8 | LN2 | 3300 | 413 |
| 429 | 1/20/2006 | Kureha PVdF | 8 | LN2 | 5390 | 674 |
| 430 | 1/24/2006 | Kureha PVdF | 8 | LN2 | 3050 | 381 |
| 431 | 1/24/2006 | Kureha PVdF | 8 | LN2 | 5730 | 716 |
| 432 | 1/24/2006 | Kureha PVdF | 8 | LN2 | 5050 | 631 |
| 433 | 1/24/2006 | TPL PMMA Sheet | 17.7 | LN2 | 8110 | 458 |
| 434 | 1/24/2006 | TPL PMMA Sheet | 17.7 | LN2 | 7730 | 437 |
| 435 | 1/24/2006 | TPL PMMA Sheet | 17.7 | LN2 | 7960 | 450 |
| 436 | 1/24/2006 | TPL PMMA Sheet | 17.7 | LN2 | 8920 | 504 |
| 437 | 1/24/2006 | TPL PVCVA Sheet | 14 | LN2 | 7370 | 526 |
| 438 | 1/24/2006 | TPL PVCVA Sheet | 14 | LN2 | 7230 | 516 |
| 439 | 1/24/2006 | TPL PVCVA Sheet | 14 | LN2 | 8230 | 588 |
| 440 | 1/24/2006 | TPL PVCVA Sheet | 14 | LN2 | 7600 | 543 |
| 441 | 1/24/2006 | TPL Loaded PVA 60wt% BSA Sheet | 15.8 | LN2 | 3750 | 237 |
| 442 | 1/24/2006 | Kureha PVdF | 8 | LN2 | 5370 | 671 |
| 443 | 1/24/2006 | Kureha PVdF | 8 | LN2 | 5800 | 725 |
| 444 | 2/15/2006 | Kureha PVdF | 8 | LN2 | 3480 | 435 |
| 445 | 2/15/2006 | Kureha PVdF | 8 | LN2 | 5530 | 691 |
| 446 | 2/15/2006 | Kureha PVdF | 8 | LN2 | 10830 | 1354 |
| 447 | 2/15/2006 | Kureha PVdF | 8 | LN2 | 4590 | 574 |
| 448 | 2/15/2006 | TPL-Loaded PMMA 50wt% BSA | 4 | LN2 | | |
| 449 | 2/15/2006 | TPL Polamer GA.08 | 8 | LN2 | | |
| 450 | 2/15/2006 | TPL PMMA | 6 | LN2 | 4680 | 780 |
| 451 | 2/15/2006 | TPL PMMA | 6 | LN2 | 4850 | 808 |
| 452 | 2/15/2006 | TPL PMMA | 6 | LN2 | 5190 | 865 |
| 453 | 2/15/2006 | TPL PMMA | 6 | LN2 | 7560 | 1260 |
| 454 | 2/15/2006 | PVCVA (TPL) | 8 | LN2 | 4460 | 558 |
| 455 | 2/15/2006 | PVCVA (TPL) | 8 | LN2 | 7280 | 910 |
| 456 | 2/15/2006 | PVCVA (TPL) | 8 | LN2 | 7090 | 886 |
| 457 | 2/15/2006 | PVCVA (TPL) | 8 | LN2 | 5130 | 641 |
| 458 | 2/15/2006 | PVCVA (TPL) 50WT% BVA | 7.5 | LN2 | 1900 | 253 |
| 459 | 2/15/2006 | PVCVA (TPL) 50WT% BVA | 7.5 | LN2 | 4160 | 555 |
| 460 | 2/15/2006 | PVCVA (TPL) 50WT% BVA | 7.5 | LN2 | 2480 | 331 |
| 461 | 2/15/2006 | PVCVA (TPL) 50WT% BVA | 7.5 | LN2 | 2200 | 293 |

Subsequent ball and plane tests verified the breakdown performance of the GA-AMT 4 micron thick PMMA with $SiO_2$ particle additives. We did not understand the magnitude of the scatter in the breakdown voltage and attempted to investigate if this variation was due to the film fabrication process. The early GA-AMT films were all fabricated in a laboratory environment, cast on 8.5 x 11 in. PET sheets. We fabricated a sheet of material and sectioned it into 9 equal areas. Samples were taken from these areas and tested in the ball and plane apparatus. Figure 7-15 shows a photograph of the polymer on a PET substrate, the lines denoting the sections on the film, and the magnitudes of breakdown voltage within those areas.

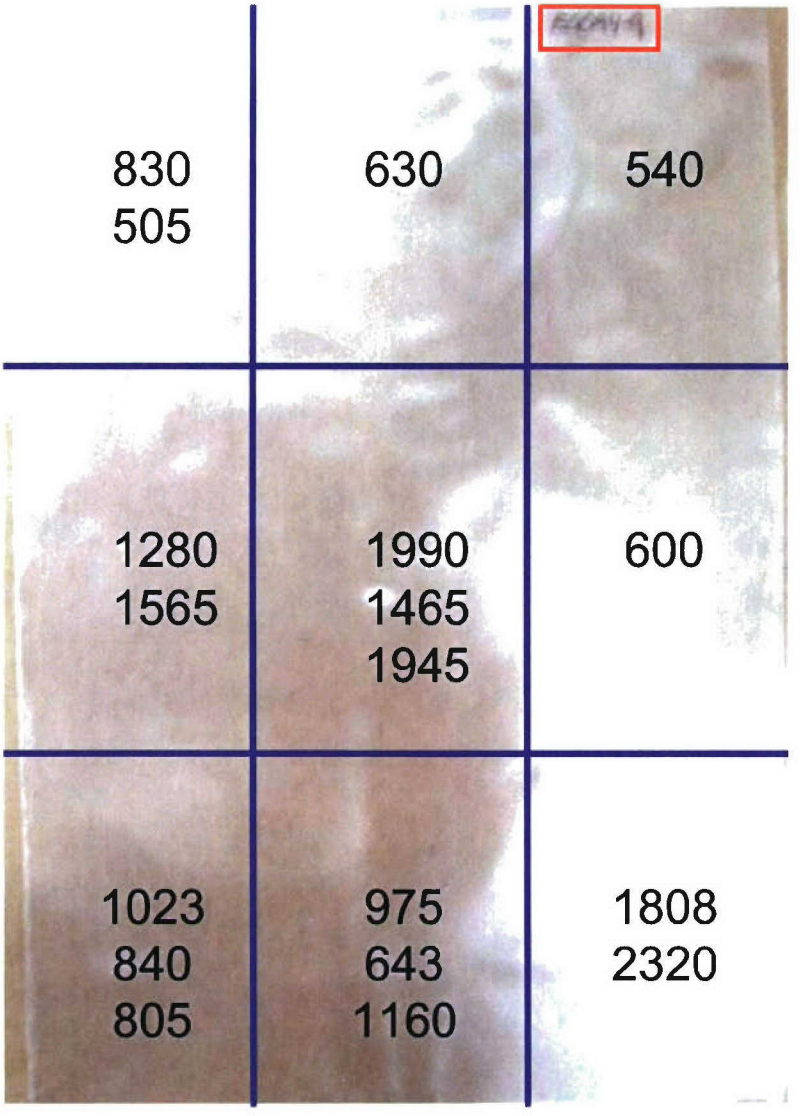


***Fig. 7-15. Dielectric breakdown strength measurements in various areas of a laboratory-cast 4 micron PMMA with $SiO_2$ film on a PET substrate***

As shown in the figure, there are areas over the film in which the breakdown strength is consistently high (such as the center), others where it is consistently low (the top). Still, in a given area there is still significant scatter. Clearly, there is a variation in some film property (thickness, $SiO_2$ concentration, morphology, chemical constituency) that leads to the variation in breakdown strength.

To address this question, a production run was made of the same material. A roll 600 ft in length by 54 in. wide was fabricated on production equipment. Scanning Electron Microscopy (SEM) of various samples of the film showed that the film thickness was fairly uniform, averaging 4.2 microns. Figure 7-16 shows two representative SEMs. The SEM on the left shows the thin PMMA film on the PET substrate film. $SiO_2$ particles are visible protruding from the top surface of the film. Other impurities on the surface are visible in the higher magnification SEM on the right.

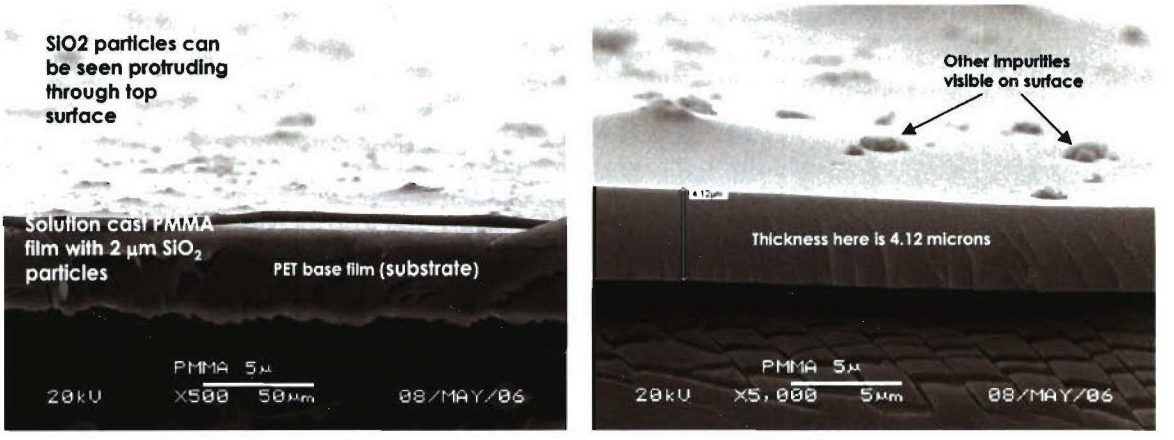


***Fig. 7-16. Scanning electron micrograph (SEM) of production PMMA with $SiO_2$ film on PET substrate***

Ten-inch square samples were cut from the left, center, and right portions of the roll (after non-uniform sections had been trimmed off), and these samples were taken every 100 ft along the roll. Ball and plane breakdown tests were performed on 12 samples from within EACH of the 10-in. square samples. Figure 7-17 shows the breakdown strength results from the left, center, and right samples 10 ft from the end of the roll.

**Results from LEFT sample**

| V/μm |
|---|
| 1602 |
| 2438 |
| 1224 |
| 3155 |
| 1233 |
| 745 |
| 1114 |
| 940 |
| 898 |
| 2655 |
| 2655 |
| 1743 |

| Average |
|---|
| 1700.2 |
| **Standard Deviation** |
| 821.1 |

**Results from CENTER sample**

| V/μm |
|---|
| 1743 |
| 1526 |
| 1145 |
| 2807 |
| 733 |
| 779 |
| 648 |
| 1962 |
| 1967 |
| 995 |
| 2655 |
| 733 |

| Average |
|---|
| 1474.4 |
| **Standard Deviation** |
| 758.5 |

**Results from RIGHT sample**

| V/μm |
|---|
| 1245 |
| 852 |
| 745 |
| 929 |
| 1005 |
| 1917 |
| 2774 |
| 2188 |
| 1624 |
| 1026 |
| 2374 |
| 1938 |

| Average |
|---|
| 1551.4 |
| **Standard Deviation** |
| 678.2 |

***Fig. 7-17. Dielectric breakdown data from first production run PMMA with $SiO_2$ film, 4.2 micron average thickness***

The peak and average values of dielectric breakdown strength are quite high, but there are still significant variations among the samples tested. The variation in breakdown strength may still be due to film variations, which in turn are caused by process variations. Particle distribution, morphology, and contaminants are again suspects, but the variation may be primarily in the ball and plane test itself. Stamp capacitor tests will give a more accurate, area-averaged measure of breakdown strength. The utility of ball and plane tests is their ability to quickly screen materials at low cost.

To summarize, all commercial films showed dielectric breakdown strengths that are below the 1000 V/μm level required to achieve 8 J/cc. This includes so-called "capacitor grade" films. Solution casting is able to produce polymer films with higher purity levels, and these films meet the dielectric breakdown strength requirements for 8 J/cc. Solution cast PMMA films with $SiO_2$ particles demonstrate high breakdown strengths, especially at thicknesses between 4 and 6 microns. Fabricating this material on production equipment reduces the variability seen in laboratory fabricated films, but some scatter remains. Overall, the quest for a material that can produce an 8 J/cc cryogenic capacitor has been successful. Improvements can be achieved by adjusting the range of the $SiO_2$ particle sizes from micron to nano sized or employing techniques to prevent film contamination during processing. Also use of Micro Gravure coater instead of a Mayer rod allows for better thickness control thus achieving better dispersion.

### *7.1.3 Integrated Coefficient of Thermal Contraction Testing*

A test rig shown in Fig. 7-18 was developed to measure the integrated coefficient of thermal contraction (CTE) of capacitor films. It involves an $LN_2$ bath over a meter long, which can be raised or lowered to submerge a test specimen in nitrogen. The test film is clamped between two supports, one of which slides on precision bearings to actuate a dial indicator to record the amount the film shrinks. From this shrinkage amount, and the initial room temperature length of the film, the Integrated Coefficient of Thermal Contraction (ICTC) can be determined.

***Fig. 7-18. Integrated thermal contraction test rig***

Because of the proximity of the nitrogen vapor to the film during the room temperature initial measurement, a thermocouple was placed on the fixed support so that more accurate readings of the thermal contraction can be measured. A small weight was connected to the sliding support and suspended over the edge of the table to put a constant small tension on the films.

### *7.1.3.1 Coefficient of Thermal Contraction Testing Results*

The test rig was used to test ICTC of rolls of material supplied by ESI. Strips 4–6 in. wide and 1-m long were sliced into 2–3 strips (~2 in. wide) for testing. The materials were Polypropylene (PPL), Polyvinylidene fluoride (PVdF), and Polyethylene Terephthalate (PET, Mylar). Results were consistent with published values for the ICTC, shown in Table 7-15.

**Table 7-15**
**CTE Measurements of Polymers at 77 K**

| Material | Exp 1 | Exp 2 | Reference* |
|---|---|---|---|
| PVdF | 1.094% | 1.198% | 1.4% |
| PPL | 0.766% | 0.786% | 1.2% |
| PET | 0.203% | 0.216% | — |

*Reference: Hartwig, Gunther. Polymer Properties at Room and Cryogenic Temperatures. New York: Plenum Press, 1994.

Since the shrinkage amount typical of these films is very small compared to the length (a few percent), long pieces are required in order to fit within the resolution of the test setup. New films delivered to GA from material suppliers are seldom longer than 8–10 in., and so their ICTC cannot be accurately measured using this setup.

### *7.1.4 Impregnation Testing*

#### *Vacuum Pressure Impregnation*

The COTS capacitors filled with rapeseed oil (RSO) were causing the windings to become wrinkled when used in $LN_2$, so an investigation was begun to find another filler material that would work better than RSO or any of the other typical capacitor (silicone oil, castor oil, etc.) impregnates. Any new filler material would need to have a high dielectric breakdown strength and low viscosity in order to penetrate the windings, and would preferably form an amorphous structure when frozen. It was hypothesized that a frozen crystalline structure might damage the very thin material of the windings.

Some candidates for new filler materials include: low viscosity silicone oil, paraffin and other waxes, epoxy, sulfur hexafluoride (SF6), and liquid argon. A listing of some important properties can be found below in Table 7-16.

A vacuum pressure impregnation system was set up to fill the capacitors with the candidate material. A paint pot was connected to a vacuum pump and cold trap to degas the material before impregnation. The capacitor was placed in a pressure vessel, which was evacuated and then filled with the filler material. A schematic of the rig is shown in Fig. 7-19, and a photograph of the system is shown in Fig. 7-29.

## Table 7-16
## Properties of Candidate Filler Materials for Capacitor Impregnation

| Impregnant | Part Number | Qty | Form | Melting Point (C) | Boiling Point (C) | Dielectric Constant | Dielectric Strength (kV/mm) | Kinematic Viscosity (cSt) |
|---|---|---|---|---|---|---|---|---|
| Epoxy | CTD-403 | 2 pts | Liquid Resin | | | | | |
| Silicone Oil | DMS-T01 | 1 gal | Liquid | -86 | 152 | | | 1.0 |
| Silicone Oil | DMS-T01.5B | 1 gal | Liquid | -86 | >150 | | | 1.5 |
| Beeswax | 1100K89 | 3 lbs | Beads | 60-70 | | | | |
| Paraffin | 1085K91 | 3 lbs | Beads | 55 | | | | |
| Bonding Wax | 1129K11 | 3 lbs | Trays | 60-65 | | | | |
| Candelilla | 7285T11 | 3 lbs | Beads | 67-74 | | | | |
| Petroleum Jelly | | 12 oz | Jar | | | | | |
| SF6 | | | Vapor | | -63.9 | 1.0 | | 2.45 @ 25C |
| LAr | | | Liquid | -189.0 | -185.0 | | 11000-14200 | |
| Fluorinert | | | Vapor? | | | 1.9 | 16.9 | 0.75 @ 25C 4 @ -40C |
| Paratherm CR | | | Liquid | -120 (Pour Point) | | | | 12 @ -88C 24.2 @ -96C |

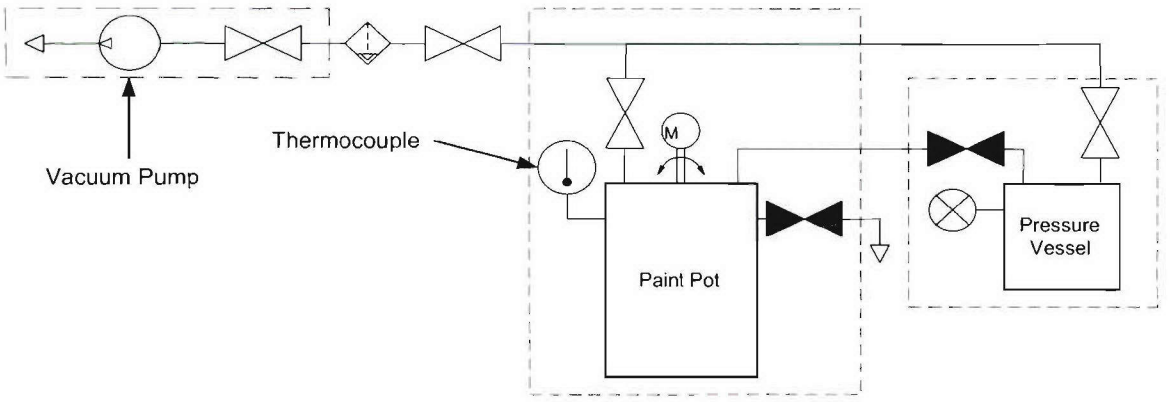


*Fig. 7-19. Schematic for VPI system*

***Fig. 7-20. Photograph of VPI system***

To fill a capacitor with the candidate material, first the capacitor top was opened to allow impregnation while still in the can (similar to the process used at ESI). It was then baked at 85 °C in a 100–200 mTorr vacuum for two days to ensure all the moisture was driven off. The candidate filler material was meanwhile heated under vacuum in the paint pot to degas it. Once everything was dry and degassed, the pressure vessel containing the capacitor was hooked up in line from the vacuum pump to the paint pot, and filler material was allowed to be sucked into the vessel. Once filled, the pressure vessel was then backfilled with compressed nitrogen gas and left overnight. The capacitor was pulled out and examined to see how well it penetrated the capacitor windings.

Low viscosity Silicone oils (1.0 and 1.5 cS) were tested, and performed well in penetrating the capacitor windings. The 1.0 cS oil, however, evaporated quickly, and was thus deemed too volatile to be used in future tests. The 1.5 cS oil penetrated the windings thoroughly, and did not evaporate as quickly as the 1.0 cS oil. It was chosen to advance to the next stage of testing, a step-charge-to-failure test with an impregnated capacitor (discussed below).

Paraffin wax was also tested to determine how far it would penetrate the capacitor windings. After heating to 85°C (well above its melting point of 55°C), the paraffin was quite liquid, and flowed easily. The same procedure was performed with the paraffin as was with the silicone oil, and upon autopsy, it was shown that the paraffin did not penetrate the inner layers of the capacitor windings more than 3–5%, which was deemed insufficient results for its advancement to the next phase of testing. Photographs of selected results are shown in Fig. 7-21.

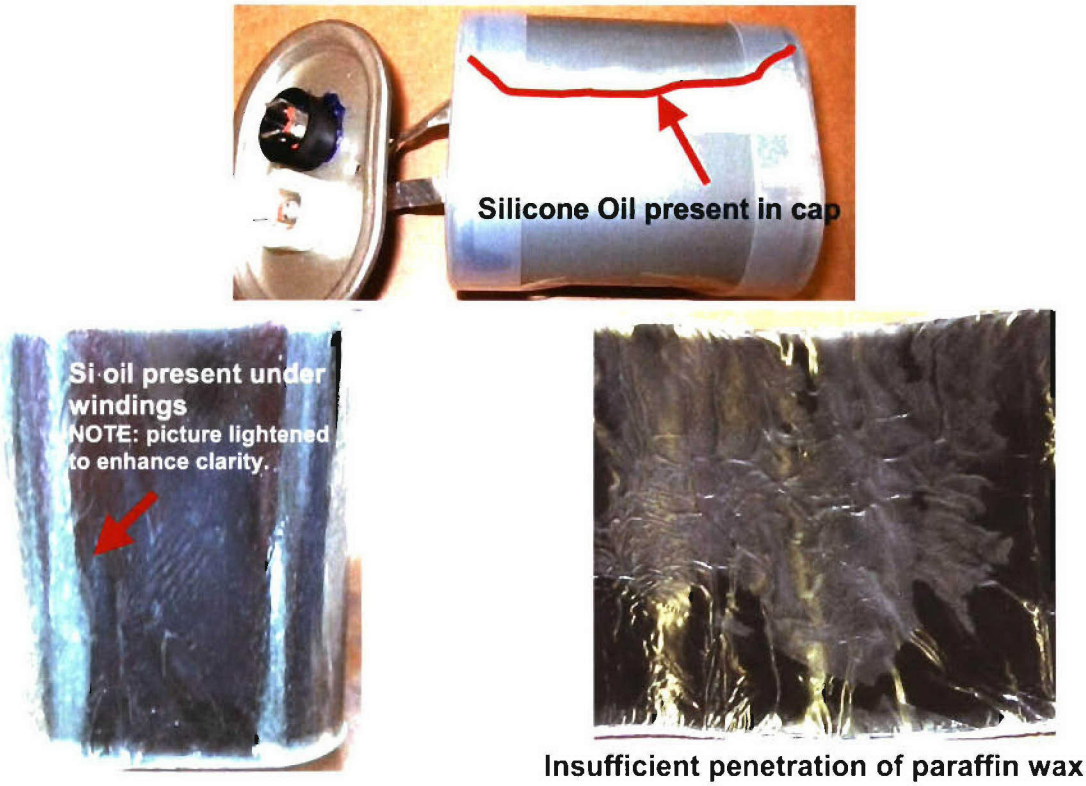


***Fig. 7-21. Photographs of results from silicone oil and paraffin impregnation***

Two more capacitors were impregnated with 1.5 cS silicone oil to be tested with a step charge to failure method as shown in Fig. 7-22. This method involves charging the capacitor to its rated voltage (2.3 kV), holding for 10 sec, and discharging. The capacitance was measured, and the charge voltage was stepped up 100 V. This procedure was continued until the measured capacitance had dropped 5% below its initial capacitance as shown in Fig. 7-23.

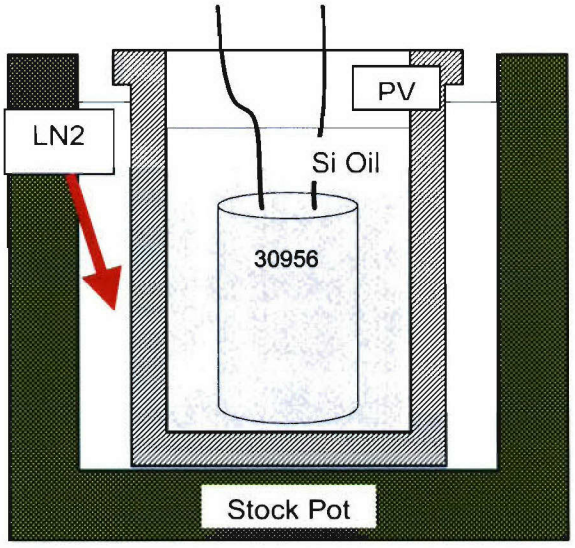

**Fig. 7-22. Schematic of setup for step charge to failure test**

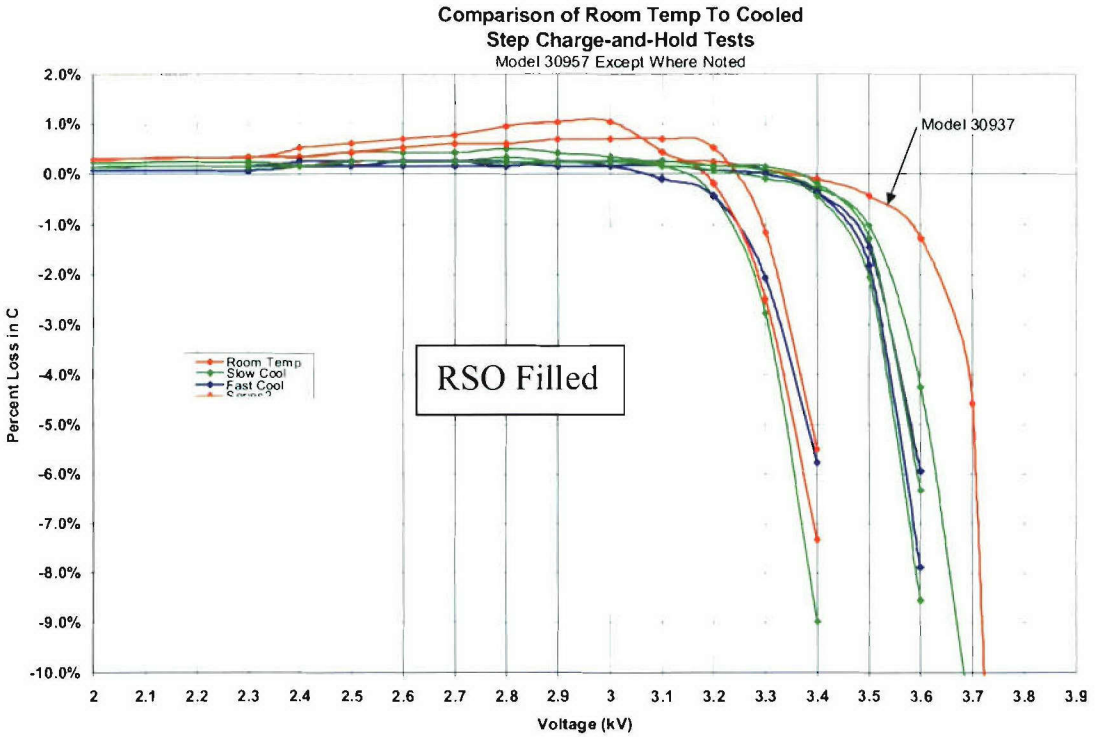


***Fig. 7-23. Results from numerous step to failure tests***

Previous tests with RSO-filled capacitors (#30957) showed an average failure at 3.6 kV. Tests with $LN_2$-filled capacitors showed an average catastrophic failure at 3.0–3.1 kV, while pressurized $LN_2$-filled capacitors failed at 3.5 kV. The 1.5 cS capacitors failed at 3.6 kV, making them better than the $LN_2$-filled caps, but about average for the RSO-filled caps. See Fig. 7-24.

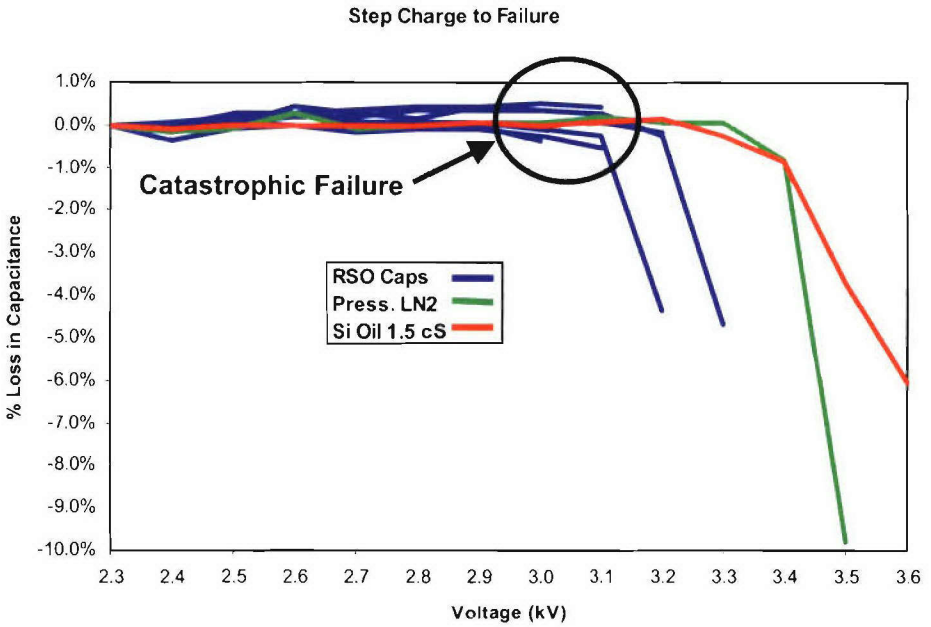


***Fig. 7-24. Step to failure details for three impregnates***

Because the silicone oil filled capacitors did not perform extraordinarily well compared to COTS designs (RSO), and because silicone oil is hazardous to work with and presents a problem in sealing the capacitors, low-viscosity silicone oil was discontinued as a filler material candidate.

Liquid argon was suggested as a possible filler material due to its low boiling point of 84 K, but was rejected because it has lower breakdown strength than $LN_2$ currently in use (LAr breaks at 1.10–1.42 MV/cm, while $LN_2$ breaks at 1.6–1.9 MV/cm). Sulfur Hexafluoride was also suggested as a filler material because of its wide use in industry as a gaseous dielectric in transformers, etc. Concern was raised over the hazardous products formed from SF6 after arcing has occurred. Under normal use, SF6 that has been subjected to arcing would be removed from the device, scrubbed, and replaced. Since in a cryo capacitor the SF6 would be subject to multiple arcing and clearings, the hazardous products would build up and may cause damage to the capacitor. Due to this, investigations into SF6 as a filler material have been placed on hold indefinitely.

After bland results of testing silicone oil and paraffin wax as possible impregnates, a cryogenic epoxy (technically a cyanate ester), CTD-403, was tested. The same VPI process was used as before, but the manufacturer of the epoxy, Composite Technologies Development, Inc., had a specific cure regimen for the epoxy:

- hour ramp from room temperature to 80°C
- 16-hour hold at 80°C (gel state)
- hour ramp from 80°C to 150°C
- 4-hour hold at 150°C

In addition, there was a caution to not let any bulk volume of epoxy exceed 100g, for risk of exotherming. To combat this, two stainless steel bars were added into the pressure vessel used for the VPI process as volume fillers. These were not in contact with the capacitors to be tested. See Fig. 7-25.

The 16-hour gel time occurred without incident, however the epoxy was still fairly liquid. Half way through the 3-hour ramp time, at 133°C, the epoxy began to release fumes. An autopsy of the PV revealed that though some of the epoxy had cured well, at some point it began to exotherm, rendering the batch, and the test capacitors, useless. See Fig. 7-26.

Upon freeing the capacitors from the burnt epoxy, it was evident that the steel outer can had split outward, presumably due to rapid expansion of the epoxy within the can.

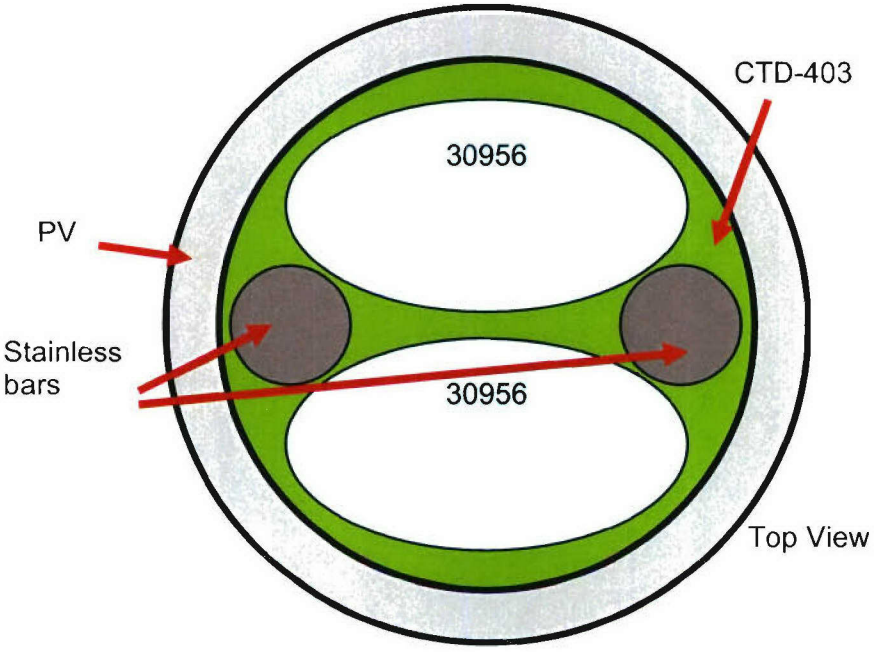


***Fig. 7-25. Schematic for CTD-403 VPI Setup***

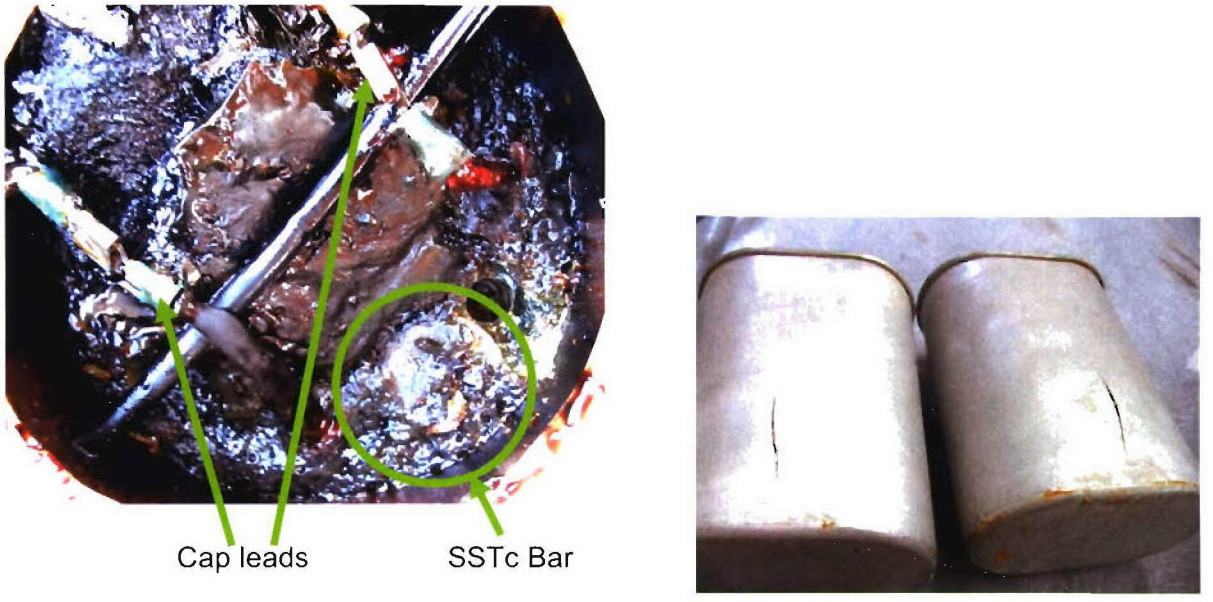


*Fig. 7-26. Results of CTD-403 attempt*

## 7.2 ESI Testing

### 7.2.1 Stamp Capacitor Testing

Stamp capacitor testing is an effective way to initially screen materials that could be used in larger sized capacitors. This can be done with a small amount of the sample material to be tested. This is useful in the case of resins or polymers that are too expensive to be manufactured in large quantities. The information obtained from stamp capacitor testing can then be used to infer what the operating voltage of a material of a given thickness can be. Stamp capacitor testing however cannot predict lifetime or any other outside factor that could affect a capacitor in real world applications. Stamp capacitor testing results are subjective and should be interpreted as such. Stamp capacitor testing technique enables determination of dielectric breakdown stress and dielectric constants.

Figure 7-27 is a chart of materials that show an increase in electrical breakdown strength in relation to temperature. This chart was used, as a guide into deciding what materials would be tested and what materials would not be tested.

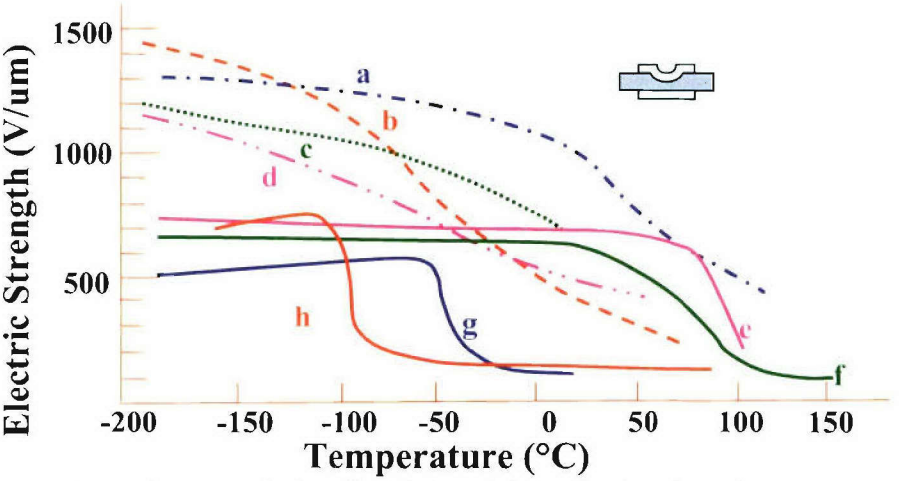


*Examples of the temperature dependence of the d-c electric strength of a range of polar (broken Lines) and nonpolar (solid lines) polymer (Refs 6, 9, and 36) (a) polymethyl methacrylate, (b) polyvinyl alcohol, (c) polyvinyl chloride acetate, (d) 55 percent chlorinated polyethylene, (e) atactic polystyrene, (f) low-density polyethylene, (g) polyisobutylene, and (h) polybutadiene.*

Ref: Engineering Dielectrics Volume IIA ASTM STP 780, Edited by A. Bradwell, ASTM Publication Code Number (PCN) 04-783000-21, Fig. 5.7

***Fig. 7-27. Temperature dependence of polymer dielectrics***

### *7.2.2 COTS Materials (Polypropylene and Polyester)*

Polypropylene (PP) and Polyester (PET) are films that are readily available and are used in capacitors manufactured at GA-ESI. These materials were tested as a baseline and were used to build a bank of materials and information on how films react to cooling in liquid nitrogen. The results from this testing can be seen in Table 7-17. Results showed that there was not a significant increase in breakdown strength or energy density when these materials were cooled from room temperature down to liquid nitrogen temperature.

**Table 7-17**
**PP and PET Stamp Capacitor Testing Results**

| Film | Manufacture | Comments | Thickness in μm | Temp in ~K | Impregnate | Avg Max V/μm | Avg Max J/CC | Dielectric Constant |
|---|---|---|---|---|---|---|---|---|
| PET | Bolmet | Metallized | 5.1 | 77 | LN2 | 678.52 | 5.46 | 2.68 |
| PET | Bolmet | Metallized | 5.1 | 77 | LN2 | 671.94 | 5.23 | 2.62 |
| PPL | Bollore | Metallized | 7.9 | 77 | LN2 | 672.59 | 4.52 | 2.26 |
| PET | Bolmet | Metallized | 5.06 | 295 | SO | 573.12 | 4.43 | 3.06 |
| PPL | Bollore | Metallized | 7.9 | 77 | LN2 | 653.55 | 4.14 | 2.18 |
| PPL | Bollore | Metallized | 7.9 | 295 | SO | 621.83 | 3.85 | 2.25 |
| PET | Bolmet | | 5.0 | 77 | LN2 | 520.00 | 3.62 | 3.00 |
| OPP | Exxon Mobil | | 13.0 | 77 | LN2 | 646.15 | 3.23 | 1.74 |
| PP | Terfilm | | 8.5 | 295 | RSO | 670.59 | 3.16 | 1.58 |
| PP | Terfilm | | 8.5 | 77 | LN2 | 572.55 | 2.86 | 1.97 |
| PET | Dupont | | 5.1 | 77 | LN2 | 528.38 | 2.61 | 2.11 |

### *7.2.3 Polyvinyl Alcohol (PVA)*

Polyvinyl Alcohol (PVA) was listed in Fig. 7-27 as the best performing material at the low end of the temperature spectrum. PVA is a water-soluble resin that is used widely in industry. Shown in Table 7-18 are the results of stamp capacitor testing on PVA. The results of this testing were not encouraging. This material has a tendency to heat up at room temperature leading to a thermal runaway problem. At cryogenic temperature it did not perform better than 400 V/μm, which is about a ¼ of values reported in Fig. 7-27. It is theorized that the purity and process used to make this material could be a factor in the results.

**Table 7-18**
**PVA Stamp Capacitor Testing Results**

| Film | Manufacture | Comments | Thickness in μm | Temp in ~K | Impregnate | Avg Max V/μm | Avg Max J/CC | Dielectric Constant |
|---|---|---|---|---|---|---|---|---|
| PVA | Kurrahay | | 40 | 295 | RSO | 196.88 | 1.58 | 9.23 |
| PVA | Monosol | LXP-6024 | 25.0 | 77 | LN2 | 386.67 | 0.92 | 1.39 |
| PVA | Monosol | A-127 | 22.0 | 77 | LN2 | 278.79 | 0.68 | 1.98 |
| PVA | Monosol | | 37.5 | 295 | Air | 164.44 | 0.67 | 5.57 |
| PVA | Monosol | M2000 | 37.5 | 295 | Air | 158.22 | 0.63 | 5.71 |
| PVA | Monosol | | 37.5 | 77 | LN2 | 243.56 | 0.61 | 2.31 |
| PVA | Monosol | M2000 | 37.5 | 77 | LN2 | 234.67 | 0.56 | 2.30 |

### *7.2.4 Polyethylene Napthalate (PEN)*

Polyethylene Napthalate (PEN) is a film that is normally used for data storage and advanced photography systems. ESI has a stock of PEN films supplied by Japanese manufacturers for sample testing. This material was tested at cryogenic temperature to determine if the breakdown strength of this film could be increased. As shown in Table 7-19 the PEN film performed worse at the lower liquid nitrogen temperature than it did at room temperature.

**Table 7-19**
**PEN Stamp Capacitor Testing Results**

| Film | Manufacture | Comments | Thickness in μm | Temp in ~K | Impregnate | Avg Max V/μm | Avg Max J/CC | Dielectric Constant |
|---|---|---|---|---|---|---|---|---|
| PEN | Teonex | | 4.3 | 295 | RSO | 524.48 | 2.44 | 2.00 |
| PEN | Teonex | | 4.3 | 77 | LN2 | 404.04 | 1.11 | 1.54 |
| PEN | Mitsubishi | | 5.0 | 77 | LN2 | 433.33 | 1.07 | 1.29 |

### *7.2.5 Polyvinylidene Fluoride (PVDF*

Polyvinylidene fluoride (PVDF) has been the baseline dielectric material for high energy density cryogenic capacitors as envisioned by ESI. Model capacitors storing about 100 J when tested at room temperature have operated for hundreds of shots at 400 V/μm voltage gradients (data from NSWC/GA Railgun program). The energy input and output of these samples has been directly measured. If scaled up to larger sizes in

the 1 to 100-kJ range, with expected packing factor of 75%, the delivered energy density at 400 V/μm is projected to be 4 J/cc. However, capacitor grade PVDF film is not currently being manufactured, but, it has been made in the past and the required technology is well established. Sufficient material is stored at ESI to build and test a large number of 1 kJ capacitor samples.

Unfortunately, stamp capacitor tests have shown that the maximum energy density in PVDF is about 6 J/cc at both room temperature and 77 K. The apparent dielectric constant of PVDF, measured using a low-voltage signal from a digital LCR meter, drops from 10.1 to 2.63 when the film is at 77 K, which offsets the fact that the breakdown strength increases from 400 V/um to 700 V/um.

**Table 7-20**
**PVDF Stamp Capacitor Testing Results**

| Film | Manufacture | Comments | Thickness in μm | Temp in ~K | Impregnate | Avg Max V/μm | Avg Max J/CC | Dielectric Constant |
|---|---|---|---|---|---|---|---|---|
| PVDF | Kureha | Metallized | 8.3 | 295 | SO | 396.16 | 7.01 | 10.08 |
| PVDF | Terphane | | 5.8 | 295 | RSO | 513.04 | 5.99 | 5.14 |
| PVDF | Kureha | Metallized | 8.3 | 77 | LN2 | 708.00 | 5.98 | 2.65 |
| PVDF | Terphane | | 5.8 | 77 | LN2 | 678.26 | 3.95 | 1.94 |
| PVDF | Kureha | Metallized | 8.3 | 77 | LN2 | 648.00 | 4.91 | 2.58 |

### *7.2.6 Commercial Plastic Wraps*

Commercial plastic wraps were obtained for the purpose of stamp capacitor testing. The results of these tests can be seen in Table 7-21. After some investigation it

of polyethylene (PE) and resulted in relatively low energy densities.

**Table 7-21**
**Plastic Wraps Stamp Capacitor Testing Results**

| Film | Manufacture | Comments | Thickness in μm | Temp in ~K | Impregnate | Avg Max V/μm | Avg Max J/CC | Dielectric Constant |
|---|---|---|---|---|---|---|---|---|
| | Saran | Plastic Wrap | 12.5 | 295 | SO | 506.00 | 2.05 | 1.81 |
| | Reynolds | Plastic Wrap | 10.8 | 295 | SO | 318.56 | 1.62 | 3.59 |
| | Ralphs | Plastic Wrap | 14.8 | 295 | SO | 377.61 | 1.44 | 2.28 |
| | Reynolds | Plastic Wrap | 10.8 | 77 | LN2 | 346.26 | 1.12 | 2.10 |
| | Rite Aide | Plastic Wrap | 28.9 | 295 | SO | 119.21 | 0.23 | 3.69 |
| | Rite Aide | Plastic Wrap | 28.9 | 77 | LN2 | 99.34 | 0.10 | 2.23 |

A Fourier Transform Infrared Spectroscopy (FTIR) was performed on the commercial plastic wraps. Results of this analysis can be seen in Fig. 7-28.

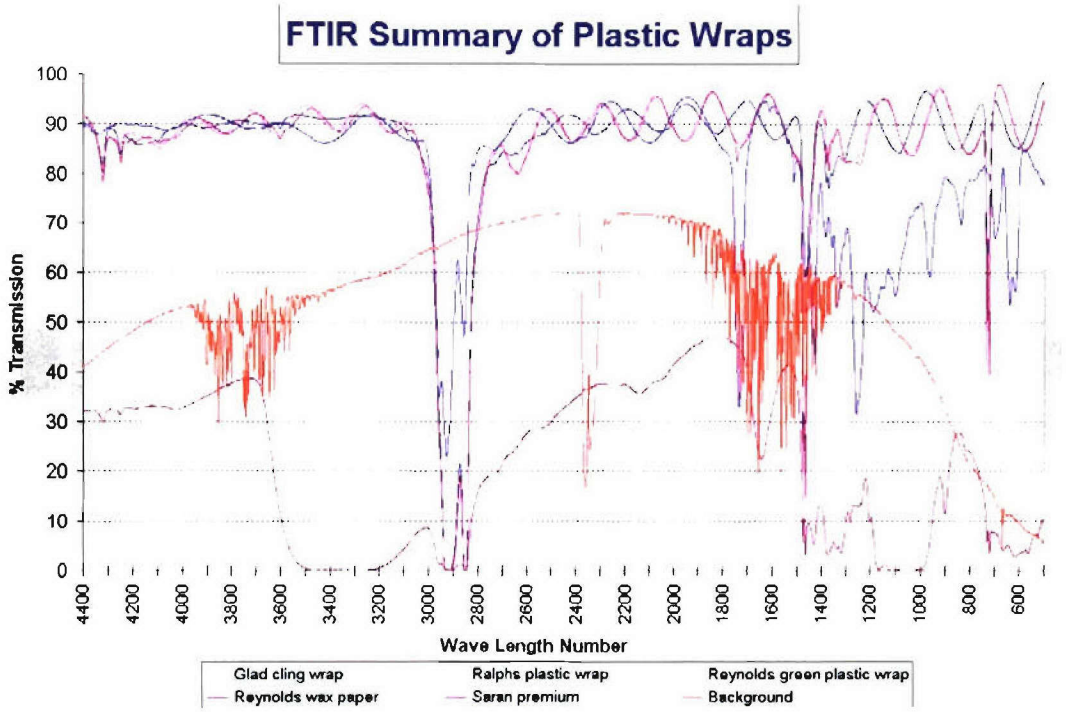


*Fig. 7-28. FTIR analysis of commercial plastic wraps*

### *7.2.7 Miscellaneous Stamp Capacitor Materials*

Numerous other materials were tested using the stamp capacitor method for quick analysis and to determine if any of the materials tested in Table 7-22 were worth investigating further. After testing it was determined that none of these materials warranted any more effort to due poor test results and lack of data in the literature.

**Table 7-22**
**Miscellaneous Stamp Capacitor Test Results**

| Film | Manufacture | Comments | Thickness in µm | Temp in ~K | Impregnate | Avg Max V/µm | Avg Max J/CC | Dielectric Constant |
|---|---|---|---|---|---|---|---|---|
| FPE | Ferrania | | 12.2 | 77 | LN2 | 439.89 | 2.01 | 2.34 |
| | Dupont | Kapton | 8.3 | 295 | RSO | 434.26 | 1.88 | 2.26 |
| PFA | PFA | McMaster Carr | 26.9 | 295 | RSO | 427.91 | 1.69 | 2.08 |
| PEEK | | | 6.25 | 77 | LN2 | 453.33 | 1.63 | 1.80 |
| | Dupont | Kapton | 8.25 | 77 | LN2 | 359.60 | 1.63 | 2.84 |
| SMK | | | 8.25 | 77 | LN2 | 311.11 | 1.47 | 3.39 |
| FEP | FEP | McMaster Carr | 24.8 | 295 | RSO | 414.14 | 1.46 | 1.93 |
| ETFE | AGC | | 12.0 | 77 | LN2 | 383.33 | 1.29 | 1.98 |
| PFA | PFA | | 26.9 | 77 | LN2 | 367.44 | 1.18 | 1.97 |
| PTFE | PTFE | | 11.1 | 295 | RSO | 392.73 | 1.13 | 1.66 |
| FEP | FEP | McMaster Carr | 24.8 | 77 | LN2 | 294.95 | 0.71 | 1.84 |
| Teflon | Teflon | McMaster Carr | 58.6 | 77 | LN2 | 200.41 | 0.37 | 2.06 |

### *7.2.8 Double Sided Metallized Stamp Capacitors*

The data obtained initially on stamp capacitor test samples of PVDF at 77 K did not indicate the x2 to x3 increase in breakdown strength that was anticipated based on the published literature. It was hypothesized that this was because the stamp capacitor configuration included gaps between the film sample under test and the metallized electrodes. This possibility was addressed by testing film samples that were metallized on both sides, thereby excluding any other material from the dielectric. Figure 7-29 shows the two-aluminum metallization layers overlapping in the "active capacitance" region on two test areas prepared on one film sample.

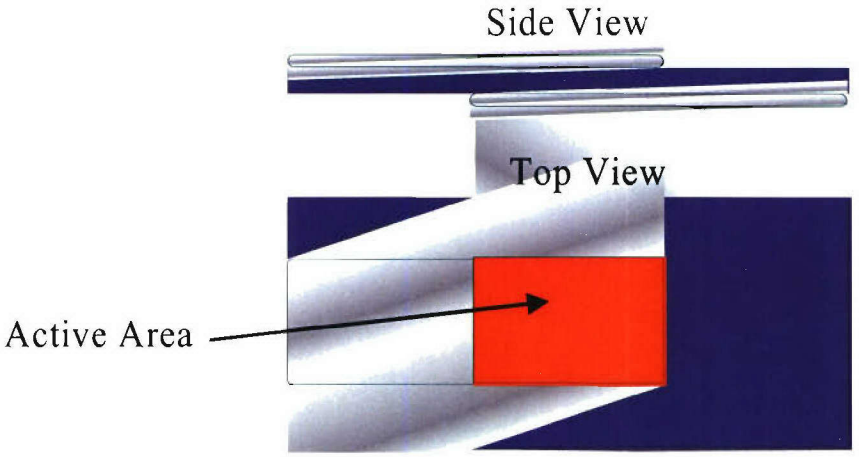


***Fig. 7-29. Double metallized sample active area***

The metallization of these samples was done by GA Display Products and the finished product can be seen in Fig. 7-30. Two samples were prepared on one sheet of film and separated before testing. This cut down on time and expense of making the samples.

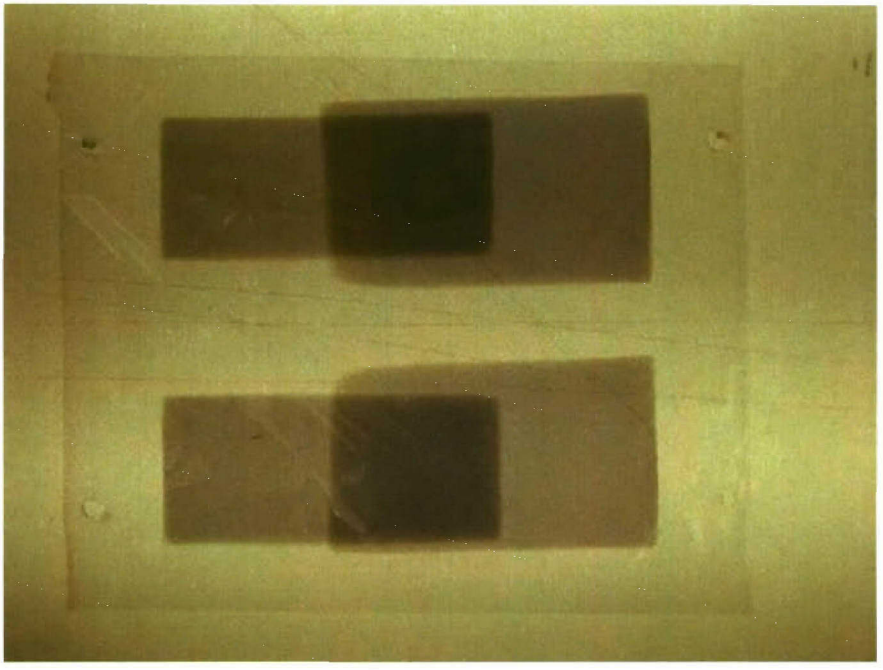

***Fig. 7-30. Double Sided Metallized film electrodes seen in transmitted light***

With this sample arrangement, ESI measured an increase in breakdown strength between room temperature and 77 K for PVDF from 396 V/μm to 672-708 V/μm (70-79%), for PET from 573 to 648-678 V/μm (13-18%), and for PPL from 622 to 654-673 V/μm (5-8%). Unfortunately, the dielectric constant of the PVDF sample fell from 10.08 to 2.63 (74%) due to the effect of temperature, so that there was *negligible net gain in energy density*. The measured energy density at breakdown in PVDF was just under 6 J/cc, as seen in Table 7-23.

**Table 7-23**
**Double Metallized Stamp Capacitor Test Results**

| Summary of Stamp Capacitor Testing Sorted By Avg Max J/CC | | | | | | | | | |
|---|---|---|---|---|---|---|---|---|---|
| Test Date | Film | Manufacture | Comments | Thickness in um | Temp in Kelvin | Impregnate | Avg Max V/um | Avg Max J/CC | Dielectric Constant |
| Metallized Room Temperture Stamp Capacitors | | | | | | | | | |
| 9-Aug | PVDF | Kureha | Metallized | 8.333 | 295 | SO | 396.16 | 7.01 | 10.08 |
| 9-Aug | PET | Bolmet | Metallized | 5.1 | 295 | SO | 573.12 | 4.43 | 3.06 |
| 9-Aug | PPL | Bollore | Metallized | 7.88 | 295 | SO | 621.83 | 3.85 | 2.25 |
| Metallized Liquid Nitrogen Stamp Capacitors | | | | | | | | | |
| 2-Aug | PVDF | Kureha | Metallized | 8.333 | 77 | LN2 | 708.00 | 5.98 | 2.65 |
| 2-Aug | PET | Bolmet | Metallized | 5.1 | 77 | LN2 | 678.52 | 5.46 | 2.68 |
| 2-Aug | PPL | Bollore | Metallized | 7.88 | 77 | LN2 | 653.55 | 4.14 | 2.18 |
| Metallized Liquid Nitrogen Stamp Capacitors | | | | | | | | | |
| 27-Jul | PET | Bolmet | Metallized | 5.06 | 77 | LN2 | 671.94 | 5.23 | 2.62 |
| 27-Jul | PVDF | Kureha | Metallized | 8.3 | 77 | LN2 | 648.00 | 4.91 | 2.58 |
| 27-Jul | PPL | Bollore | Metallized | 7.88 | 77 | LN2 | 672.59 | 4.52 | 2.26 |

### *7.2.9 Miscellaneous PVDF Stamp Capacitor Testing*

Other tests were performed on PVDF stamp capacitors to determine if any more information could be obtained from the samples.

#### *7.2.9.1 PVDF Energy Measurements*

Measurements of energy input and output during PVDF stamp capacitor charge/discharge cycles were attempted in order to characterize the ferroelectric behavior of PVDF at 77 K and determine if the effective dielectric constant was reduced to low values as observed at low fields with an LCR meter. Unfortunately the noise using the available equipment was enough to overwhelm measurements of the very small currents involved. It was decided to test PVDF model capacitors instead. Ten units were transferred from the NSWC/GA Railgun project for this purpose and the results for this testing are discussed in Section 7.2.10.4.

#### *7.2.9.2 PVDF Poling Process Experiments*

It was hypothesized that a higher dielectric constant might be obtained in PVDF by applying a moderate electric field to orient the dipoles or "pole" the film, and then cooling to cryogenic temperature. A PVDF stamp capacitor was held at 2000 Vdc (250 V/μm) for one hour at room temperature and then cooled to 77 K while held at voltage. The voltage was held for an additional hour, and then the capacitance was measured. The apparent dielectric constant had decreased from 10.4 at room temperature to 2.53 at 77 K.

#### *7.2.9.3 PVDF Voltage Coefficient Measurements*

The apparatus shown schematically in Fig. 7-31 was used to measure the apparent dielectric constant, proportional to dQ/dV, as a function of DC bias voltage. Figure 7-32 shows the results, with the dielectric constant measured in this way decreasing from 10.0 at near-zero volts to 7.0 at 2000 V (250 V/μm).

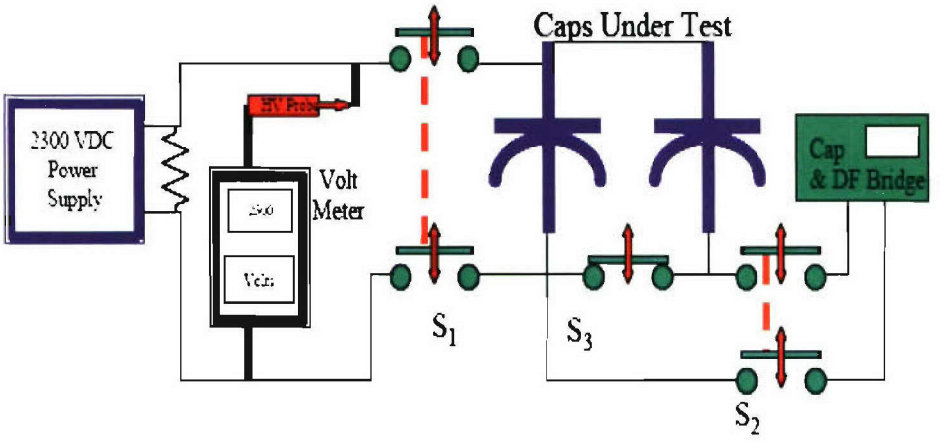


***Fig. 7-31. Sawyer-tower circuit used for measuring voltage coefficient of capacitance and dielectric constant***

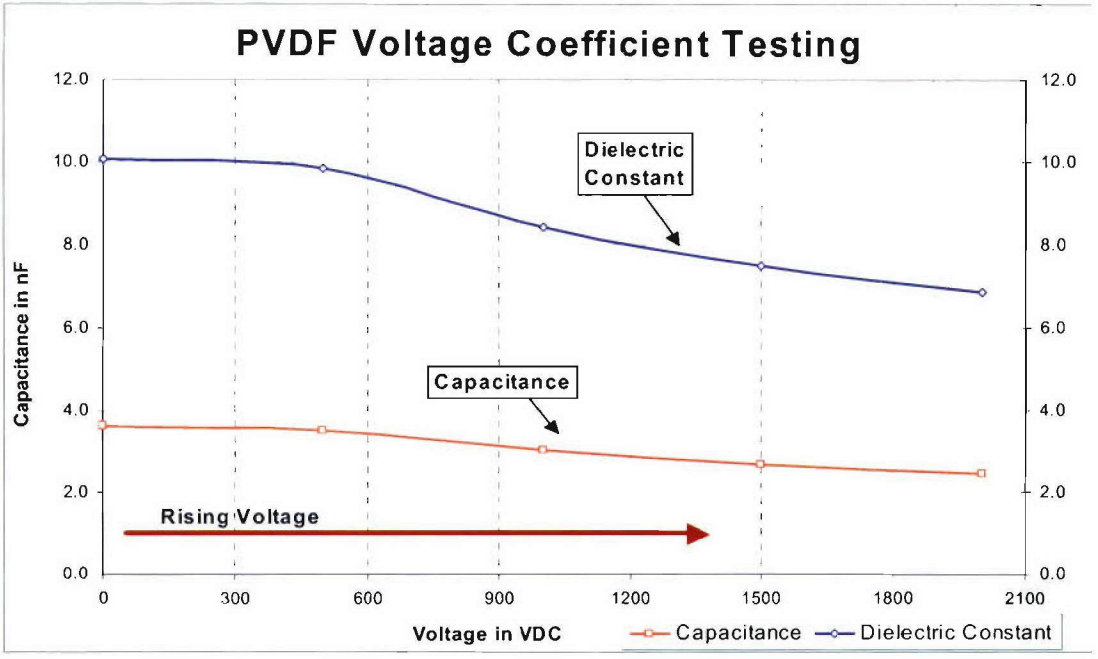


*Fig. 7-32. PVDF voltage dependence of capacitance and dielectric constant*

### *7.2.9.4 PVDF Frequency Scan*

A metallized PVDF stamp capacitor immersed in $LN_2$ was measured for capacitance and dissipation factor as a function of frequency from 10 Hz to 1 MHz. The relative dielectric constant (normalized at the 10 Hz value) and the dissipation factor are shown in Figures 7-33 and 7-34, respectively. The dielectric constant decreases rapidly between about 1 kHz and 10 kHz, eventually stabilizing at about 30% of its low frequency value above 100 kHz. It is presumed that the low frequency value still includes dipole rotation, which is unable to respond in phase at higher frequencies, and that the highest frequency value includes only electronic polarization. The dissipation factor shows that the dipole rotation becomes a major loss mechanism in the kHz-frequency band, then decreases. Above 100 kHz the rapidly increasing DF is due to ohmic resistance in the electrodes, since the ESR (graph not shown) is seen to become constant in this band.

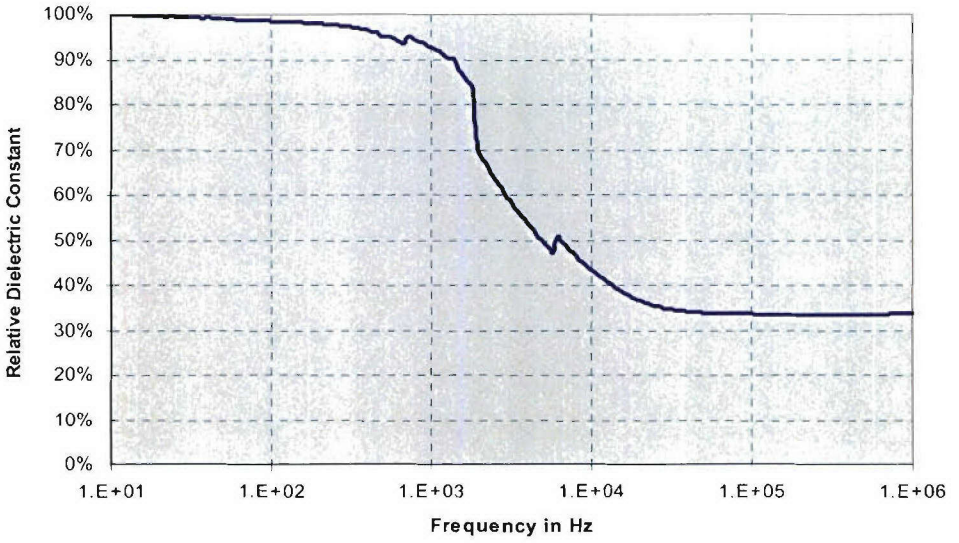


*Fig. 7-33. Relative dielectric constant of PVDF at 77 K as a function frequency*

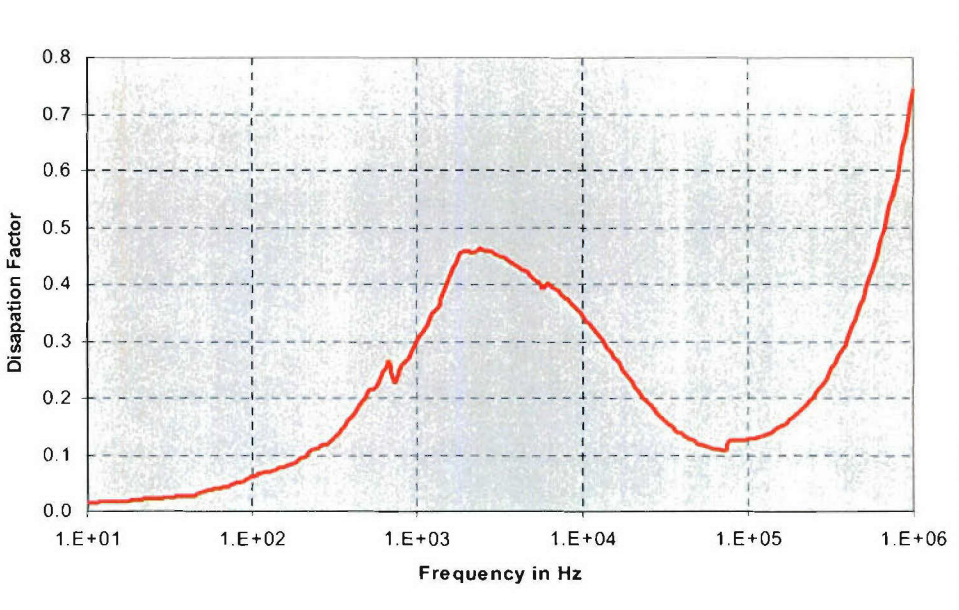


*Fig. 7-34. Dissipation factor of PVDF at 77 K as a function of frequency*

### *7.2.9.5 PVDF Temperature Scan*

The dielectric constant of PVDF was measured as a function of temperature using a stamp capacitor to determine the effect that cooling the capacitor to liquid nitrogen temperatures. As seen in Fig. 7-35, the large decrease in dielectric constant observed at cryogenic temperature actually occurs at about –40°C, the glass transition temperature for this polymer. This confirms our hypothesis that this effect is due to the "freezing out" of dipole motion.

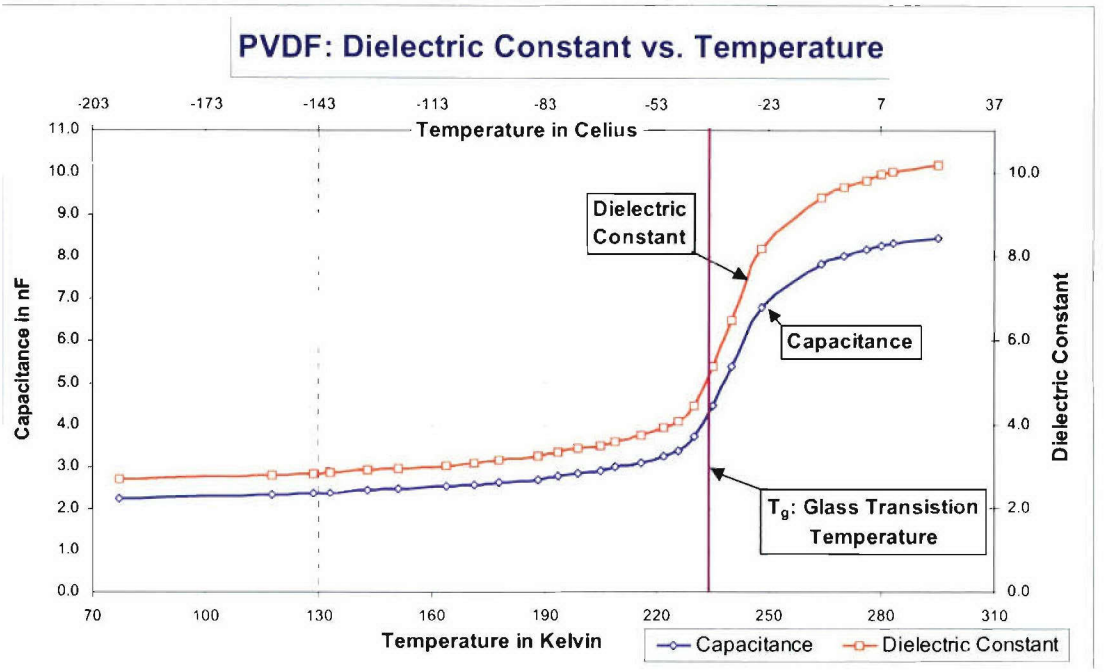


*Fig. 7-35. Dielectric constant of PVDF vs. temperature*

### *7.2.9.6 Pressurized Vessel Stamp Capacitor Test*

In order to initially test the effect of pressurization, it was decided to test a stamp capacitor in one of the reusable vessels built for the program. The breakdown strength (500 V/μm) of the PVDF sample did not increase between ambient pressure in $LN_2$ and 3 bars pressurized LN2 at 77 K. This test measured the breakdown strength of a film sample, however, and may not be a good indication of the breakdown strength of $LN_2$ or of surface flashover in $LN_2$.

### *7.2.10 Model Capacitor Testing*

PN 30956 is a polypropylene capacitor that is readily available and was chosen for nearly all of the model sized capacitor testing.

#### *7.2.10.1 Maximum Voltage Test PN 30956*

Testing was conducted to determine the maximum breakdown voltage of model-sized capacitor made from polypropylene at cryogenic temperatures. As seen in Fig. 7-36 the breakdown voltage was between 3000 and 3300 VDC. For the 4.8 μm film used in this capacitor the voltage levels translated to breakdown strength of 625 to 687 V/μm.

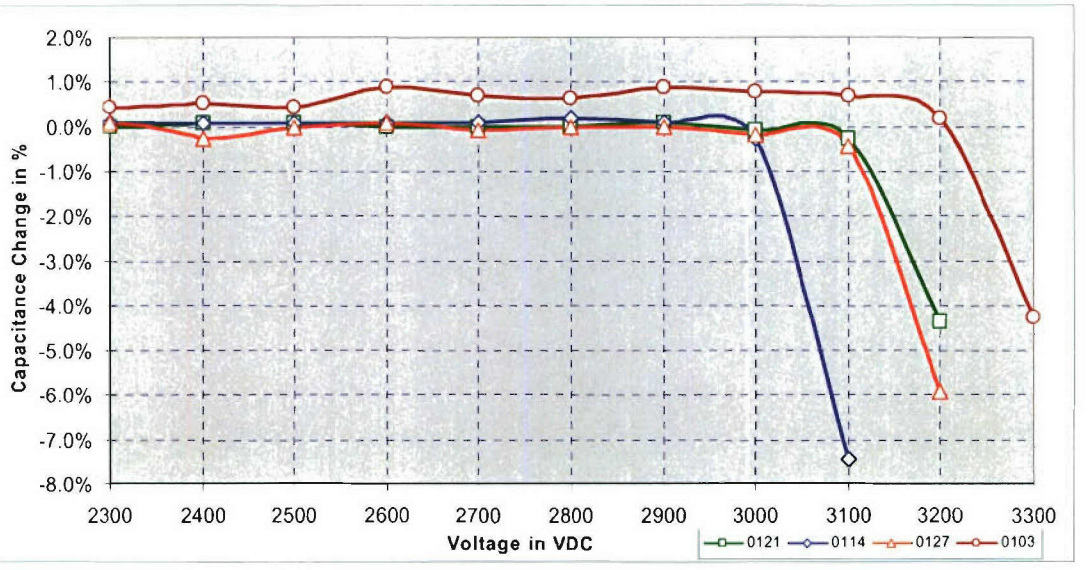


***Fig. 7-36. Maximum voltage test results of PN 30956 in $LN_2$***

The maximum voltage test results were then calculated to determine the energy density in just the winding of the capacitor. These results can be seen in Fig. 7-37 and show that the energy density never got higher than 4.00 J/cc.

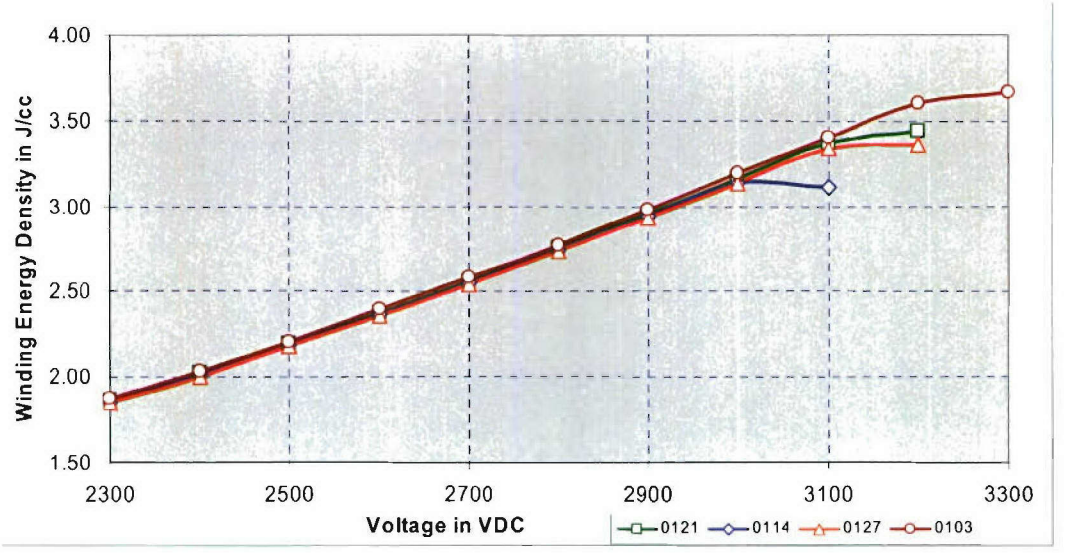


***Fig. 7-37. Maximum voltage resulting energy density***

### *7.2.10.2 Room Temperature Cycle Testing (PN 30956)*

Life cycle testing was performed on three capacitors of PN 309556 at a voltage of 2.5 kV. Results of this testing can be seen in Fig. 7-38. The life of these capacitors, determined after 5% capacitance loss, was 17,000 for two of the units and 22,000 for the other. This testing was done for comparison with $LN_2$ temperature testing done at

the same voltage being performed at GA. Results from that test showed that the capacitors could last over 75,000 cycles with little or no capacitance loss.

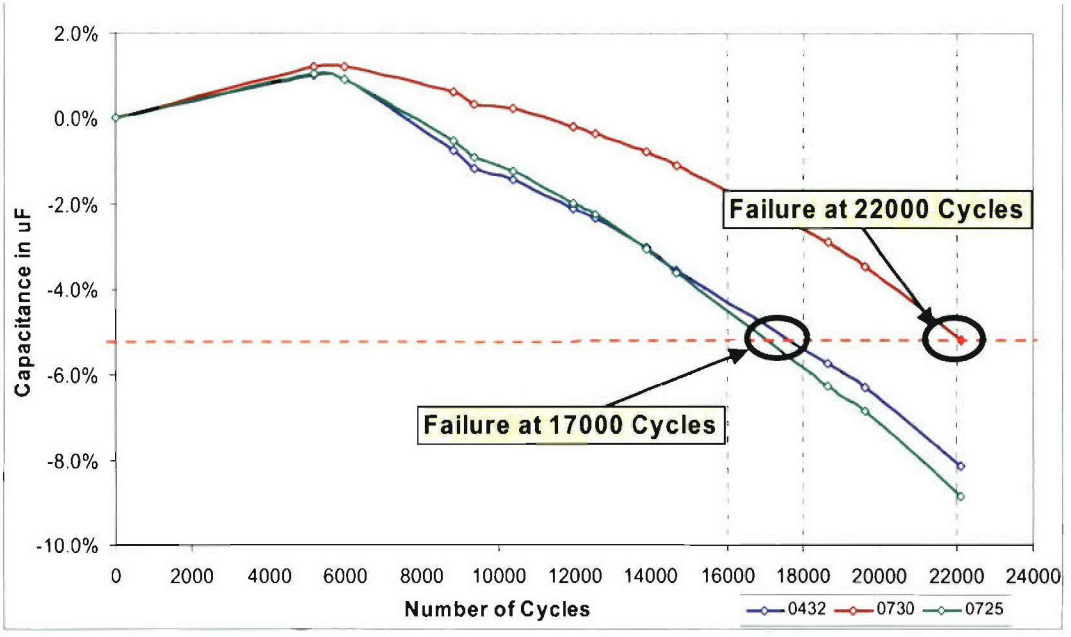


***Fig. 7-38. Room temperature cycle testing of PN 30956***

### *7.2.10.3 DC Life Testing*

DC life testing consists of charging a capacitor to a set voltage and maintaining that voltage for an extended period of time. Capacitance is measured at intervals that allow for the observation of a sample that is losing capacitance. The failure criterion for this test is a capacitance loss of greater than 5%.

The capacitors tested at ESI were varied in test voltage and in test temperature. The test voltages were 2.5 and 2.9 kV. The temperatures used were room and cryogenic temperature.

### *7.2.10 3.1 2.5 KV DC Life Test*

PN 30956 has a rated voltage of 2.3 kV. It was decided that a voltage that was a higher voltage than the rated voltage was needed to speed up the failure of the capacitor. 2.5 kV was the first voltage chosen for this series of tests. After 200 hours the capacitor being tested it showed no capacitance loss as shown in Fig. 7-39. This test was stopped after 220 hours after it determined that the capacitor could last much longer than initially anticipated.

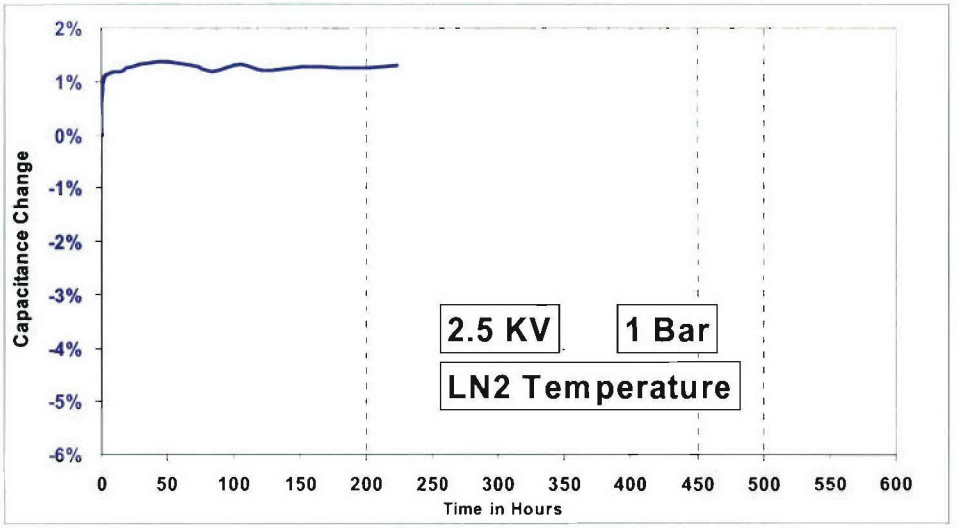


*Fig. 7-39. Cryogenic DC life test of PN 30956 at 2.5 kV*

Room temperature data from another program for two capacitors with the same parameters for testing with the exception of temperature was located. This data is shown in Fig. 7-40. This confirmed earlier thoughts that the testing would last well into the 1000's of hours since the room temperature capacitors lasted over 400 hours.

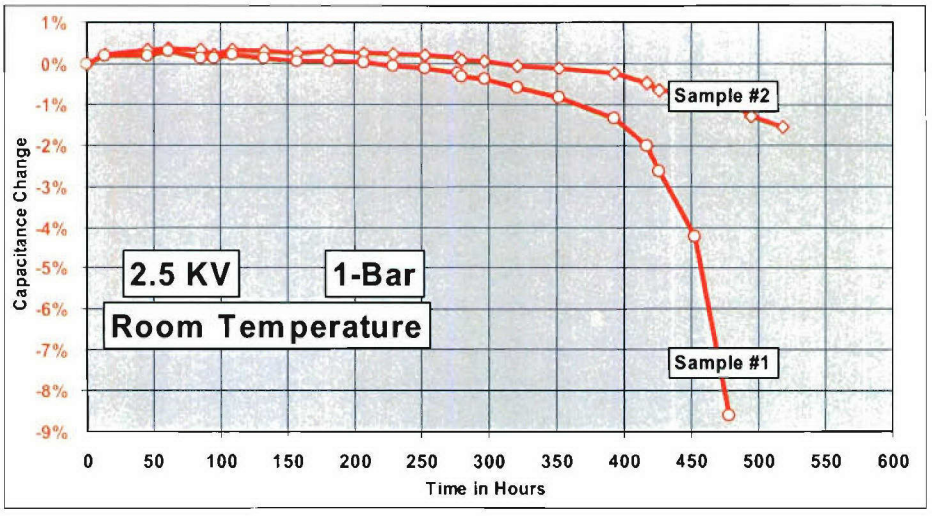


*Fig. 7-40. Room temperature DC life test at 2.5 kV*

### *7.2.10.3.2 2.9 kV DC Life Testing*

After it was determined that the capacitors tested at 2.5 kV would not fail within a reasonable time frame the testing voltage was increased to 2.9 kV. The 2.9 kV level was chosen because it seem to be the highest voltage level that could be achieved without a flashover failure becoming a problem.

Two capacitors were tested in liquid nitrogen at atmospheric pressure (1 bar). The results of this testing can be seen in Fig. 7-41. Only one of the two capacitors tested failed from capacitance loss and this happened at around 26 hours. The other capacitor failed when a flashover occurred in the margin of the capacitor. The result of this failure can be seen in Fig. 7-42. The failure was catastrophic and destroyed the dewar that was being used. This failure was observed in another capacitor tested under the same conditions. From these failures it was determined that a flashover failure has a high likeliness of occurring in these capacitors under the conditions tested, i.e., 2.9 kV, 1 bar. Flashover failures were not observed in capacitors tested at the same voltage but at 3 bar. This is due to the increased withstand voltage of liquid nitrogen at increased pressures.

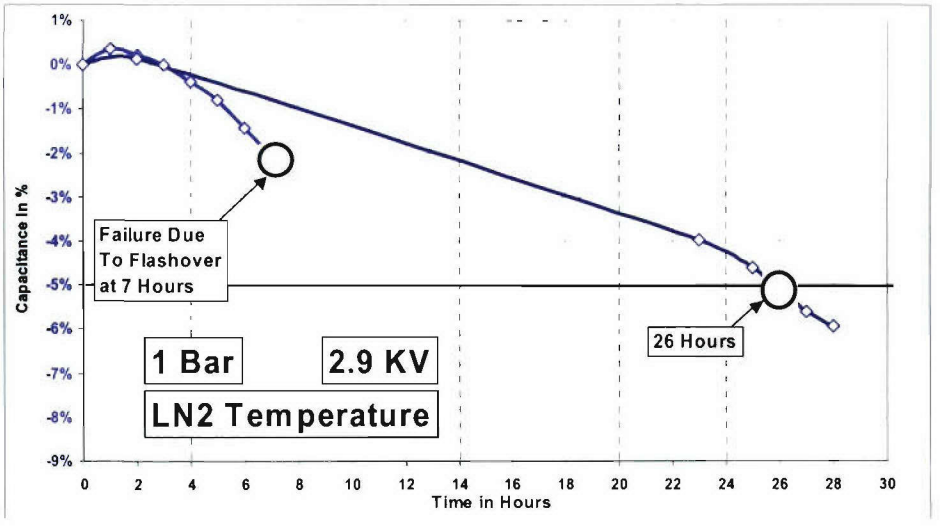


***Fig. 7-41. $LN_2$ temperature DC life test PN 30956 at 2.9 kV***

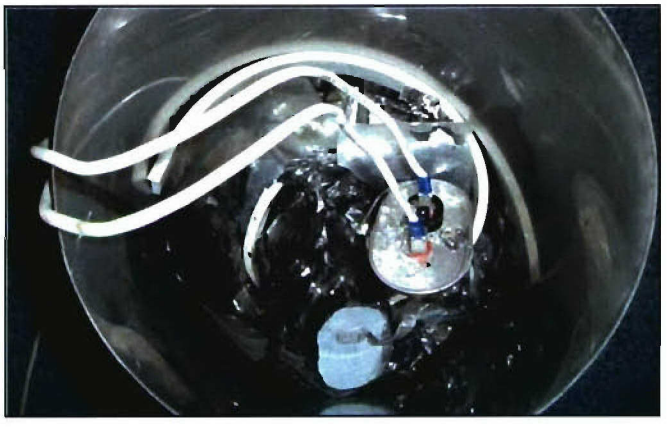

***Fig. 7-42. Flashover failure result***

Life tests at 2.9 kV were also performed at room temperature on three separate capacitors. The results of this testing showed that the failure time was between 17 and 19 hours as shown in Fig. 7-43. While this data is not impressive when compared to the $LN_2$ tested samples at 1 bar, it is when compared to the 3-bar samples which lasted nearly 50 times longer at the same voltage.

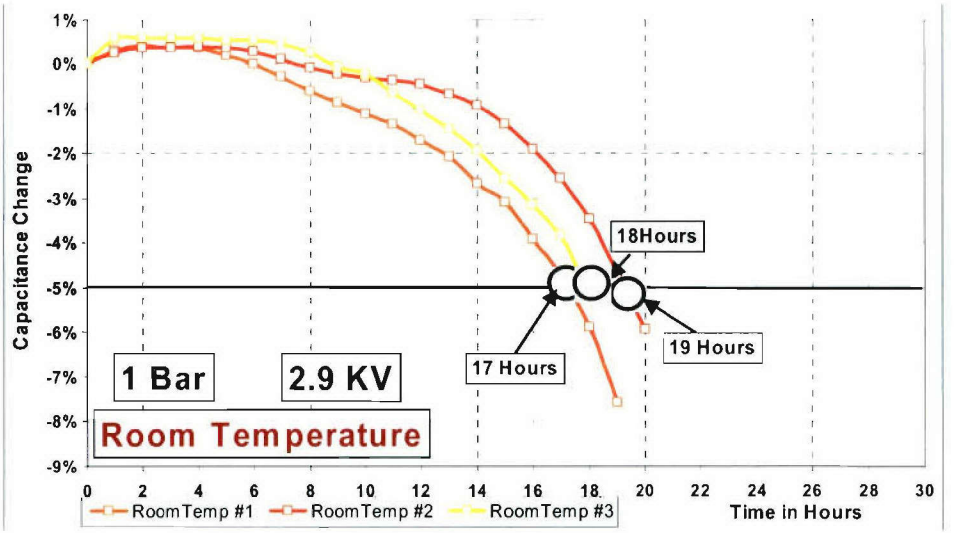


*Fig. 7-43. Room temperature DC life test PN 30956 at 2.9 kV*

### *7.2.10.4 PVDF Energy Measurements*

Measurements of energy input and output during PVDF stamp capacitor charge/discharge cycles were attempted in order to characterize the ferroelectric behavior of PVDF at 77 K and determine if the effective dielectric constant was reduced to low values as observed at low fields with an LCR meter. Unfortunately the noise using the available equipment was enough to overwhelm measurements of the very small currents involved. It was decided to test PVDF model capacitors instead. Ten units were transferred from the NSWC/GA Railgun project for this purpose.

With these transferred capacitors the energy in and out from them could be more readily made. An experiment was conducted using voltage levels of 2, 3, and 4 kV at $LN_2$ temperature to determine both the energy put into the capacitor and the energy received from the capacitor. Calculated energy values were predetermined by using the capacitance found with a low level field and the voltage level at the time of discharge. The values from this portion of the experiment can be seen in Table 7-24. Measured energy values were taken and are displayed in Table 7-25.

**Table 7-24**
**PVDF Model Cap Calculated Energy Values**

| Calculated Energy Values | | |
|---|---|---|
| **Voltage** | **Cap in uF** | **Calc. Energy** |
| 1966 | 8.06 | 15.58 |
| 1966 | 8.11 | 35.67 |
| 3980 | 8.13 | 64.39 |

**Table 7-25**
**PVDF Model Cap Measured Energy Values**

| Measured Energy Values | | | |
|---|---|---|---|
| Voltage | Energy Out in Joules | Energy In in Joules | $E_{out}/E_{in}$ |
| 2000 | 12.18 | 16.95 | 71.88% |
| 3000 | 30.38 | 40.81 | 74.45% |
| 4000 | 56.88 | 74.03 | 76.83% |

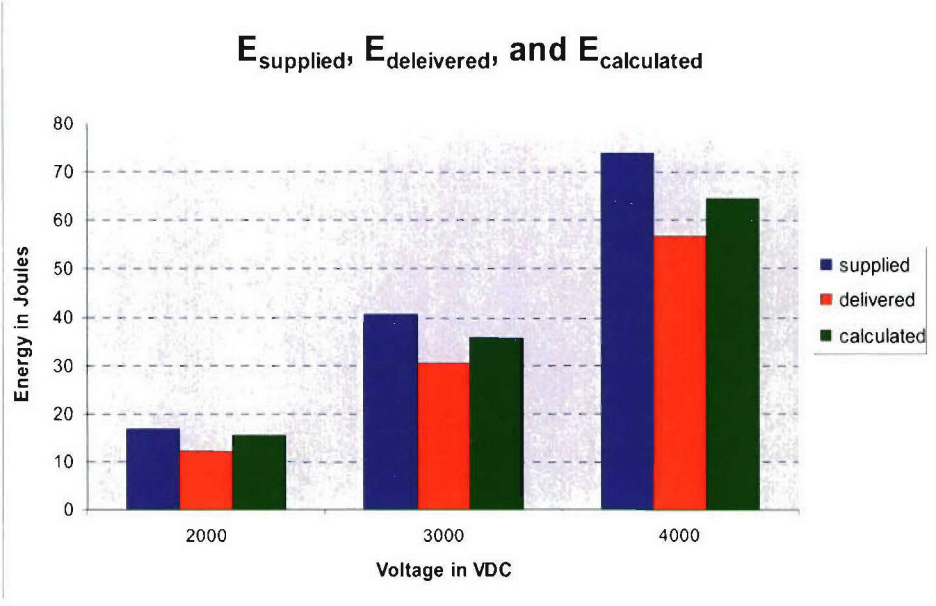


***Fig. 7-44. PVDF energy efficiency***

The energy out value from the table above at 4 kV has an energy density of about 2 J/cc, which is actually lower than the values obtained for the same capacitor at room temperature. At this time PVDF does not seem like a usable option for the cryocapacitor due to the properties it has at the $LN_2$ temperature.

### *7.2.10.5 Miscellaneous Testing*

Other tasks were performed to aid in the development of the cryo-capacitor. This ranges from impregnate investigations to the autopsy of capacitors to determine failure modes. The following sections are the result of this and other work performed in this area.

#### *7.2.10.5.1 Failure Analysis of 1-Bar and 3-Bar Life Tested Capacitors*

Two capacitors of PN 30956 were cycle life tested at 77 K. One capacitor was tested at atmospheric pressure while the other was tested at 3 bar. The remaining parameters for this test can be seen in Table 7-26.

**Table 7-26**
**Cycle Testing Parameters**

| | Sample #1 | Sample #2 |
|---|---|---|
| Pressure | 1 bar | 3 bar |
| Temperature | 77 K | 77 K |
| Voltage | 2.87 kV | 2.87 kV |
| No. of Cycles | 11,000 | 70,000 |
| Cap Loss | > 5% | ~ 3% |

With the results of the test it was obvious that the capacitor tested at the higher pressure performed significantly better than the one tested at atmospheric pressure. Autopsies were performed on both capacitors at ESI to determine the differences in the failures.

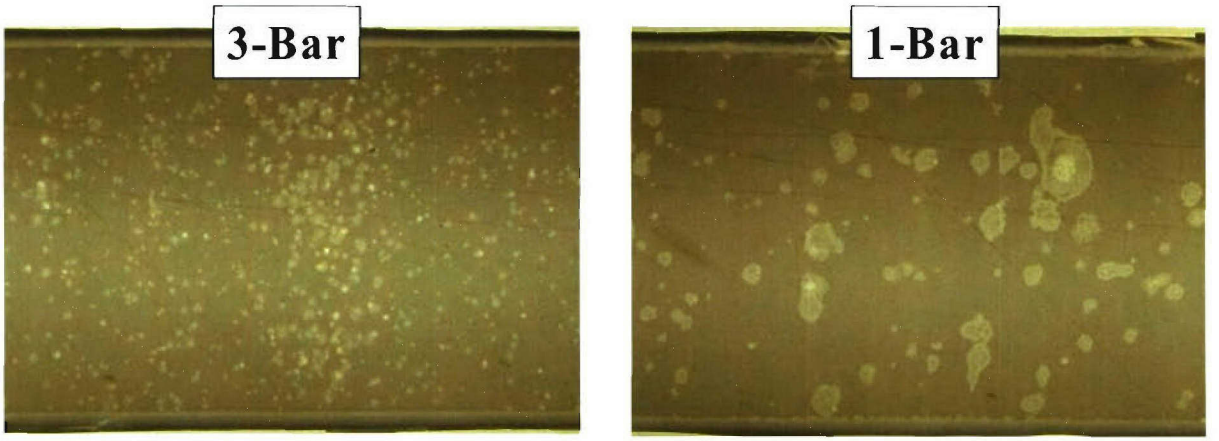


***Fig. 7-45. Typical sections of the 1-bar and 3-bar capacitors with backlighting***

From the results of the autopsy it was noted that the 1-bar sample had large clearing areas while the 3-bar sample had numerous small clearing areas. The theory is that bubbles of nitrogen gas are generated at the clearing sites during the self-healing process. Partial discharges (corona) occur in these nitrogen bubbles at 1 bar which in turn erodes the metallization around the clearings. The pressurization at 3-bar reduces the size of the nitrogen gas bubbles and increases the dielectric strength of the nitrogen gas.

It was determined from this testing that pressurization of the cryocapacitor could aid in the increase of life of the capacitor and prevent possibility of flushover.

#### *7.2.10.5.2 Silicon Oil Breakdown Test*

AC breakdown voltage testing was performed on two oils provided to ESI at room temperature. As a control ESI's normal silicon oil was added. This test was performed at 60 Hz. The results of this test can be seen in Table 7-27 and in Fig. 7-46.

**Table 7-27**
**Silicon Oils AC Breakdown Voltages (in kV)**

| | 1.5 cs Silicon Oil | 1.0 cs Silicon Oil | 200 cs Silicon Oil |
|---|---|---|---|
| 1st | 17.3 | 26 | 21 |
| 2nd | 19.5 | 26.8 | 21.5 |
| 3rd | 17.5 | 26.5 | 21 |
| **Average** | **18.1** | **26.4** | **21.2** |

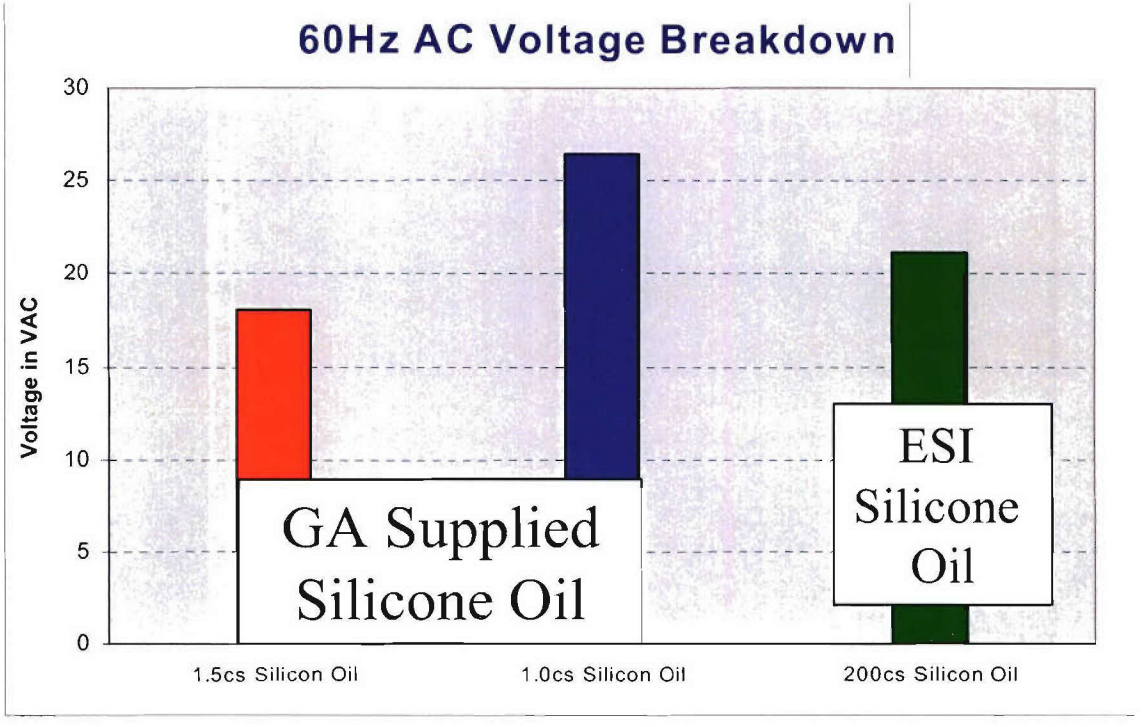


***Fig. 7-46. 60 Hz AC breakdown of various silicon oils***

Testing of these oils was done before it was determined that liquid nitrogen would be the impregnate of the cryocapacitor.

### *7.2.10.5.3 Alternate Impregnation Search*

An investigation was conducted to determine if alternate impregnation materials for the cryocapacitor would be possible. The issue with the usual room temperature impregnates is they become solid and shrink at cryogenic temperatures. It is theorized that as they become solid these impregnates form crystalline structures. These structures are then jagged and when voltage is applied the electrostatic forces of the capacitor causes the film to contract against the impregnate thereby damaging the film. For this purpose and for the removal of heat within the capacitor it was determine that an impregnate that remained a liquid or semi-liquid at 77 K was needed.

One of the possible impregnates discussed was $CO_2$. After investigation into the phase diagram of $CO_2$ it was determined that this would not be a suitable impregnate because of the pressure needed to maintain it as a liquid. This can be seen in Fig. 7-47.

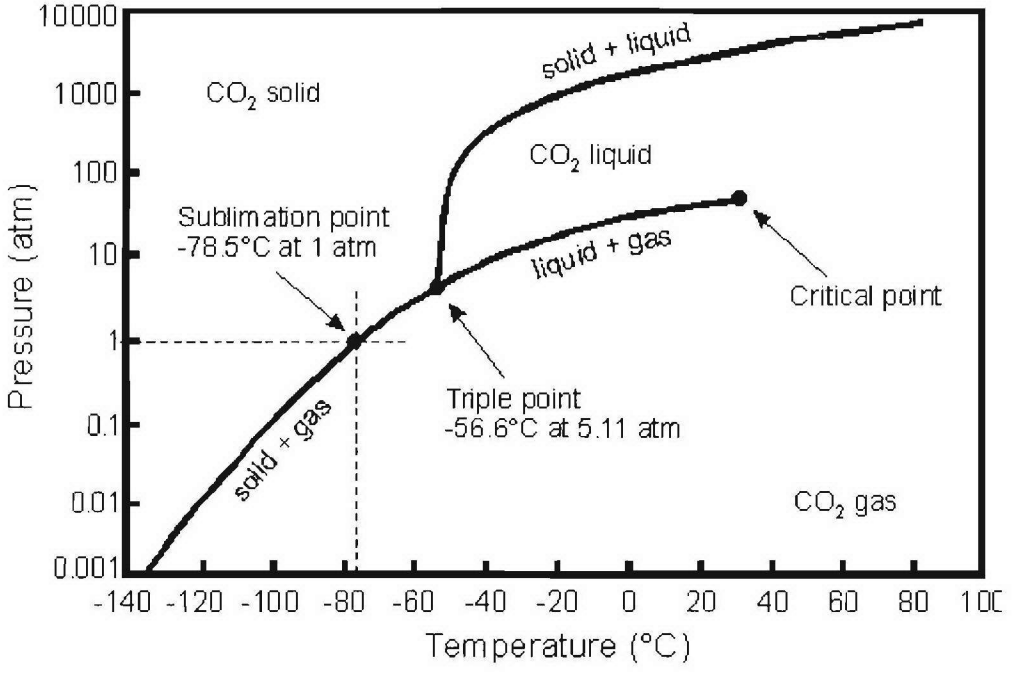


***Fig. 7-47. Phase diagram of $CO_2$***

## *7.3 MTECH*

### *7.3.1 MTECH Test Results*

#### *7.3.1.1 Saran Premium Films*

The first stamp tests at MTECH were performed on Saran Premium (low density polyethylene) films, used to calibrate the metallization process and to test the data acquisition capabilities of the setup, which had previously only been tested on packaged COTS devices. The dimensions of the overlapping metallized sides of the film were 3.175 cm by 2.540 cm (1.250 in. by 1.000 in.), giving a total surface area of 8.0645 $cm^2$. There were three stamps per plate, with 9 plates per evaporation run (27 stamps per run). Results are summarized in Tables 7-28 and 7-29.

**Table 7-28**
**Test Results for Saran Premium Stamp Capacitors**

| Sample Number | Initial Capacitance | Final Capacitance | Onset of Clearing | Onset of Significant Clearing | Highest Test Voltage |
|---|---|---|---|---|---|
| 1a | 1.0 nF | 0.00133 nF | 2100 V | 3100 V | 9100 V |
| 1b | 1.1 nF | 0.0038 nF | 1590 V | 3600 V | 5000 V |
| 1c | 1.1 nF | 0.0054 nF | 2800 V | 4500 V | 5052 V |
| 2a | 1.07 nF | 0.0012 nF | 2000 V | 2500 V | 4500 V |
| 2b | 1.13 nF | 0.0012 nF | 1400 V | 2700 V | 4000 V |
| 2c | 1.12 nF | 0.0017 nF | 800 V | 2500 V | 4100 V |
| 3a | 1.168 nF | 1.104 nF | 3258 V | 3258 V | 3800 V |
| 3b | 1.147 nF | 1.147 nF | 3135 V | 3135 V | 3135 V |
| 3c | 1.178 nF | 1.076 nF | 3935 V | 3935 V | 4200 V |

**Table 7-29**
**Further Test Results for Saran Premium Stamp Capacitors**

| Sample Number | Initial Capacitance | Dielectric Constant | Onset of Significant Clearing | Breakdown Strength* | Energy Density |
|---|---|---|---|---|---|
| 1a | 1.0 nF | 2.10 | 3100 V | 207 V/μm | 0.40 J/cc |
| 1b | 1.1 nF | 2.31 | 3600 V | 240 V/μm | 0.59 J/cc |
| 1c | 1.1 nF | 2.31 | 4500 V | 300 V/μm | 0.92 J/cc |
| 2a | 1.07 nF | 2.24 | 2500 V | 167 V/μm | 0.28 J/cc |
| 2b | 1.13 nF | 2.37 | 2700 V | 180 V/μm | 0.34 J/cc |
| 2c | 1.12 nF | 2.35 | 2500 V | 167 V/μm | 0.29 J/cc |
| 3a | 1.168 nF | 2.45 | 3258 V | 217 V/μm | 0.51 J/cc |
| 3b | 1.147 nF | 2.41 | 3135 V | 209 V/μm | 0.47 J/cc |
| 3c | 1.178 nF | 2.47 | 3935 V | 262 V/μm | 0.75 J/cc |

*Assumes a film thickness of 15 microns; based on voltage for onset of significant clearing.

The expected dielectric constant was between 2.2 and 2.35, so the assumption of a film thickness of 15 μm seems to be accurate enough for the purposes of the test setup evaluation. The measured breakdown strengths were also close to the expected value of 200 V/μm. Again, the main goal of these tests was to verify that the test setup was working correctly, and that the metallization process did not damage the films.

### *7.3.2 Results for Goodfellow Films*

MTECH ordered a number of films from a British company called Goodfellow (www.goodfellow.com). The films and their thicknesses are shown in Table 7-30.

**Table 7-30**
**Materials Ordered from Goodfellow**

| Material | Thickness | Material | Thickness |
|---|---|---|---|
| Polyamide (Nylon-6) | 15 μm | PEI | 25 μm |
| Polyimide | 25 μm | PPS | 25 μm |
| Polyimide | 8 μm | PEN | 25 μm |
| PVDF | 50 μm | PVDC | 12.5 μm |
| PVDF | 4.5 μm | PVF | 25 μm |
| PMMA | 50 μm | PVF | 13 μm |
| E-CTFE | 12.5 μm | Cellulose Acetate | 25 μm |
| Polycarbonate | 6 μm | PTFE | 10 μm |
| PEEK | 25 μm | FEB | 25 μm |
| PES | 25 μm | ETFE | 25 μm |

Polyimide: Treated and untreated films (CN, HR, KJ Types)
PVDF: Biaxially and uniaxially oriented films
PVF: Modified and unmodified films

After consulting with General Atomics, a selection of these films was sent to Albany NanoTech for metallization, including two sheets of 15-μm -thick Nylon-6, two sheets of 4.5-μm PVDF, two sheets of 13-μm PVF, and one sheet of 50-μm PMMA. Each sheet of film yielded three stamp capacitors, each with a plate area of 8.0645 $cm^2$.

Table 7-31 shows the measured capacitance values for 300 K and 77 K, and the calculated relative dielectric constants. For Nylon-6, the second batch yielded slightly higher capacitance values. This could be the result of variations in film thickness from sheet to sheet. In general, the dielectric constants, and therefore the measured capacitance values, decreased significantly when the stamps were cooled to 77 K. For Nylon-6, this decrease represented a factor of 2.2, compared to a factor of 3.6 for PVDF, and 2.8 for PVF. The dielectric constant of PMMA dropped by about 35% at low temperatures.

The breakdown voltages of these films are shown in Table 7-32. To measure these, the applied voltage was increased in 100-V steps. After each step in voltage, the capacitance was re-measured. The breakdown voltage was defined as the applied voltage that resulted in a 5% drop in capacitance due to clearing effects. In general, the breakdown voltages at 77 K were significantly higher than those measured at 300 K. Despite the decrease in relative dielectric constant, and therefore in capacitance, at low temperatures, the increase in energy density was significant for some films. For Nylon-6, for example, the energy density improved by a factor of about 2. In the case of Polyvinyl Fluoride (PVF), the energy density improved by a factor of 3 to 8.

## Table 7-31
## Measured Capacitance and Calculated Relative Dielectric Constants of Various Goodfellow Films

**The plate area of each stamp capacitor was 8.0645 $cm^2$.**

| *Material* | *Designation* | *Cap* | *C, 300 K (nF)* | *C, 77 K (nF)* | *Thickness ( μ m)* | *Diel. Const., 300 K* | *Diel. Const., 77 K* |
|---|---|---|---|---|---|---|---|
| Nylon-6 | MT4A | A | 2.67 | -- | 15 | 5.6 | -- |
| | | B | 2.67 | -- | 15 | 5.6 | -- |
| | | C | 2.80 | -- | 15 | 5.9 | -- |
| Nylon-6 | MT4B | A | 3.16 | 1.36 | 15 | 6.6 | 2.9 |
| | | B | 3.20 | 1.41 | 15 | 6.7 | 3.0 |
| | | C | 3.21 | 1.44 | 15 | 6.7 | 3.0 |
| PVDF | MT4G | A | 17.2 | -- | 4.5 | 10.8 | -- |
| | | B | 16.5 | -- | 4.5 | 10.4 | -- |
| | | C | 16.7 | 4.59 | 4.5 | 10.5 | 2.9 |
| PVDF | MT4H | A | 17.5 | -- | 4.5 | 11.0 | -- |
| | | B | 16.6 | -- | 4.5 | 10.5 | -- |
| | | C | 16.5 | 4.56 | 4.5 | 10.4 | 2.9 |
| PVF | MT5C | A | 5.37 | -- | 13 | 9.8 | -- |
| | | B | 5.23 | -- | 13 | 9.5 | -- |
| | | C | 5.19 | -- | 13 | 9.5 | -- |
| PVF | MT5D | A | 5.19 | -- | 13 | 9.5 | -- |
| | | B | 5.24 | 1.88 | 13 | 9.5 | 3.4 |
| | | C | 5.00 | 1.77 | 13 | 9.1 | 3.2 |
| PMMA | MT4C | A | 0.50 | 0.37 | 50 | 3.5 | 2.6 |
| | | B | 0.49 | 0.37 | 50 | 3.5 | 2.6 |
| | | C | 0.49 | 0.36 | 50 | 3.5 | 2.5 |

## Table 7-32
## Breakdown Voltages and Energy Densities of Various Goodfellow Films

**Breakdown voltage was measured as the applied voltage that resulted in a 5% decrease in capacitance.**

| *Material* | *Designation* | *Cap* | *C, 300 K (nF)* | *C, 77 K (nF)* | *d ( μ m)* | *V Brk 5%, 300 K (V)* | *V Brk 5%, 77 K (V)* | *ED, 300 K (J/cc)* | *ED, 77 K (J/cc)* |
|---|---|---|---|---|---|---|---|---|---|
| Nylon-6 | MT4A | A | 2.67 | -- | 15 | 2600 | -- | 0.746 | -- |
| | | B | 2.67 | -- | 15 | 2400 | -- | 0.636 | -- |
| | | C | 2.80 | -- | 15 | 2500 | -- | 0.723 | -- |
| Nylon-6 | MT4B | A | 3.16 | 1.36 | 15 | -- | -- | -- | -- |
| | | B | 3.20 | 1.41 | 15 | -- | -- | -- | -- |
| | | C | 3.21 | 1.44 | 15 | -- | >5000 | -- | >1.488 |
| PVDF | MT4G | A | 17.20 | -- | 4.5 | 1900 | -- | 8.555 | -- |
| | | B | 16.50 | -- | 4.5 | 1900 | -- | 8.207 | -- |
| | | C | 16.70 | 4.59 | 4.5 | -- | 3000 | -- | 5.692 |
| PVDF | MT4H | A | 17.50 | -- | 4.5 | 1700 | -- | 6.968 | -- |
| | | B | 16.60 | -- | 4.5 | 400 | -- | 0.366 | -- |
| | | C | 16.50 | 4.56 | 4.5 | -- | 1750 | -- | 1.924 |
| PVF | MT5C | A | 5.37 | -- | 13 | 1500 | -- | 0.576 | -- |
| | | B | 5.23 | -- | 13 | 1700 | -- | 0.721 | -- |
| | | C | 5.19 | -- | 13 | -- | 5300 | -- | -- |
| PVF | MT5D | A | 5.19 | -- | 13 | 1000 | -- | 0.248 | -- |
| | | B | 5.24 | 1.88 | 13 | -- | 4800 | -- | 2.066 |
| | | C | 5.00 | 1.77 | 13 | -- | 4900 | -- | 2.027 |
| PMMA | MT4C | A | 0.50 | 0.37 | 50 | -- | -- | -- | -- |
| | | B | 0.49 | 0.37 | 50 | -- | -- | -- | -- |
| | | C | 0.49 | 0.36 | 50 | -- | >10,000 | -- | >0.448 |

The test setup was limited to voltages of 10 kV, and since no clearing occurred in the PMMA film below this voltage, we were not able to destroy this film and obtain a measured value for breakdown voltage. PMMA was not available from Goodfellow in thicknesses below 50 μm, and since the breakdown strength increases for thinner films, there was not much interest in testing to higher voltages. However, the voltage capability of the test setup could be increased to 30 kV for future testing.

The only film for which the energy density decreased at low temperatures was PVDF. This was due mainly to the enormous drop in dielectric constant through cryogenic cooling, a decrease of about a factor of 4. Table 7-33 summarizes the voltage breakdown data in terms of breakdown strength (V/μm).

**Table 7-33**
**Breakdown Strengths of Various Films Obtained from Goodfellow**
**The breakdown strength is derived from the breakdown voltages given in Table 7-31.**

| Sample | Material | Thickness | 300K Breakdown Strength | 77 K Breakdown Strength |
|---|---|---|---|---|
| MT4A(a) | Nylon-6 | 15 μm | 173 V/μm | --- |
| MT4A(b) | Nylon-6 | 15 μm | 160 V/μm | --- |
| MT4A(c) | Nylon-6 | 15 μm | 167 V/μm | --- |
| MT4B(c) | Nylon-6 | 15 μm | --- | >333 V/μm |
| MT4G(a) | PVDF | 4.5 μm | 422 V/μm | --- |
| MT4G(b) | PVDF | 4.5 μm | 422 V/μm | --- |
| MT4G(c) | PVDF | 4.5 μm | --- | 667 V/μm |
| MT4H(a) | PVDF | 4.5 μm | 378 V/μm | --- |
| MT4H(c) | PVDF | 4.5 μm | --- | 389 V/μm |
| MT5C(a) | PVF | 13 μm | 115 V/μm | --- |
| MT5C(b) | PVF | 13 μm | 131 V/μm | --- |
| MT5C(c) | PVF | 13 μm | --- | 408 V/μm |
| MT5D(b) | PVF | 13 μm | --- | 369 V/μm |
| MT5D(b) | PVF | 13 μm | --- | 377 V/μm |
| MT4C(c) | PMMA | 50 μm | --- | >200 V/μm |

One effect observed only in PVDF films was a change in capacitance after low voltages were applied, as illustrated in Table 7-34. This effect was only observed at 300 K [samples (a) and (b) in Table 7-33], and not at 77 K [sample (c)].

**Table 7-34**
**Increase in Dielectric Constant and Capacitance of 4.5-μm-thick PVDF Films at Room Temperature [Samples MT4G(a) and MT4G(b)] as a Result of the Application of Low Voltages**

**This polarization effect was not observed at 77 K [sample MT4G(c)].**

| Sample | Capacitance before voltage applied* | Capacitance after voltage applied* | Dielectric constant before voltage | Dielectric constant after voltage |
|---|---|---|---|---|
| MT4G(a) 300 K | 17.19 nF | 22.40 nF | 10.8 | 14.1 |
| MT4G(b) 300 K | 16.45 nF | 23.20 nF | 10.4 | 14.6 |
| MT4G(c) 77 K | 4.60 nF | 4.60 nF | 2.9 | 2.9 |

*Capacitance measured at 1 kHz.

Finally, each of these films exhibited a significant improvement in the dissipation factor, as shown in Table 7-35. The improvement for Nylon-6 was almost two orders of magnitude, although it was only a factor of about 3.5 for PVDF. The dissipation factor of PMMA decreased by about a factor of 40. These results are significant for applications where losses are important.

**Table 7-35**
**Comparison of Dissipation Factor Between Room Temperature and 77 K**

**Capacitance and breakdown voltages are also shown again for completeness.**

| | | | 300K @ 1kHz Vm=1.00V | | | 77K @ 1kHz Vm=1.00V | | |
|---|---|---|---|---|---|---|---|---|
| Material | Designation | Cap | Capacitance (nF) | D | V Break 5% (V) | Capacitance (nF) | D | V Break 5% (V) |
| Nylon-6 | MT4A | A | 2.67 | 0.1186 | 2600 | -- | -- | -- |
| | | B | 2.67 | 0.1230 | 2400 | -- | -- | -- |
| | | C | 2.80 | 0.1290 | 2500 | -- | -- | -- |
| Nylon-6 | MT4B | A | 3.16 | 0.1544 | -- | 1.36 | 0.0012 | -- |
| | | B | 3.20 | 0.1476 | -- | 1.41 | 0.0015 | -- |
| | | C | 3.21 | 0.1459 | -- | 1.44 | 0.0013 | >5000 |
| PVDF | MT4G | A | 17.20 | 0.0142 | 1900 | -- | -- | -- |
| | | B | 16.50 | 0.0140 | 1900 | -- | -- | -- |
| | | C | 16.70 | 0.0141 | -- | 4.59 | 0.0039 | 3000 |
| PVDF | MT4H | A | 17.50 | 0.0145 | 1700 | -- | -- | -- |
| | | B | 16.60 | 0.0141 | 400 | -- | -- | -- |
| | | C | 16.50 | 0.0142 | -- | 4.56 | 0.0042 | 1750 |
| PVF | MT5C | A | 5.37 | 0.0296 | 1500 | -- | -- | -- |
| | | B | 5.23 | 0.0304 | 1700 | -- | -- | -- |
| | | C | 5.19 | 0.0310 | -- | -- | -- | 5300 |
| PVF | MT5D | A | 5.19 | 0.0181 | 1000 | -- | -- | -- |
| | | B | 5.24 | 0.0185 | -- | 1.88 | 0.0036 | 4800 |
| | | C | 5.00 | 0.2636 | -- | 1.77 | 0.0037 | 4900 |
| PMMA | MT4C | A | 0.50 | 0.0404 | -- | 0.37 | 0.0011 | -- |
| | | B | 0.49 | 0.0403 | -- | 0.37 | 0.0010 | -- |
| | | C | 0.49 | 0.0404 | -- | 0.36 | 0.0010 | >10,000 |

### *7.3.2.1 PMMA Results (GA and TPL Films)*

PMMA samples obtained from GA and TPL were also tested by MTECH. The films came with an aluminum backing attached to one side, so the films were sent to ANT for metallization on the remaining side. The original aluminum backing was left attached. These films were difficult to handle for several reasons. First, there was a mylar film covering the aluminum backing, and this film was sometimes difficult to remove without causing damage to other parts of the stamp. Second, since the original aluminum backing was covered on both sides with plastic, there was a difficulty in attaching leads to the original aluminum backing, and a new test fixture was required. Most problematic was the fact that the application of even slight pressure would affect the measurement. Therefore, the new electrodes were developed using a very thin metal foil, as shown in Fig. 7-48.

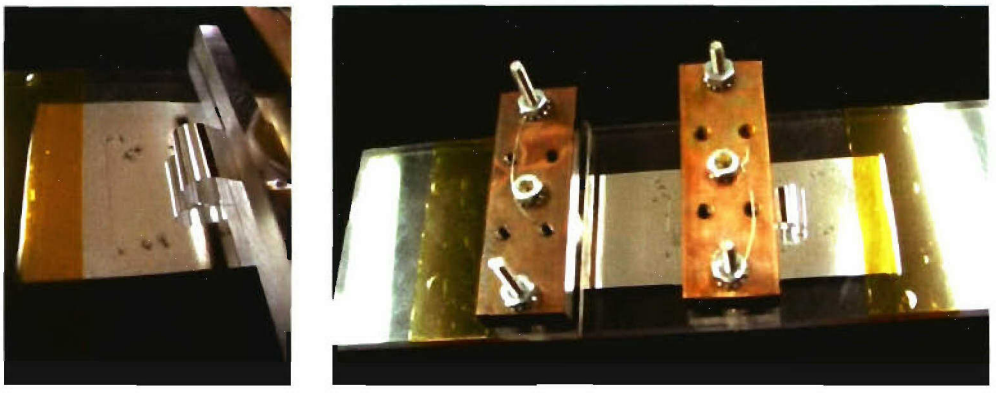

***Fig. 7-48. Test fixture used to hold the PMMA samples***

***It was important not to place any pressure on the films.***

The very thin metal electrode did not always behave well in liquid nitrogen, and was sometimes pushed around by bubbles. In some instances, frost formation affected the contact between the metal electrode and the sample. After some careful adjustments, however, we were able to obtain reasonable results.

Table 7-36 shows the relative dielectric constants and measured capacitance values of the PMMA films supplied by GA. Included in the table are results for other films, including PVCA and PVA. The data show a general decrease in relative dielectric constant at low temperatures. The reduction was significant (almost 93%) for PVCA (which exhibited a phenomenally high dielectric constant of nearly 60 at room temperature). For the remaining films, the decrease in dielectric constant was typically between 20% and 50% for the remaining films.

**Table 7-36**
**Relative Dielectric Constants ($e_r$) and Measured Capacitance Values for PMMA and Other Films Received from GA and TPL, Again Showing a General and Sometimes Significant Decrease in Dielectric Constant at Low Temperatures**

| Film | d (μm) | $e_r$ (300K) | $e_r$ (77K) | Reduction (%) | 300 K Capacitance | 77 K Capacitance |
|---|---|---|---|---|---|---|
| E00095-4 A3 (PMMA/Si) * | 4 | --- | --- | --- | --- | --- |
| E00095-4 A2 (PMMA/Si) | 4 | 7.56 | 5.57 | 26% | 26.97 nF | 19.894 nF |
| E00095-4 A1 (PMMA/Si) ** | 4 | 7.58 | 5.09 | 33% | 27.06 nF | 18.162 nF |
| E00094-6 B1 (PMMA/Al) | 4 | 5.96 | --- | --- | 21.26 nF | --- |
| E00094-6 B5 (PMMA/Al) * | 4 | --- | --- | --- | --- | --- |
| E00094-6 B4 (PMMA/Al) *** | 4 | 6.67 | --- | --- | 23.79 nF | --- |
| E00094-6 B6 (PMMA/Al) ** | 4 | 6.17 | 4.02 | 35% | 22.03 nF | 14.35 nF |
| E00094-6 B7 (PMMA/Al) ** | 4 | 5.91 | --- | --- | 21.10 nF | --- |
| (TPL) PVCA 8 μm | 8 | 59.63 | 4.34 | 93% | 112.00 nF | 8.15 nF |
| (TPL) PVA 7.2 μm | 7 | 6.27 | 3.12 | 50% | 12.78 nF | 6.365 nF |
| (TPL) Poly GA 0.89-9 μm | 9 | 4.72 | 3.23 | 32% | 7.93 nF | 5.42 nF |
| (TPL) PMMA 6 μm | 6 | 3.33 | 2.28 | 32% | 7.93 nF | 5.42 nF |
| (TPL) 50wt% BSA/PMMA 7.6 μm **** | 8 | 9.25 | 4.04 | 56% | 16.50 nF | 7.2 nF |
| (TPL) 50wt% BSA/PMMA 4 μm **** | 4 | 6.48 | 3.46 | 47% | 23.14 nF | 12.35 nF |
| (TPL) 15v% BSA in TPL Poly 6 μm | 6 | 6.83 | 5.50 | 20% | 16.25 nF | 13.082 nF |

* Returned to GA untested

** Returned to GA after testing

*** Room temperature testing only

**** Turned white, cracked and peeled after testing in LN2

Unexpectedly, the PMMA films broke down at low voltages (below 500 V) at both room temperature and 77 K. We suspect the low breakdown voltages were a result of defects in the films. Table 7-37 summarizes the data.

**Table 7-37**
**Breakdown Strength, Breakdown Voltage, and Dissipation Factor Measured for PMMA and Other Films Received from GA and TPL**

| Film | Breakdown Strength | 300K Breakdown voltage (V) | 300K Breakdown voltage (V) | 300K Dissipation Factor | 77K Dissipation Factor |
|---|---|---|---|---|---|
| E00095-4 A3 (PMMA/Si) * | --- | --- | --- | --- | --- |
| E00095-4 A2 (PMMA/Si) | --- | --- | < 500 V | 0.01690 | 0.00177 |
| E00095-4 A1 (PMMA/Si) ** | --- | --- | < 500 V | 0.01620 | 0.00330 |
| E00094-6 B1 (PMMA/Al) | --- | < 500 V | --- | 0.026 | --- |
| E00094-6 B5 (PMMA/Al) * | --- | --- | --- | --- | --- |
| E00094-6 B4 (PMMA/Al) *** | --- | --- | --- | 0.0241 | --- |
| E00094-6 B6 (PMMA/Al) ** | --- | < 500 V | --- | --- | --- |
| E00094-6 B7 (PMMA/Al) ** | --- | < 500 V | --- | 0.0252 | --- |
| (TPL) PVCA 8 μm | --- | --- | < 500 V | 2.7 | 2.24 |
| (TPL) PVA 7.2 μm | 429 V/μm | --- | 3000 V | 0.0449 | 0.0249 |
| (TPL) Poly GA 0.89-9 μm | 235 V/μm | --- | 2000 V | 0.009 | 0.0037 |
| (TPL) PMMA 6 μm | --- | < 500 V | --- | --- | --- |
| (TPL) 50 wt% BSA/PMMA 7.6 μm **** | --- | --- | < 500 V | 0.028 | 0.008 |
| (TPL) 50 wt% BSA/PMMA 4 μm **** | --- | --- | < 500 V | 0.0458 | 0.0021 |
| (TPL) 15 v% BSA in TPL Poly 6 μm | 250 V/μm | --- | 1500 V | 0.009 | 0.0044 |

* Returned to GA untested
** Returned to GA after testing
*** Room temperature testing only
**** Turned white, cracked and peeled after testing in $LN_2$

### *7.3.3 Testing on Liquid-Nitrogen-Filled Capacitors*

Apart from the stamp data described above, MTECH also tested utilizing liquid nitrogen as a filler in place of the vacuum, air, or oils that are typically used for this purpose. The device under test was received from GA/ESI, and carried the part number 30956-X580. We began by carefully cutting vents into the capacitor's container, as shown in Fig. 7-49. Doing so revealed an inner case made of plastic (white material visible inside the metal container. No holes were cut into the plastic case for fear of damaging the capacitor film. Therefore, liquid nitrogen probably did not permeate into the film windings. Nevertheless, capacitance and dissipation factor data were taken, and are shown in Table 7-38. These are compared to the data in Table 7-39, taken from a capacitor of the same part number (30956-X581), but which was left sealed. The dissipation factor was 2-3 times lower for the sealed capacitor, but the capacitance was higher for the $LN_2$-filled device.

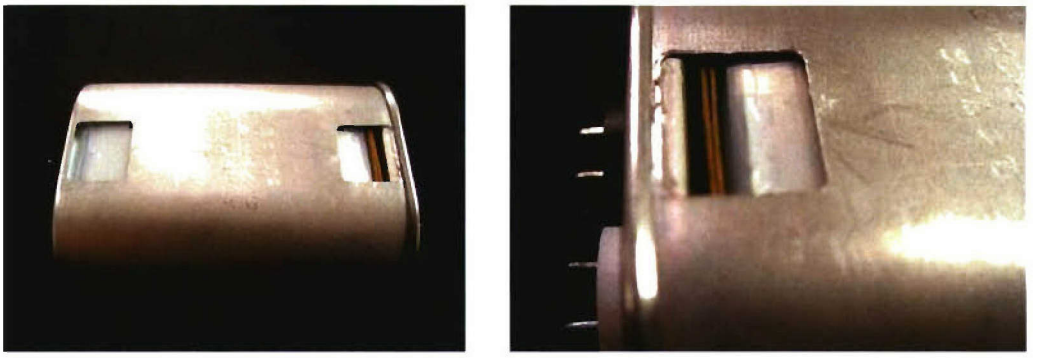

*Fig. 7-49. Holes were cut into a capacitor's housing to allow liquid nitrogen to permeate the capacitor more directly.*

*A second plastic housing inside the metal outer case was not, however, removed.*

**Table 7-38**
**Capacitance and Dissipation Factor Data from a Packaged Capacitor, Part Number 30956-X580, Into Which Fill and Vent Holes Were Cut to Allow Liquid Nitrogen to Permeate the Outer Metal Case**

**The inner, plastic case was not touched. 77 K data were taken after a two-hour cool-down period. The resonant frequency of the capacitor was ~45 kHz at 300 K, and ~55 kHz at 77 K**

| Frequency | Capacitance (300 K) | Dissipation Factor (300 K) | Capacitance (77 K) | Dissipation Factor (77 K) |
|---|---|---|---|---|
| 20 Hz | 108.34 μF | 0.000767 | 114.14 μF | 0.000632 |
| 60 Hz | 108.32 μF | 0.001857 | 114.13 μF | 0.001533 |
| 1 kHz | 108.42 μF | 0.029308 | 114.22 μF | 0.024545 |
| 10 kHz | 116.05 μF | 0.334820 | 120.08 μF | 0.271304 |

**Table 7-39**
**Capacitance and Dissipation Factor Data from a Packaged Capacitor, Part Number 30956-X581, Which Was Left Sealed**

**77-K data were taken after a two-hour cool-down period. The resonant frequency of the capacitor was ~45 kHz at 300 K, and ~45 kHz at 77 K.**

| Frequency | Capacitance (300 K) | Dissipation Factor (300 K) | Capacitance (77 K) | Dissipation Factor (77 K) |
|---|---|---|---|---|
| 20 Hz | 108.15 μF | 0.000421 | 112.08 μF | 0.000225 |
| 60 Hz | 108.14 μF | 0.000981 | 112.07 μF | 0.000589 |
| 1 kHz | 108.22 μF | 0.014904 | 112.16 μF | 0.009639 |
| 10 kHz | 112.75 μF | 0.181401 | 116.86 μF | 0.115929 |

Mtech's testing results were similar to GA's in that the COTS and commercial materials are not adequate for the 8J/CC. A significant change in "K" was observed between 300 and 77K for both commercial and COTS materials. It was noticed that the polarization with low voltages do not have any positive effects at 77K and also the dielectric constant reduction is lower with the use of $SIO_2$ particles.

### *7.3.4 New Capacitor Concepts*

MTECH also evaluated some new concepts in capacitor design, geared especially toward low-temperature operation. Figure 7-50 illustrates one of these, which involves utilizing a special polymer with periodic cooling channels to allow the flow of liquid nitrogen throughout the capacitor for more direct cooling.

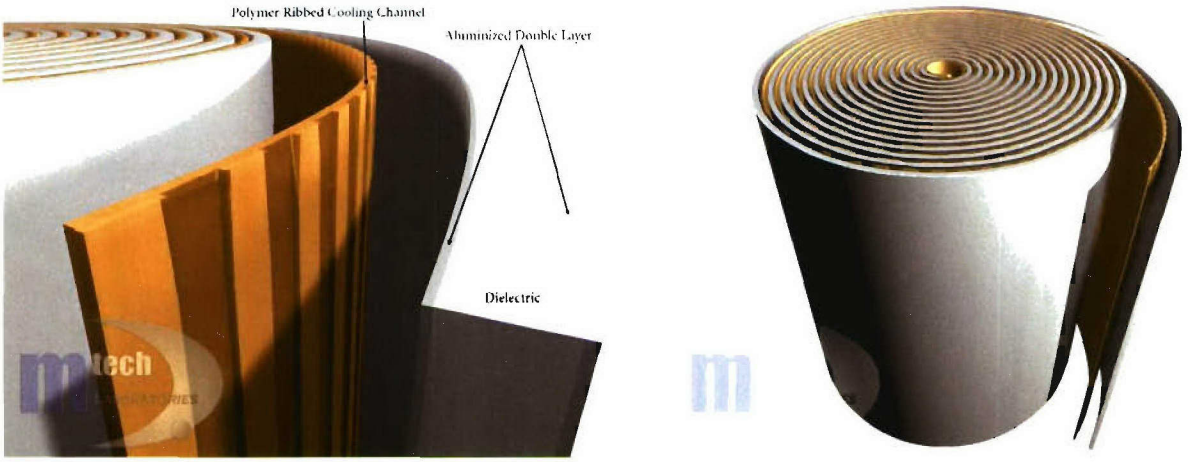


***Fig. 7-50. An example of a new capacitor design concept being developed by MTECH.***

***The cooling channels in the special ribbed polymer layer allow for the free flow of liquid nitrogen throughout the capacitor, in close contact to the dielectric.***

A second design is shown in Fig. 7-51. Here, the capacitors are wound using a special mandrel, allowing for the center of the capacitor to remain open. This increases the surface area with which liquid nitrogen can come into contact, and also leaves room for cryogenic electronic components to be housed inside the capacitor. Although not appropriate for the rail gun applications that are the focus of this program, such a concept may find use as a filter in high-frequency cryogenic circuits.

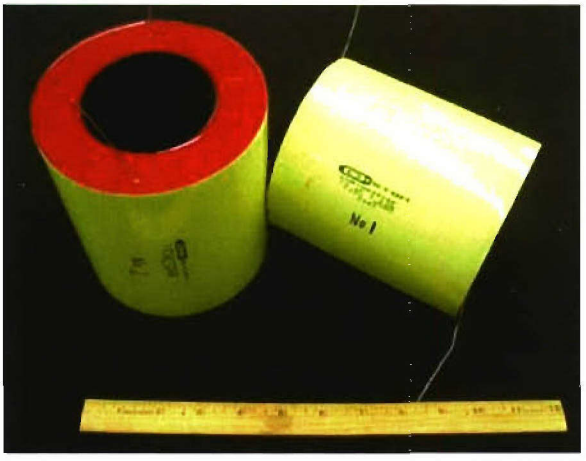

*Fig. 7-51. A second cryogenic capacitor concept explored by MTECH in a separate SBIR program.*

*A special mandrel is used to wind the capacitor, leaving the center of the device free for liquid nitrogen flow and/or the inclusion of cryogenic electronics within close proximity to the filter capacitors. This may be especially useful for high-frequency applications.*